

School of Doctoral Studies in Biological Sciences
University of South Bohemia in České Budějovice
Faculty of Science

Mitochondrial gene expression in trypanosomatids

PH.D. THESIS

Mgr. Michaela Procházková

Supervisor: RNDr. Alena Zíková, Ph.D.
Biology Centre of the Czech Academy of Sciences
Institute of Parasitology, České Budějovice, CZ
&
University of South Bohemia in České Budějovice
Faculty of Science

České Budějovice 2018

This thesis should be cited as:

Procházková, M., 2018: Mitochondrial gene expression in trypanosomatids. Ph.D. Thesis. University of South Bohemia, Faculty of Science, School of Doctoral Studies in Biological Sciences, České Budějovice, Czech Republic, 116 pp.

Annotation

This thesis comprises of diverse projects all focused towards analysis of mitochondrial translation in unicellular parasites. As only two mitochondrially encoded genes are required during the life cycle stage when *Trypanosoma brucei* resides in the bloodstream of a mammalian host, this protist provides a simplified background in which to study mitochondrial translation termination phase. The leading project utilizes *T. brucei* to examine mitochondrial translation termination factor TbMrf1 by gene knockout. Subsequently, it is suggested that the peptidyl-tRNA hydrolase TbPth4 is able to abate the TbMrf1 knockout phenotype by its ability to rescue mitoribosomes that become stalled when TbMrf1 is absent. Additionally, modifying methyltransferase of TbMrf1, the TbMTQ1, was characterized. And finally, this work contributed to the development of the protein expression regulation method in *Leishmania* parasites, a protocol for measurement of proton pumping activity of F₀F₁ ATPase complex in native mitochondria, and optimization of purification protocol for hydrophobic recombinant proteins.

Declaration [in Czech]

Prohlašuji, že svoji disertační práci jsem vypracovala samostatně pouze s použitím pramenů a literatury uvedených v seznamu citované literatury.

Prohlašuji, že v souladu s § 47b zákona č. 111/1998 Sb. v platném znění souhlasím se zveřejněním své disertační práce, a to v nezkrácené podobě elektronickou cestou ve veřejně přístupné části databáze STAG provozované Jihočeskou univerzitou v Českých Budějovicích na jejich internetových stránkách, a to se zachováním mého autorského práva k odevzdanému textu této kvalifikační práce. Souhlasím dále s tím, aby toutéž elektronickou cestou byly v souladu s uvedeným ustanovením zákona č. 111/1998 Sb. zveřejněny posudky školitele a oponentů práce i záznam o průběhu a výsledku obhajoby kvalifikační práce. Rovněž souhlasím s porovnáním textu mé kvalifikační práce s databází kvalifikačních prací Theses.cz provozovanou Národním registrem vysokoškolských kvalifikačních prací a systémem na odhalování plagiátů.

V Českých Budějovicích, 11.4.2018

.....

This thesis originated from a partnership of Faculty of Science, University of South Bohemia and the Institute of Parasitology, Biology Centre CAS supporting doctoral studies in the Molecular and Cellular Biology and Genetics study programme.



Přírodovědecká
fakulta
Faculty
of Science



BIOLOGICKÉ
CENTRUM
AV ČR, v. v. i.

Financial support

This work was supported by:

Ministry of Education ERC CZ grant no. LL1205

EMBO 649 Installation grant no. 1965

Grant Agency of the University of South Bohemia grant no. 093/2012/P

Acknowledgements

I wish to express my gratitude to the whole team of Laboratory of Functional Biology of Protist, predominantly its leader Alena Zíková, who took me under her wings and hoped for the best. Thanks to this young and dynamic group (Brian, Eva, Ondra, Dave, Karolína, Honza, Hanka, Zuzka, Míša, Carol, and Gergana), I learned a great deal about laboratory work, science life, and myself. I thank especially my former colleague David Wildridge, who kindly provided his proofreading skills.

I cannot forget to mention my kind hosts for an international study visit in Boston, USA. Inna and Ruslan Aphasizhev (School of Dental Medicine, BU) put up with me most kindly for three months during which I learned a lot about scientific excellence, work with RNA, and American culture.

More than a year before even a line of this thesis was written, my time was up in Dr. Zíková's team and I was fortunate to get accepted by Dr. Pavel Plevka as a member of his team on CEITEC-MU in Brno, where I currently reside. I am very grateful for a chance to work in this progressive and fruitful environment.

And last but not least, I am forever in debt to my husband and broader family who always stood by me regardless of the level of frenzy I was exhibiting.

Publication and author's contribution statement

1. **Procházková, M.**, Panicucci, B. & Zíková, A. Cultured bloodstream *Trypanosoma brucei* adapt to life without mitochondrial translation release factor. *Sci. Rep.* 8, 1–15 (2018).

This study was designed by BP, MP, and AZ. MP performed all the experiments, analyzed data and contributed to the writing process.

- Experimental contribution: 100%

- Contribution to the writing: 50%

2. Doleželová, E., Terán, D., Gahura, O., Kotrbová, Z., **Procházková, M.**, Keough, D., Špaček, P., Hocková, D., Guddat, L., Zíková, A. Evaluation of the *Trypanosoma brucei* 6-oxopurine salvage pathway as a potential target for drug discovery. *PLoS Negl. Trop. Dis.* 12, e0006301 (2018).

This study is not included in Ph.D. thesis. M.P. contributed to the preliminary results generation and data curation. The approximate level of contribution is 10%.

I agree with the given level of contribution of Mgr. Michaela Procházková to both publications.

.....
RNDr. Alena Zíková, PhD.

(Corresponding author)

Contents

<i>List of abbreviations</i>	v
<i>List of figures and tables</i>	vii
1. INTRODUCTION	1
1.1 SALIVARIAN TRYPANOSOMES AS CAUSATIVE AGENTS OF HUMAN AND ANIMAL TRYPANOSOMIASES.....	1
1.2 STERCORARIAN TRYPANOSOMA CRUZI AS CAUSATIVE AGENT OF CHAGAS DISEASE.....	4
1.3 LEISHMANIA SPECIES AND LEISHMANIASES.....	6
1.4 UNIQUE FEATURES OF <i>TRYPANOSOMA BRUCEI</i> CELL.....	8
1.5 ROLE OF MITOCHONDRION IN BOTH LIFE STAGES.....	11
1.6 MITOCHONDRIAL GENE EXPRESSION	13
1.6.1 Mitochondrial translation – initiation.....	18
1.6.2 Mitochondrial translation – elongation.....	19
1.6.3 Mitochondrial translation – termination and mitoribosome recycling	20
2. AIMS AND COURSE OF RESEARCH	22
PART I - MITOCHONDRIAL RELEASE FACTORS IN BLOODSTREAM FORM TRYPANOSOME	24
I.1. INTRODUCTION.....	24
I.2. METHODS.....	27
I.2.1 Preparation of constructs.....	27
I.2.2 Native electrophoresis.....	29
I.2.3 Sucrose gradient with dot blot analysis.....	29
I.2.4 Isolation of total RNA and Northern blot.....	30
I.3. RESULTS & DISCUSSIONS.....	31
I.3.1 Cultured bloodstream <i>Trypanosoma brucei</i> adapt to life without <i>TbMrf1</i> [Publication].....	31
I.3.1.1 Additional unpublished data.....	47
Loss of <i>TbMrf1</i> decreases mt transcript levels.....	47
Mt transcripts accumulate when <i>TbPth4</i> is down-regulated in the dKO <i>TbMrf1</i> cell line.....	49
I.3.2 Identification of cytosolic class 1 release factor - <i>TbeRF1</i>	51
I.3.3 Characterization of mt MTase <i>TbMTQ1</i>	53
PART II – OPTIMIZATION OF THE SAFRANINE O ASSAY FOR MEASUREMENT OF F_0F_1 ATPASE ACTIVITY	60
II.1 INTRODUCTION.....	60
II.1.1 F_0F_1 ATPase composition and function in BF trypanosomes	61
II.2 PROTOCOL.....	63
II.3 RESULTS WITH DISCUSSION.....	63
PART III - DESTABILIZATION DOMAIN TECHNIQUE IN MITOCHONDRION	66
III.1 INTRODUCTION	66
III.2 METHODS.....	69
III.3 RESULTS WITH DISCUSSION.....	70
PART IV – RESPIRATORY COMPLEX IV- ASSOCIATED PROTEIN MIX IN BLOODSTREAM FORM TRYPANOSOME	77
IV.1 INTRODUCTION	77
IV.2 METHODS.....	78
IV.3 RESULTS WITH DISCUSSION.....	79
3. SUMMARY	82
4. REFERENCES	84
5. SUPPLEMENTARY MATERIAL	101

List of abbreviations

A6	F ₀ F ₁ ATPase subunit 6, in the mammalian system designated subunit <i>a</i>
AAC	ADP/ATP carrier
AOX	trypanosome alternative oxidase, sometimes abbreviated as TAO
BF	bloodstream form of <i>Trypanosoma brucei</i>
Complex I	NADH : ubiquinone oxidoreductase
Complex II	succinate : ubiquinone oxidoreductase
Complex III	ubiquinol : cytochrome c oxidoreductase
Complex IV	cytochrome c : oxygen oxidoreductase
ETC	electron transport chain
eRF1	human cytosolic release factor 1
eRF1L	human cytosolic release factor 1-like protein
eRF3	human cytosolic release factor 3
F ₀ F ₁ ATPase	complex V, inner mt membrane ATP synthase/hydrolase
G3PDH	glycerol-3-phosphate dehydrogenase
GRBC1/2	gRNA binding complex, a heterodimer
HmPrmC	human mitochondrial methyltransferase
IF1,2,3	bacterial initiation factor 1, 2, 3
KPAF1,2	kinetoplast polyadenylation factor 1,2
KPAP1	kinetoplast polyadenylation protein 1
KREN1,2,3	kinetoplast RNA editing endonuclease 1, 2, 3
KREPB6	kinetoplast RNA editing protein B6
KREPB7	kinetoplast RNA editing protein B7
KREX1	kinetoplast RNA editing exonuclease 1
LSU	large subunit of the ribosome
mt	mitochondrial
mmp	mitochondrial membrane potential
mRF1	human mitochondrial release factor 1
Mrf1	yeast mitochondrial release factor 1
Mtq1	yeast mitochondrial methyltransferase
Mtq2	yeast cytosolic methyltransferase
NTDs	neglected tropical diseases
ORF	open reading frame
PAMC	polyadenylation mediator complex
PF	procyclic form of <i>Trypanosoma brucei</i>
PrmC/HemK	bacterial methyltransferase
RECC	RNA editing core complex
REMC	RNA editing mediator complex
RESC	RNA editing substrate binding complex or MRB1 complex
RET1	RNA editing TUTase 1
RET2	RNA editing TUTase 2
RF1,2,3	bacterial release factor 1, 2, 3
RNAi	RNA interference
RPS12	ribosomal protein 12, SSU subunit
RRF	yeast mitochondrial ribosome recycling factor

Subunit <i>a</i>	mammalian pore forming subunit of F_0 moiety of ATPase
Subunit β	subunit of F_1 moiety of F_0F_1 ATPase
SSU	small subunit of the ribosome
TbRGG1/2	protein containing RGG motif, mt RNA binding in RESC complex
VSG	variable surface glycoprotein
WHO	World Health Organization

List of figures and tables

Figure 1: The life cycle of <i>Trypanosoma brucei</i>	3
Figure 2: The life cycle of <i>Trypanosoma cruzi</i>	5
Figure 3: The life cycle of <i>Leishmania sp</i>	7
Figure 4: Mitochondrion of procyclic form trypanosome	11
Figure 5: Mitochondrial gene expression and translation	16
Figure 6: Elimination of TbMrf1 causes a decrease in mt transcript levels	48
Figure 7: The A6 and RPS12 transcripts accumulate upon downregulation of TbPth4 in dKO TbMrf1 cells	50
Figure 8: A – The TbeRF1-PTP constructs is expressed in wild-type and dKO TbMTQ1 background. B –TbeRF1 is localized in mitochondrion. C – Growth curve. D – RT-PCR analysis of TbeRF1 knockdown cell line	52
Figure 9: A – Verification of dKO TbMTQ1 cell line by PCR. B – Growth curve. C – Doubling time. D – Mitochondrial membrane potential. E – Level of mt F ₀ F ₁ ATPase moieties in dKO TbMTQ1 compared to BF427	57
Figure 10: A, B –dKO TbMTQ1 cell sensitivity to specific inhibitors. C, D – Level of individual ribosomal RNAs, E – Parasitemia levels in mouse blood. F – survival of animals infected with wild-type BF 427 and dKO TbMTQ1 cells	59
Figure 11: A – Solvent controls. B – Relative quenching of safranin O fluorescence signal by addition of specific inhibitors. C – Analysis of ATPase activity in ATPaseTb1 knockdown cell line	65
Figure 12: Schematic overview of destabilization domain technique	67
Figure 13: A – Titration of stabilization ligand, FK506. B – Detection of stabilized eGFP individual reporter cell line. C – Subcellular fractionation	72
Figure 14: A – Schematics of dd_T7 polymerase construct for incorporation into the SSU rDNA. B – Verification of correctly incorporated dd domain by PCR. C – Stabilization of T7 RNA polymerase N – terminal dd domain in response to the addition of FK506 ligand	75
Figure 15: A – Schema of the cassette for genomic integration to the LD1 locus. B – The endogenous LD1 locus scheme. C – The MIX protein integration scheme. D – Immunoblotting analysis of cassette expression	76
Figure 16: A – Growth curve of RNAi TbMIX in PF cells. B – Growth curve of RNAi and genetically silenced dKO TbMIX in BF cells, C – Purification profile of the antigen. D – Anti-TbMIX antibody verification by immunoblotting	81
Supplementary Table 1: List of nucleotides used in unpublished projects	101
Supplementary materials from publication	103

1. INTRODUCTION

While the majority of infectious diseases can be either prevented or effectively treated, there is a group of fatal illnesses still evading our efforts. The World Health Organization (WHO) defines neglected tropical diseases (NTDs) as a diverse group of highly transmittable pathogens prevalent in rural tropical areas. Three NTDs are caused by protozoan parasites belonging to the class *Kinetoplastida*, from the order *Trypanosomatida*. These are Human African Trypanosomiasis (HAT) in equatorial Africa, Chagas disease in America, and leishmaniasis in tropical regions around the globe. In addition to the medical issues caused by these parasites, there is an economic burden that hinders social development in endemic areas.

1.1 SALIVARIAN TRYPANOSOMES AS CAUSATIVE AGENTS OF HUMAN AND ANIMAL TRYPANOSOMIASES

Trypanosoma brucei is an extracellular protozoan parasite relying on its insect vector, the tsetse fly for transmission between hosts. Both subspecies of *T. brucei*: *T.b. gambiense* and *T.b. rhodesiense*, cause HAT but they differ in geographical distribution as well as in character of disease they cause. *T.b. gambiense* is prevalent in central and western Africa and causes chronic trypanosomiasis accounting for 97% of reported HAT cases. In contrast, *T.b. rhodesiense* is more common in southern and eastern Africa and its infection is characteristic by acute progress. Zoonotic subspecies *T.b. brucei*, *T.b. equiperdum*¹ and *T.b. evansi*² cause Animal African Trypanosomiasis in livestock and wild animals with devastating effect on agriculture in the endemic areas. Interestingly,

Introduction

the latter two subspecies lost the ability to survive in the insect vector as a consequence of partial or complete loss of mitochondrial genome. Both subspecies are transmitted mechanically, either sexually or by hijacking the proboscis of bloodsucking insects.

Trypanosoma is a digenetic parasite with a complex life cycle alternating between an insect vector and a mammalian host (Figure 1). It infects the mammalian host as the stage of metacyclic trypomastigote during a blood meal of the infected tsetse fly (genus *Glossina*). The parasite spreads via the lymphatic system to the bloodstream and undergoes transformation to the bloodstream trypomastigote (referred to as the slender form, BF). This stage is characterized by rapid multiplication and spreading to the blood, lymph, cerebrospinal fluid, and adipose tissue ³. The patient's immune system is temporarily able to slow down the infection, however, the parasite changes its surface molecules through the process of antigenic variation (reviewed in ⁴). The antigenic variation of surface glycoproteins (VSGs) is a rapid replacement of original VSGs with a new type of the molecule, which is unknown to host's immune system. As a result, periodic waves of parasitemia occur in patient's blood and cause typical symptoms of the HAT: a headache, fever, and weakness. After the blood-brain barrier is compromised by the parasite, the neurological symptoms such as disturbed sleep cycle, ataxia, and seizures set in and the host eventually dies of the exhaustion from a constant parasitic challenge.

The parasite cell possesses a density sensing mechanism responding to the concentration of a stumpy induction factor (SIF). At the cell density exceeding 10^6 parasites/ml, this SIF signal induces first G1 phase arrest and subsequently change in cell morphology to the stumpy form in preparation for the transmission to the insect vector ⁵⁻⁸. Next, the tsetse fly ingests host's blood and the parasite enters the midgut where it undergoes a transformation into the procyclic trypomastigote (PF). PF multiplies and migrates to the salivary glands

where it transforms to epimastigote and the infective metacyclic trypomastigote. The life cycle is concluded when another host becomes infected.

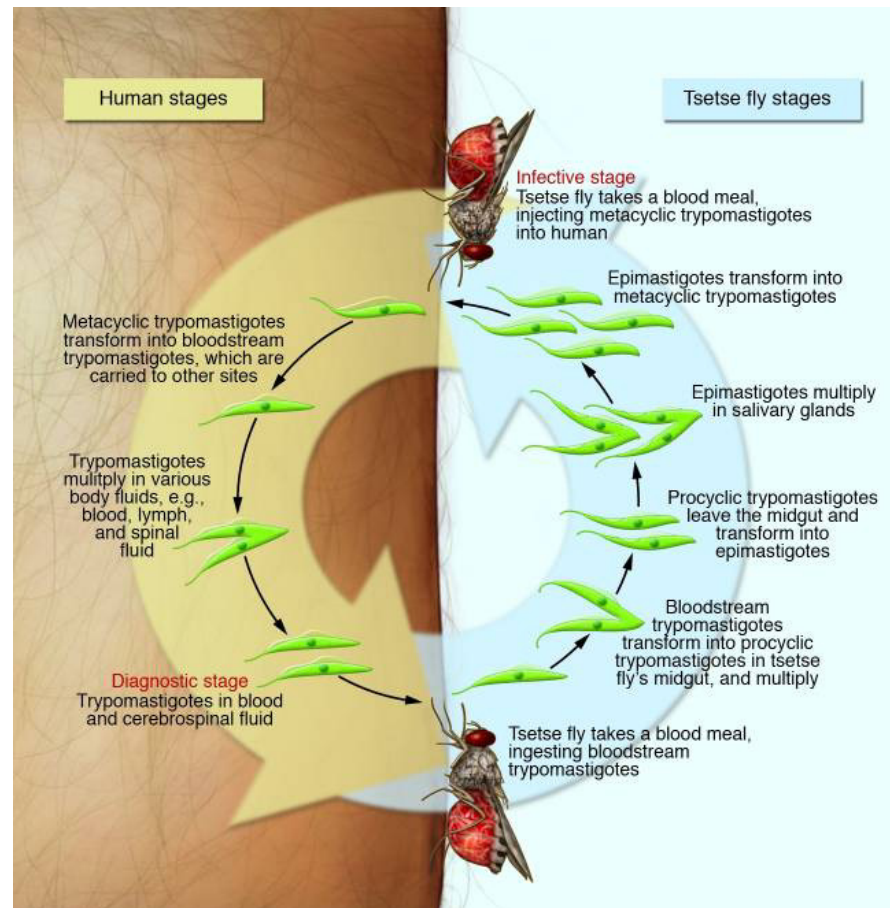


Figure 1: Life cycle of *Trypanosoma brucei* as adapted from ⁹.

The treatment of the HAT relies on highly toxic compounds ¹⁰. There are currently five approved drugs used in specific stages of disease progress. Pentamidine and suramin are administered to treat an initial haemolympathic stage. Both drugs were developed in an early 20th century and may cause the following side effects; diarrhea, vomiting, abdominal pain, various skin reactions, and rarely liver dysfunction developing into jaundice ¹¹. The treatment of choice for the second HAT stage is melarsoprol for infection by *T.b.rhodesiense* and Nifurtimox-Eflornithin combination therapy (NECT) in case of infection by *T.b.gambiense*. Melarsoprol was manufactured in 1940's as an anti-cancer drug and has been used for the treatment of the second stage of the HAT since 1949. It

Introduction

is a highly toxic organic compound of arsenic with severe side effects including encephalopathy ¹² in 3-10% of treated patients, with subsequent 40% lethality ¹³. Approval of NECT in 2009 simplified previously complex Eflornithine treatment regimen of chronic HAT ¹⁴. Recently, DNDi group from Switzerland reported the success of oral drug Fexinidazole in stage 3 clinical trials in field treatment of second stage HAT ¹⁵. The development of a vaccine against HAT is difficult due to the process of antigenic variation of surface glycoproteins in infective BF, and thus the generation of efficacious, safe and affordable drugs is desirable.

1.2 STERCORARIAN TRYPANOSOMA CRUZI AS CAUSATIVE AGENT OF CHAGAS DISEASE

Chagas disease, endemic in south America, is caused by *Trypanosoma cruzi* transmitted by 'kissing bug' from family *Triatominae* (Figure 2). Affected are predominantly inhabitants of traditional mud-walled houses that serve as habitats for the insects. Moreover, the natural reservoirs of *T. cruzi* parasite include both wild and domestic animals, which are living as a part of the household in these areas. Infection by *T. cruzi* usually arises from contamination of opened wound (insect bite) by insect feces containing infective trypomastigotes, but can additionally originate from ingestion of contaminated food ¹⁶, blood transfusion or organ transplant, and also congenitally. The parasite exists in two forms; the first form is a non-dividing extracellular stage of metacyclic trypomastigote that travels through the bloodstream and infects multiple tissues, whereas the second form is an intracellular dividing amastigote. Transformation of amastigote to trypomastigote occurs in cycles and allows the parasite to infect different tissues.

The infection has usually a short asymptomatic initial phase and long (decades) chronic phase during which the persistent interaction of host immune

system with infected tissues gradually develops into typical symptoms. Chagas disease symptoms include cardiomyopathy in 30% of patients, gut enlargement and neural alterations in 10% of patients^{17,18}. The vector eradication combined with an efficient screening of patients and early therapy represents a successful approach to control the Chagas disease in endemic areas. Nevertheless, the numbers of people infected by *T. cruzi* are estimated by WHO to be 6 – 7 million, worldwide¹⁹. Current therapy employs existing anti-parasitic drugs Nifurtimox and Benznidazole with high efficiency shortly after infection. Progressed chronic phase cannot be fully treated however, treatment can slow down the onset of symptoms.

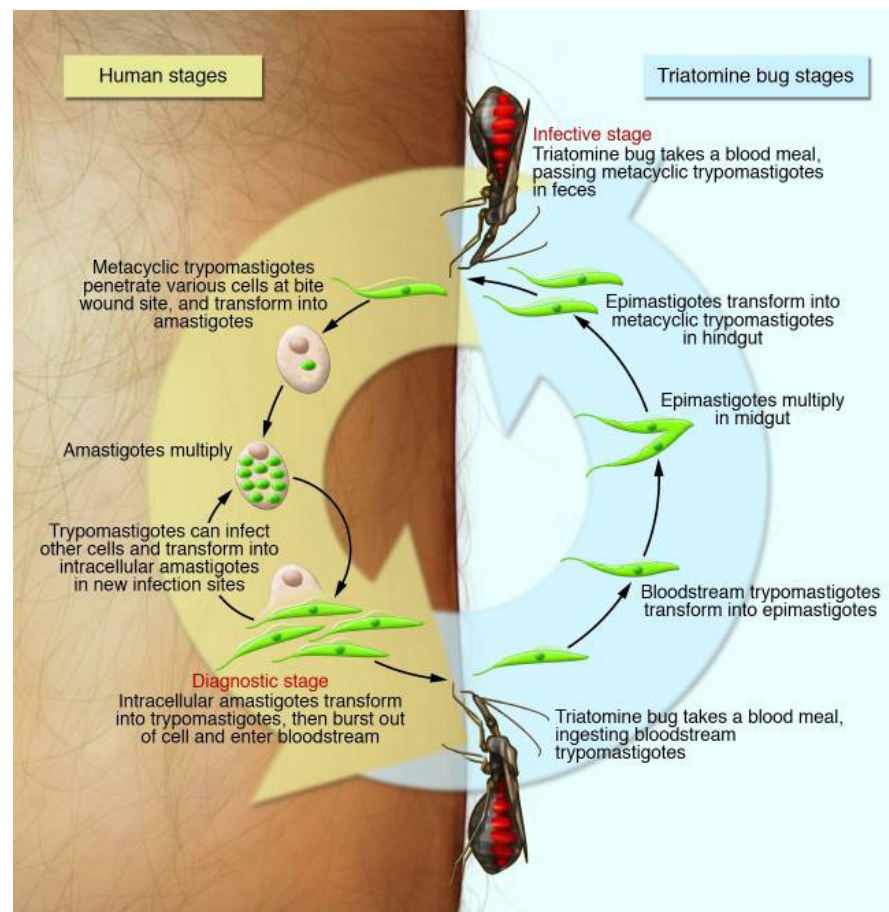


Figure 2: Life cycle of *Trypanosoma cruzi* as adapted from⁹.

1.3 LEISHMANIA SPECIES AND LEISHMANIASES

Leishmaniasis is a common designation for a group of diseases caused by protozoan parasites of genus *Leishmania* (order *Trypanosomatida*). There are currently 21 species known to infect human²⁰. WHO divides leishmaniasis based on an afflicted tissue type to cutaneous, mucocutaneous, and visceral forms. Cutaneous leishmaniasis (CL) agents include *L. major*, *L. tropica*, *L. aethiopica*, *L. mexicana*, and typically cause self-healing ulcers in soft tissues exposed to bite of the insect vector, the sand-fly (genus *Phlebotomus* in Asia and Africa; genus *Lutzomyia* in Americas). Mucocutaneous leishmaniasis (MCL) is more severe and is usually caused by members of subgenus *Viannia* (*L. braziliensis* and *L. guyanensis*) prevalent in South America. Untreated infection results in destruction of mucous parts of the face. It was shown that aggravated symptoms of MCL are the consequence of viral infection of the parasite by Leishmania RNA virus 1 (LRV, Totiviridae). Research on a mouse model revealed that host immune system responds differently to infection by virus-free leishmania compared to parasite containing the virus. LRV is able to efficiently divert the immune response by activating production of pro-inflammatory cytokines that leads to a destruction of large patches of tissue²¹⁻²³. Interestingly, species infected with LRV are almost exclusively members of subgenus *Viannia* with functional RNAi pathway shown to be able to limit LRV infection²⁴.

The most severe form of leishmaniasis is the visceral leishmaniasis (VL). Symptoms include enlargement of internal organs (spleen and liver) and bone marrow failure caused by massive migration of the parasite into these organs. The causative species are *L. donovani* or *L. infantum*. The disease is fatal if left untreated consequently, VL earned itself several names like kala azar, black or dum dum fever. In isolated cases, a seemingly healed patient can harbor parasite in skin eventually relapsing in form of post-kala-azar dermal leishmaniasis

(PKDL)^{25,26}. With thousands of cases *per annum*, *Leishmania* is the second largest parasitic "killer" in the world after *Plasmodium spp* ⁹.

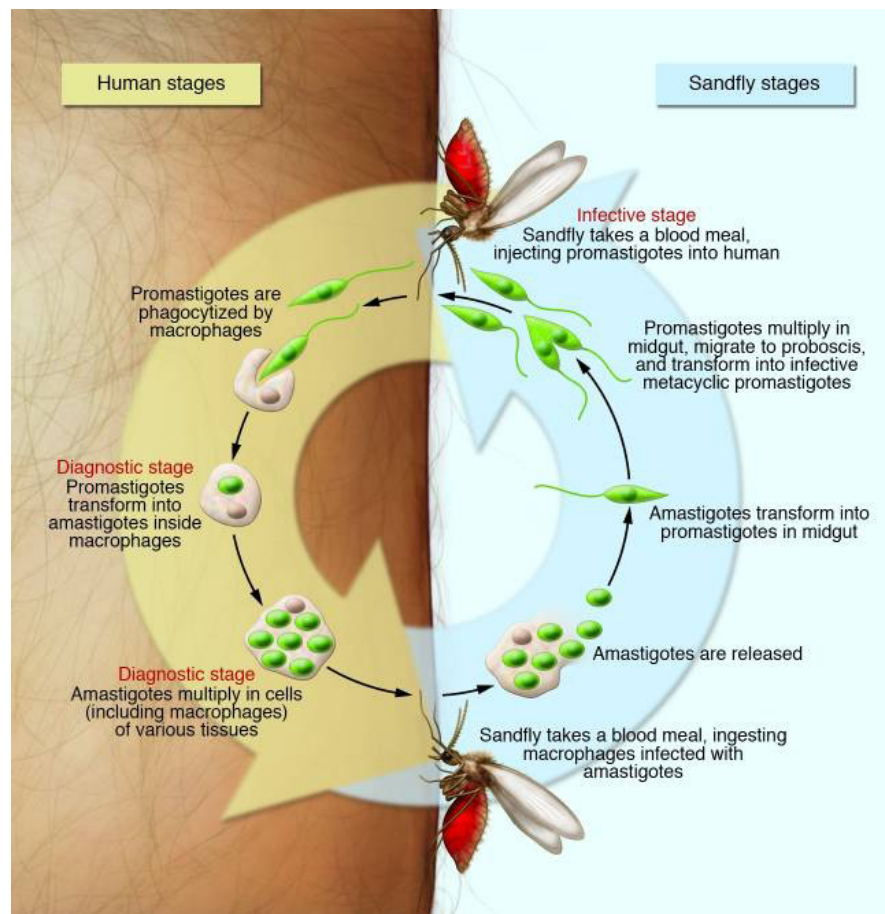


Figure 3: Life cycle of *Leishmania* sp. adapted from ⁹

Leishmania lifecycle differs from that of *T. brucei*. As an intracellular parasite, leishmania undergoes dramatic changes in cell morphology (Figure 3). The initial wave of parasites is phagocytized by macrophages that have migrated to the site of the sand-fly bite. Later, *Leishmania* further infects other immune cell types by receptor-mediated endocytosis ^{27,28}. Metabolic adaptation to low pH and high amino-acid concentration allows the parasite to rapidly multiply in endosomes. From the original site of a bite, the parasite spreads through blood and lymph to internal organs. When the next sand fly takes a blood meal on an infected individual, it ingests immune cells (predominantly macrophages) that are full of amastigotes. Ingested amastigotes are released in the midgut of a sand

Introduction

fly and transform into promastigotes that further multiply and migrate to proboscis where they await transfer to another host in form of metacyclic promastigotes.

The standard course of treatment includes pentavalent antimonial compounds (Pentostam, Glucantim). In India, the antimonials have been completely replaced with antibiotic amphotericin B due to the emerging resistance in parasites ²⁹. Alternative treatments are Paronomycin and Miltefosine, both efficient but either costly or causing undesirable side effects (diarrhea, vomiting, abdominal pain, skin reaction, fever, kidney and liver problems) ⁹.

In contrast to improbable vaccine development to protect against HAT, the vaccine against leishmaniasis might be a viable option. A prophylactic vaccine seems to be feasible based on current knowledge of protective immunity after 'leishmanisation' with a live attenuated parasite and recognized specific antigens conserved between individual *Leishmania* species ³⁰. Currently, efforts continue to develop and prepare a universally safe vaccine against all species of *Leishmania* with prophylactic as well as therapeutic effects ^{31,32}.

1.4 UNIQUE FEATURES OF *TRYPANOSOMA BRUCEI* CELL

Of the aforementioned TriTryp species i.e. *Leishmania* sp., *T. cruzi* and *T. brucei*, the *Trypanosoma brucei brucei* subspecies (the causative agent of nagana in cattle will be further addressed as the trypanosome), has become the best established laboratory model organism for several reasons. The genomes of widely used laboratory strains (TREU927, Lister strain 427) have been sequenced and are freely available at the TriTrypDB database ³³ together with the related proteomic and transcriptomic data. Trypanosomes are also amenable to genetic manipulations utilized in forward and reverse genetic approaches – homologous

recombination, introduced gene expression, and RNA interference. The parasite has short generation time and it is possible not only to keep the procyclic and bloodstream trypomastigotes in culture but also run through the whole life cycle *in vitro* ³⁴. As a counterpart to *Opisthokont* model organisms such as mammalian cells or yeast, this ancient parasite proved to contain a series of interesting traits ³⁵. In next few paragraphs, I will briefly introduce some of the peculiarities which are observed in trypanosome transcription, surface molecule variation, and energy metabolism.

The first unique trait is found in trypanosome nucleus where the genome is organized in eleven pairs of large chromosomes (0.9 – 6 Mbs) which are polycistronically transcribed and consequently post-transcriptionally processed into individual mRNAs ³⁶. Post-transcriptional processing of the majority of the open reading frames (only two exceptions exist, poly A polymerase and DEAD/H RNA helicase ³⁷) is performed by *trans*-splicing and polyadenylation ^{38–41}. To create individual mature mRNA molecules through the *trans*-splicing, the 39 bp spliced-leader RNA (SL-RNA) molecule is required. SL-RNA is encoded by series of repetitive genes throughout the trypanosome genome ³⁸ and transcribed from a specific promoter by RNA polymerase II ⁴². SL-RNA contains modified nucleotides on its 5' end: first 7-methylguanosine is followed by four more nucleotides with defined modifications. As a result, one of the most complicated cap structures is formed, the cap 4: m⁷Gpppm_{6,6}AmpAmpCmpm₃Ump-SL-RNA ^{43,44}. *Trans*-splicing is based on a nucleophile attack performed by SL-RNA terminal nucleotide towards branching adenine situated between the two coding genes ⁴¹. The 3' end of the now capped mRNA is polyadenylated by polyA polymerase in a reaction immediately following *trans*-splicing (reviewed in ⁴⁰). Significant effort was invested to map the splicing sites in trypanosome genome revealing over one thousand novel sites often active in dependence on the life cycle stage ⁴⁵. Due to a missing regulation by transcription factors, it is presumed

Introduction

that trypanosome evolved trans-splicing as a tool to influence mRNA stability, thus adding a missing level of gene expression regulation ⁴⁶.

The second mechanism found exclusively in trypanosome allows the parasite to effectively evade detection while living in the host's bloodstream. The expression of VSG on the cellular surface creates a dense coat eventually recognized by immune cells ⁴⁷. Once it is recognized, the original type of VSG is rapidly replaced by another to avoid the host's immune system. Genes encoding VSG molecules are found on separate circular mini-chromosomes (30 – 150 kb), which are transcriptionally silent. The switching event itself is performed by duplicative recombination of VSG from mini-chromosome into an active VSG expression site on a large chromosome ⁴⁸. VSGs are transcribed by RNA polymerase I at localized clusters called transcription factories in the extranucleolar body, which is a structure specific to BF ⁴⁹. Such a system allows the parasite to retain access to a considerable repertoire of VSG gene variants. The surface coat can be replaced in a matter of minutes through the clathrin-mediated endocytosis that occurs exclusively in flagellar pocket ^{50,51}.

The third peculiar trait of trypanosome is a sequestration of the glycolytic pathway into peroxisome-like organelles, glycosomes ⁵². In BF parasites, the first seven of the ten glycolytic enzymes are localized to this organelle. ^{53,54}. The remaining three steps representing substrate level phosphorylation occur in the cytosol. Formed NADH+H⁺ is oxidized by DHAP/G3P shuttle to regenerate cytosolic NAD⁺ ⁵⁵. The compartmentalization of glycolysis is essential and it seems to facilitate regulation of energy metabolism through short periods of anaerobiosis ⁵³. Additionally, compartmentalization allows the maintenance of a redox balance and ATP/ADP balance in glycosome. As the BF relies on glucose and glycolysis to generate energy, any glucose that enters the glycosome is trapped after phosphorylation and is committed to glycolytic flux ^{56,57}. Moreover, glycosomes contain additional metabolic pathways such as pentose-phosphate pathway, purine salvage pathway, β -oxidation of fatty acids, and pyrimidine

biosynthesis. Importantly, glycolysis is the only source of ATP for BF cells making some of the glycolytic enzymes very promising drug target⁵⁸.

Glycosomes are not the only unconventional attribute of trypanosome energy metabolism. In the final part of this chapter, I will introduce the trypanosome single mitochondrion, the source of parasite's ability to adapt to various environments encountered during its life cycle.

1.5 ROLE OF MITOCHONDRION IN BOTH LIFE STAGES

Trypanosomes possess a single tubular mitochondrion spanning the length of the cell (Figure 4). The mitochondria of different life stages are morphologically and metabolically different⁵⁹.

PF parasites proliferate in the glucose-poor but the amino acid-rich environment of the tsetse fly midgut. To produce a sufficient quantity of ATP, the parasite relies on the substrate and oxidative phosphorylation pathways occurring in the mitochondrion^{60,61}. In addition to the canonical electron transport chain (ETC), PF mitochondrion contains an alternative pathway located in the inner mitochondrial membrane. The canonical

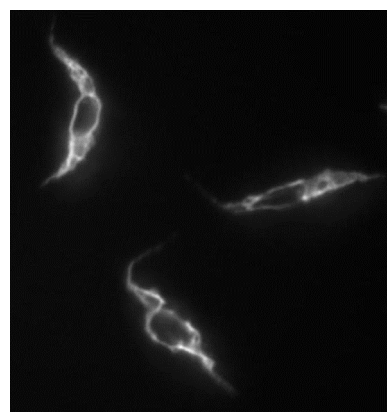


Figure 4: Fluorescent image of PF mitochondrion.

Trypanosome is immuno-labeled with primary antibody against mt-specific marker Hsp70. Primary antibody is recognized by secondary antibody conjugated to TexasRed.

ETC comprises four complexes; NADH:ubiquinone oxidoreductase (complex I), succinate:ubiquinone oxidoreductase (complex II), ubiquinol:cytochrome c oxidoreductase (complex III), and cytochrome c oxidase (complex IV), is complemented by an alternative oxidase (AOX)⁶² and alternative dehydrogenase Ndh2⁶³. Electrons from reducing equivalents, the NADH and FADH₂ are transferred from complex I and II by membrane submerged ubiquinol to complex

Introduction

III. In complex III, electrons are handed over to soluble cytochrome *c* shuttling them to complex IV that uses oxygen as a terminal acceptor of electrons, thus forming a molecule of water. During the process, electrochemical gradient is established by proton pumping activity of complexes I, III and IV. This gradient is utilized by membrane bound complex, F_0F_1 ATP synthase, to synthesize ATP from ADP and P_i ⁶¹.

In contrast to PF, the infective BF stage lives in glucose rich mammalian bloodstream. The complexity of mt energy metabolism of BF is reduced, as is the volume of imported proteins ⁶⁴. Electron transport chain complexes are either partially active (complex I), or not active at all (complex III and IV) ^{64,65}. The electron transport chain is reduced to the Gly-3-P/DHAP shuttle operated by mitochondrial glycerol 3-dehydrogenase, which is coupled to AOX via ubiquinone/ubiquinol pool. Importantly, this pathway does not produce ATP or generate membrane potential ⁶⁶. However, mitochondrion still harbors vital processes such as iron-sulfur clusters formation, Ca^{2+} homeostasis ⁶⁷, production of acetate ⁶⁸, and RNA editing ⁶⁹, consequently the proton gradient across the inner mt membrane remains essential. The gradient is maintained by the F_0F_1 ATPase complex that operates in reverse – hydrolyzing ATP to fuel the proton translocation to intermembrane space ^{64,70}. As a result, the F_0F_1 ATP synthase complex is crucial for the survival of all life cycle stages of trypanosome.

The investigation of individual ETC complexes and F_0F_1 ATP synthase is facilitated by specific inhibitors; complex I – rotenone ⁷¹, complex II – carboxin ⁷², complex III – Antimycin A ⁷³, complex IV – cyanide and azide ⁷¹, F_0 moiety – oligomycin ⁷⁴. The inhibitor of AAC, atractyloside, is able to completely abolish mt metabolism by blocking ADP translocation ⁷⁴. In trypanosome, the additional plant-like cyanide-insensitive alternative oxidase was found to be inhibited by salicylhydroxamic acid (SHAM) ⁶². In the infective BF trypanosome, ETC undergoes massive remodeling. The cell becomes less sensitive to cyanide and azide as it lacks all cytochromes, and barely reacts to rotenone ⁶⁵. However, the

sensitivity to oligomycin and atractyloside is retained and the inhibitors are widely employed in functional assays.

1.6 MITOCHONDRIAL GENE EXPRESSION

Trypanosome's single mitochondrion contains an independent genome as well as means for replication, transcription, and translation (Figure 5). Mt genome is organized into electron-dense structure termed kinetoplast (kDNA) – hence the name of the order Kinetoplastida. The kDNA is formed by a tightly organized net of circular DNA molecules of two types: maxicircles (20 – 40 kb), and minicircles (0.5 – 1 kb). Maxicircles encode rRNA (9S and 12S), subunits of mt respiratory complexes I (ND1, 3, 4, 5, 7, 8, 9), III (cyb), IV (coxI, II, III) and F₀F₁ ATPase (subunit A6), ribosomal protein S12 (RPS12), and several other proteins (cr2, cr3, murf 1, 2, 5) with so far undetermined functions ⁷⁵. Minicircles encode guide RNAs (gRNA), a short 35 bp RNA molecules serving as a guide for re-organization of 12 out of 18 maxicircles open reading frames by RNA editing ⁷⁶. The extent of uridine insertion/deletion is different for each gene, but the mechanism is similar as described below.

Editing of transcribed pre-mRNA molecule requires complex machinery of enzymes and co-factors catalyzing the sequence of reactions, which leads to mature edited mRNA. RNA editing substrate binding complex (RESC, also known as MRB1 complex) binds and stabilizes gRNA while RNA editing core complex (RECC) recruits pre-edited mRNA ⁷⁷. Contact of RESC and RECC is followed by mRNA cleavage, insertion or deletion of a precise number of uridines depending on information contained in the gRNA, and re-ligation of mRNA. In more detail, the initial requirement for editing of pre-edited transcripts is the presence of gRNAs transcribed from minicircles and processed by RET1 (RNA editing TUTase) ⁷⁸. The RESC contains TbRGG1/2 dimeric

Introduction

module capable of binding the gRNA and hetero-tetrameric gRNA binding module GRBC1/2 responsible for stabilization of gRNA. To form active RESC, additional two modules seem to be required: the RNA editing mediator complex (REMC) responsible for interaction with RECC, and the polyadenylation mediator complex (PAMC) ⁷⁹. RESC-bound gRNA is uridylated at 3' by RET1 and the gRNA hybridization to pre-edited mRNA initiates the editing process. Annealing of gRNA to pre-edited mRNA further induces the formation of short A-tail at the 3' of pre-edited mRNA, which appears to stabilize the molecule ⁸⁰. By improving mRNA stability during the editing, the A-tail serves to sequester pre-edited mRNA from the surplus transcripts otherwise directed for degradation, thus possibly serving as a means to regulate expression ⁸¹.

Initial binding of gRNA anchor region to pre-edited mRNA and cleavage of mRNA at the site of mismatch directly upstream of anchor region is catalyzed by RNase III-like enzyme. Downstream enzymatic activities are catalyzed by RECC (or 20S editosome) complex with 12 common and 2-3 alternating auxiliary factors recruited in specific steps of the process, thus forming three distinct editosomes ⁸². If the gRNA contains an extra site, the uridine(s) have to be inserted to edit mRNA and thus the insertion-specific factors bind to RECC: TUTase 2 (RET2), endonuclease KREN2, and zinc-finger protein KREPB7 ^{82,83}. Analogically, the deletion event requires core RECC augmented by endonuclease KREN1, U-specific exoribonuclease KREX1, and zinc-finger protein KREB8 ^{83,84}. Finally, CoII is processed by cis-editing which requires specific factors bound to RECC complex: endonuclease KREN3 and zinc-finger protein KREPB6 ^{76,82}.

Editing is performed sequentially from 3' to 5' end of mRNA. Once the first gRNA binding site is processed, the novel sequence reveals binding site for the next gRNA, and so forth, until the process runs out of gRNA binding sites. The edited transcripts at this stage contain complete information about amino acid sequence and are equipped with short poly-A tail on 3' end. However, it has been shown that mt translation machinery does not recognize "short-tailed" mRNA as

a substrate for translation. Instead, short-tailed fully edited molecules are further processed by polyadenylation/uridylation catalyzed by KPAP1 and RET1 with help of KPAF1/2 factors ⁷⁹. Only 'long-tailed' mRNA, which contains 200 – 300 nt long poly-A/U tail on its 3' end, is recognized by mitoribosome and translated ^{77,79}. Complete editing machinery is present and essential in both life cycle stages of trypanosome ⁸⁵. It is presumed that in contrast to high demand for mt encoded ETC subunits in PF, the BF can minimize editing to only two transcripts: A6 ⁶⁴ and RPS12 ⁸⁶, which are essential for this life cycle stage.

Introduction

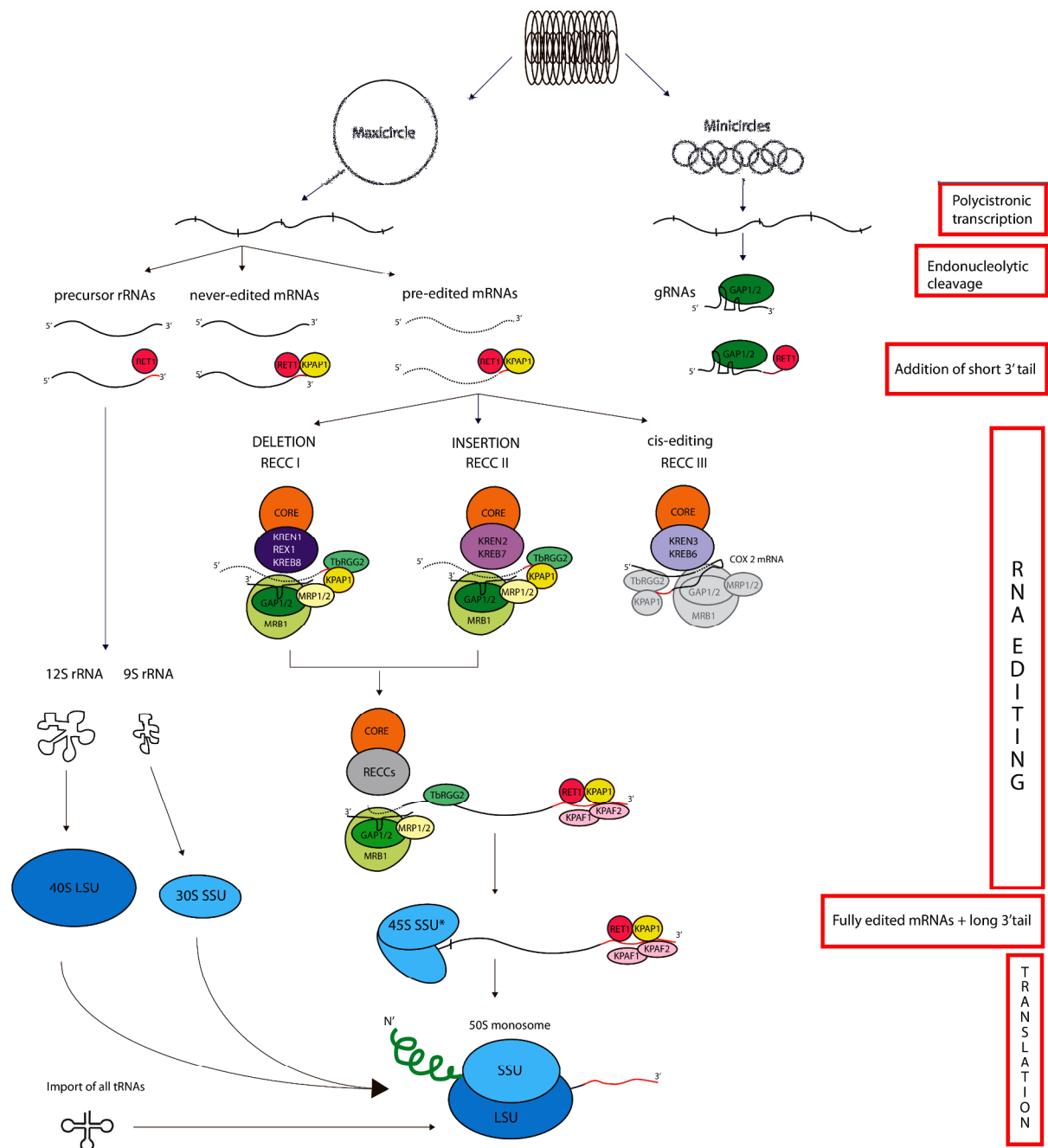


Figure 5: Mitochondrial gene expression and translation. Transfer of information from the kDNA (top) to the translation of mature mRNA (bottom) is depicted. Labels on the right mark major steps. The kDNA composed of maxicircles (left) encode rRNA and protein-coding genes, and minicircles (right), encode gRNA genes. RET1 – terminal uridylyl transferase 1; KPAP1 – Kinetoplastid poly(A) polymerase; GAP1/2 complex – gRNA binding and stabilizing complex; MRB1 – mt RNA binding complex 1; CORE – RECC (RNA editing core complex) isoforms I – III with variant modules for mRNA:gRNA duplex recognition depicted; MRP1/2 – mt RNA binding protein 1 and 2; KREN1 – kinetoplast RNA editing endonuclease 1; REX1 – RNA editing exonuclease 1; KREPB8 – kinetoplast RNA editing U1-like zinc finger protein B8;

KPAF1,2 – kinetoplast polyadenylation/uridylation factors; TbRGG2 – RNA RGG motif binding protein 2; 9S rRNA – small subunit ribosomal RNA; 12S rRNA large subunit ribosomal RNA; 40S LSU – large ribosomal subunit; 30S SSU – small ribosomal subunit; 45S SSU* - intermediate small ribosomal subunit; Adapted from ⁸⁷.

In contrast to its bacterial ancestor, eukaryotic mitoribosome is tailored to produce fewer proteins in a stoichiometric ratio suitable for respiratory complexes assembly. At the same time, they contribute to correct folding of highly hydrophobic subunits in exit tunnel and their co-translational incorporation to the inner mt membrane ^{88,89}.

The SSU of trypanosome mitoribosome contains 56 proteins associated with the single molecule of 9S rRNA (611 bp), whereas LSU contains 77 proteins and 12S rRNA (1150 bp) ^{90,91}. In contrast, human mt SSU contains 12S rRNA and 27 proteins, and the LSU is formed by 16S rRNA with 53 proteins bound. Overall the trypanosome mitoribosomes contain one of the shortest known rRNA and in turn are more protein rich, which results in more porous structure compared to its human counterpart ⁹². Trend leading to rRNA shortening and increase in the number of mitoribosome proteins is clear in higher eukaryotes. It is speculated that extra ribosomal proteins, of which only a few were functionally assigned to date, functionally substitute missing rRNA regions ⁹³, particularly in functional hotspots such as the exit tunnel (reviewed in ⁸⁹).

The translation mechanism in trypanosomes requires an intermediate SSU complex with kinetoplastid-specific ribosomal pentatricopeptide-containing proteins (KRIPPs). This complex was originally purified from *Leishmania tarentolae* and termed 45S SSU* ⁹⁴. It was shown that in trypanosome, this sub-complex 45S SSU* contains in addition to KRIPPs also Rhodanese-like protein (Rhod), and large coiled-coil domain protein (200 kDa) that are not part of fully assembled monosome ⁹⁵. Considering the role of penta-tricopeptide motif containing factor KPAF1 and 2, which form the core of adenylation/uridylation complex ⁷⁹, it is presumed that 45S SSU* could serve as a mRNA quality control

Introduction

hub to prevent translation of incompletely edited transcripts⁹⁵. Although it was conclusively shown that mt translation is the essential process in both life stages of trypanosome, the volume of translation can differ⁸⁵. The translation mechanism itself generally resembles the prokaryotic type with a few adaptations discussed further in this section.

With the exception of the SSU-associated ribosomal protein 12 (RPS12), which is encoded in kDNA^{96,97}, all ribosomal proteins, translation factors, and a full set of tRNAs are encoded in the nucleus, expressed in the cytoplasm and imported into mitochondrion^{98,99}. The cytosolic tRNAs are imported by active translocation at the expense of ATP. As the trypanosome mitochondrion requires specific initiator tRNA_i, the pool of cytosolic elongation tRNA^{Met} imported into the organelle has to be formylated on amino-group to form N-formylmethionine (fMet)¹⁰⁰. Additionally, the cytosolic set of tRNAs imported into the organelle contains the tRNA^{Trp} with anticodon CCA, which is not able to decode the mitochondrial codon for tryptophan (UGA)^{101,102} and has to be altered by C to U editing of first anticodon position 34, which is performed by editing machinery, and thiolated at position 33^{101,103}. Modified mt-tRNA^{Trp} is charged by Trp-specific aminoacyl-tRNA synthetase expressed in mt matrix¹⁰². As apparent from the list of cytosolic factors operating in trypanosome mitochondria, the originally bacterial translation mechanism had to adapt to utilize eukaryotic tools for translation of mt proteins. This trend is clear in case of trypanosome mt methionyl-tRNA formyltransferase modifying also cytosolic elongator tRNA^{Met} in contrast to its mammalian or yeast homologs that process only mt specific initiator tRNA¹⁰⁴.

1.6.1 Mitochondrial translation – initiation

Translation initiation phase¹⁰⁵ commences with the binding of initiation complex to the translation initiation site on mRNA. In bacteria, initiation complex is formed by SSU attached to factors IF3 and IF1, and IF2 carrying charged

initiator tRNA^{fMet}. This complex binds to a conserved Shine-Dalgarno sequence and the release of IF3 serves as a signal for LSU to assemble into a full monosome. In mammalian mitochondrion, the IF1 homolog is completely missing but it was shown that IF2_{mt} can compensate for the absence of IF1 as it contains a 37-residue insertion¹⁰⁶. The current model assigns the function of IF2_{mt} in directing recognition of start codon by tRNA^{fMet} and IF3_{mt} prevents association of SSU and LSU. As eukaryotic mt mRNA does not contain Shine-Dalgarno sequence and has only several nucleotides preceding the start codon, it is presumed that ribosomal binding site is not structurally demarcated but rather that the initiation complex simply scans for first start codon from the 5' end^{107,108}. Correct positioning of initiation complex is ensured by IF2_{mt}, and once the position is found, the IF3_{mt} is released and binding of LSU initiates GTP hydrolysis followed by the release of IF2_{mt}. In yeast, mt mRNAs contain long 5' UTRs targeted by translation activators showing partial transcript specificity and serving as molecular ruler for determining the position of ribosome binding^{109,110}. There is no universal mechanism for eukaryotic mt translation initiation. Instead, the pathway seems to demonstrate species specific traits.

Trypanosome contains also two mt initiation factors, TbIF2 and TbIF3. The initiator tRNA^{fMet} positioned in ribosome SSU P-site scans 5' end of mRNA for start codon. In kDNA, canonical AUG start codon is supplemented by UUA, UUG and CUG¹⁰³. Once the start codon is found and base paired to tRNA^{fMet} in ribosomal P-site, the complex of mRNA with TbIF2-tRNA^{fMet} is recognized by LSU leading to the monosome assembly and the elongation phase starts¹¹¹. The detailed mechanism of translation initiation in trypanosome mitochondrion is yet to be investigated.

1.6.2 Mitochondrial translation – elongation

Mt-specific elongation factors Tu (EF-Tu), Ts (EF-Ts), and G (EF-G) in trypanosome are functionally orthologous to bacterial factors¹¹². In bacteria, the

Introduction

small EF-Tu shuttles amino acids to the ribosome by forming a complex with GTP and amino-acylated tRNAs, EF-Ts functions as a GDP recycling factor for EF-Tu, and EF-G1 plays a role in translocation step. Elongation is a repetitive process alternating three steps. Initially, the ribosomal A-site display codon which gets recognized by matching aminoacyl-tRNA::EF-Tu complex and aminoacyl-tRNA is locked in place by interaction with acceptor stem of LSU. A peptide bond is formed with the amino acid brought by previous/initiator aminoacyl-tRNA. During coordinated movement catalyzed by the EF-G1 factor, peptidyl-tRNA is shifted to P-site, still connected to a newly nascent peptide, which is protruding through the exit channel. Finally, when the next aminoacyl-tRNA::EF-Tu complex arrives in A-site new peptide bond is formed and the ribosome movement translocates empty tRNA to E-site for recycling by aminoacyl-tRNA transferases ¹¹³. In mammals, EF-Tu_{mt} and EF-Ts_{mt} are assembled to a heterodimer presumably for efficiency reasons ¹¹⁴ and EF-G2_{mt} serves as a sole recycling factor ¹¹⁵. In contrast to a mammal, budding yeast completely lack the regeneration factor EF-Ts. Instead, the EF-Tu is capable of GDP regeneration, presumably due to a single point mutation in its C-terminal domain ¹¹⁶. In trypanosome, elongation mechanism seems to generally follow convention except in contrast to bacteria, it has two EF-G factors: TbEF-G1 and G2. TbEF-G1 playing role during elongation mitoribosome movements and TbEF-G2 catalyze ribosome recycling ¹¹².

1.6.3 Mitochondrial translation – termination and mitoribosome recycling

There are two class 1 release factors in bacteria, RF1 and RF2, and a class 2 release factor RF3 acting as a GDP recycling factor for both RF1 and RF2. Both RF1 and RF2 are able to recognize UAA stop codon but differ in specificity towards the second and third position in the codon. Consequently, RF1 is specific for UAG, and RF2 releases UGA stop codon ^{117,118}. An ortholog to bacterial RF2 is

generally missing in eukaryotic mitochondria, except for several plants and fungi taxons ¹¹⁹. In mammalian mitochondrion, single class 1 release factor Mrf1 recognizes both available stop codons, UAA or UAG ^{87,120}. When the stop codon is locked to the A-site, TbMrf1 binds to the codon and catalyzes a hydrolysis of the bond between tRNA in P-site and the final incorporated amino acid ¹²¹. An orthologue of bacterial RF3 playing a role in ribosome recycling was not identified in human mitochondrion. Instead, RRF1_{mt} together with EF-G2_{mt} serve as a mitoribosome recycling factors. Additionally, IF3_{mt} was shown to be recruited to prevent premature re-association of ribosomal subunits during the recycling process ¹²².

Trypanosome orthologue of release factor 1 TbMrf1 was shown to be essential for the survival of insect stage of trypanosome. Upon downregulation of TbMrf1 expression with RNAi, the growth arrest was observed the seventh day after induction. Additionally, cells exhibit impairment of oxidative phosphorylation and decreased levels of mt-produced proteins ^{85,112,123}. It was naturally expected, that loss of TbMrf1 in infective bloodstream stage will have a similar effect. However, no data were available for BF to support this assumption.

As a component of adaptation to life in mammalian bloodstream, the mt translation in BF is limited to produce only two proteins (A6 and RPS12). This relatively reduced, yet functional, mitochondrion presents an advantageous environment for the investigation of mechanisms underlying mt translation.

2. AIMS AND COURSE OF RESEARCH

During my doctoral studies, I worked simultaneously on disparate projects. The first project described in Part I is a continuation of my diploma work focused on the functional characterization of mt methyltransferase (MTase) in *T. brucei* cell. I have extended my studies to a cellular target of this enzyme, the mt release factor 1, TbMrf 1, and to the stop codon-independent release factor-like protein TbPth4. To functionally characterize these key players of mt translation termination I proposed to:

- generate and examine BF TbMTQ1 double knockout (dKO) cell line
- purify PTP-tagged mitochondrial TbMRF1 and cytosolic TbeMRF1 from wild-type and dKO cells to detect the presence and absence of methylation at the GGQ motif
- generate and examine BF TbMrf1 double knockout cell line
- investigate a role of stop codon-independent release factor-like protein TbPth4 in the wild-type and TbMrf1 dKO cells

A major part of this work is presented as a research paper with additional unpublished data added after manuscript. In Part II, I present a project aimed to establish inducible protein expression system utilizing the destabilization domain (dd) dependent on the FK506 ligand to regulate expression of a dd-fused protein of interest in the mitochondrion of *Leishmania major*. As a representative target, we chose mitochondrial protein X (MIX) a subunit of cytochrome c oxidase complex and a virulence factor. I planned two different strategies; the first one is based on directly attaching the dd to a protein of interest. The second strategy is

based on expression regulation of T7 RNA polymerase by dd. In order to optimize the technique, I proposed to:

- generate *L. major* cell expressing cytosolic and mitochondrial green fluorescent protein (eGFP), which is tagged with dd and its expression regulated by FK506 ligand
- generate *L. major* cell line in which expression of dd-tagged T7 RNA polymerase will be regulated by presence or absence of FK506 ligand
- employ this optimized dd technique to study *L. major* virulence factor MIX

And finally, I participated in several other projects, to which I contributed significantly to development and optimization of the methodology (part III & IV).

PART I MITOCHONDRIAL RELEASE FACTORS IN BLOODSTREAM FORM TRYPANOSOME

I.1. INTRODUCTION

In this chapter, I will focus on termination factors that play a role in cytosolic as well as in mitochondrial translation. There are two release factors, eRF1 and eRF3, that serve as effectors in cytosolic translation termination in eukaryotes ¹²⁴. The eRF1 is a class 1 release factor, which recognizes all three stop codons (UAA, UGA, and UAG) displayed in ribosomal A-site, catalyzes the hydrolysis of the aminoacyl-tRNA bond. The structure of class 1 release factors resembles the tRNA's "L" shape in its three-domain architecture with domain 1 corresponding to the anticodon loop, domain 2 to an aminoacyl acceptor stem, and domain 3 to T-stem of tRNA ^{125,126}. The mammalian eRF1's domain 1 contains Asn-Ile-Lys-Ser (NIKS) motif responsible for stop codon recognition, domain 2 harbors universally conserved Gly-Gly-Gln (GGQ) motif performing aminoacyl-tRNA hydrolysis in ribosome peptidyl-transferase center (PTC), and domain 3 is responsible for binding to class 2 release factor eRF3 ¹²⁵. The eRF3 is a GTP-binding protein serving as a co-factor for recycling of eRF1 as well as for ribosomal recycling. Depletion or mutation of any cytosolic release factor results in higher stop codon read-through in a variety of human cell lines (reviewed in ¹²⁷) ¹²⁸. On the other hand, overexpression of eRF1 in human 293 cells improves the translation efficiency independently on the expression level of the eRF3, which argues against eRF3 essential role in translation ¹²⁹. In yeast, the genetic knockout of each gene encoding the eRF1 and eRF3 (*sup45* and *sup35*,

respectively) demonstrates lethal phenotype^{130,131}. A common feature of class 1 release factors ranging from bacteria to humans is a posttranslational methylation of the glutamine residue in the conserved GGQ motif^{123,132–134}.

Methylation is a frequent modification of DNA, RNA or proteins performed by the superfamily of methyltransferases [SCOP 53335] (MTases) that share the ability to utilize S-adenosylmethionine (AdoMet) as a source of a free methyl group. All MTases possess distinct conserved features in their primary protein sequence, the catalytic motif Asn-Pro-Pro-Tyr (NPPY) and AdoMet binding site conserved to a various degree. Except for these motives, the primary sequence or secondary structure is rarely conserved. The methylation of proteins does not change the charge of amino acid residues however, the addition of the methyl group increases the steric hindrance and removes hydrogens that might participate in the formation of hydrogen bonds, thus modulating molecular interactions of the target proteins, for example RNA binding¹²³. The N-methylation of aliphatic side chains (Lys, Arg, Glu, Asp) or carboxymethylation (O-methylesterification) of Gln or Asn occurs often as a posttranslational modification in histones¹³⁵. On the other hand, methylation of Gln side chain on N⁵ is a rare modification observed only in a handful of proteins, e.g. *E. coli* ribosomal protein L3^{136,137} and release factors. The methylated Gln residue interacts with the PTC of the large ribosomal subunit, triggering hydrolysis of the ester bond in peptidyl-tRNA. Based on molecular simulation models, the hydrolysis is performed either by coordinating water molecule for nucleophile attack or by creating a space for rRNA to perform the reaction¹³⁸. In bacteria, this modification is introduced by the activity of MTase HemK/PrmC encoded by the *prfB* gene, which is placed directly downstream of *prfA* (encoding for RF1). The modification is essential for a proper function of the bacterial release factors^{133,139,140}. Later it was shown that also the mammalian cytosolic release factor eRF1 is methylated on the GGQ motif by N6amt1 MTase. Deletion of its gene *N6amt1* causes embryonic lethality in knockout mice¹⁴¹. Similarly in yeast the essential

PART I

methylation of eRF1 is performed by MTase Mfq2 (product of gene *YDR140w*)¹³². The Mfq2^{-/-} cells demonstrate multiple phenotypic defects including increased sensitivity to cold, high salt concentration, and translation fidelity antibiotics geneticin and paromomycin¹²³.

In the mitochondrion, there is only a single class 1 release factor. The yeast and mammalian mRF1 are able to recognize both stop codons (UUA, UAG) present at the end of mt transcripts^{142,143}. The orthologues of cytosolic eRF3 have not been identified to date. Generally, mt RFs display low sequence similarity to cytosolic RFs with exception of highly conserved GGQ motif. This motif is, similarly to cytosolic factors, post-translationally modified by mt MTases: human mRF1 is methylated by HMPmC while the yeast Mrf1 is methylated by Mfq1. Interestingly, the modification was shown to be essential for normal proliferation of yeast cells only when grown in non-fermentable media¹²³ or human cell in presence of translation fidelity antibiotic streptomycin¹⁴⁴. The data suggest that methylation is required mainly during translation of proteins involved in oxidative phosphorylation¹⁴⁵.

An additional group of release factor-like proteins has been identified in the yeast (Pth4) and human (ICT1, C12orf65) mitochondrion. These proteins are homologous to the bacterial codon independent peptidyl-tRNA hydrolase (ArfB), suggesting that they might be able to release nascent peptide from the ribosome in codon independent manner and thus rescue the ribosomes stalled at the end of incomplete transcripts or in response to the secondary structure of mRNA¹⁴⁶⁻¹⁴⁹.

Trypanosome cytosolic and mt translation pathways follow the eukaryotic convention, although individual factors were only partially annotated in trypanosome genome at the time of this study, with information on termination factors being completely absent. Using BLAST search, we identified candidates for trypanosome orthologues to yeast and mammalian release factors; TbMrf1 – homolog of yeast mitochondrial Mrf1 release factor; TbPth4 – homolog of yeast Pth4p rescue factor; and TbeRF1 homolog of yeast cytosolic Sup45 release factor

^{123,150–152}. Research performed on TbMrf1 and TbPth4 is thoroughly described in the research paper included in the results section one. In the second results section, I share the unpublished data on TbeRF1 generated in parallel with the published research. To complement the story, I included third results section with research on trypanosome MTase TbMTQ1 originally revealed by *in silico* search for DNA MTases related to vaccinia virus VP39 cap 2'-O-methyltransferase/poly(A) polymerase ^{153,154}. As the TbMTQ1 bears a structural similarity to VP39, it was speculated that TbMTQ1 plays a role in a mRNA cap methylation in trypanosome ¹⁵⁵. Only during the research on my diploma thesis, the TbMTQ1 was assigned to N5-glutamine methyltransferases group modifying release factors on conserved GGQ motif ¹⁵⁶.

I.2. METHODS

In addition to methods described in Procházková et al. , we used the following methodology:

I.2.1 Preparation of constructs

To facilitate detection of TbeRF1 without specific antibody, one allele of *TbeRF1* gene was in situ tagged with C-terminal PTP tag in BF cells as described in ¹⁵⁷. Briefly, the pC-PTP Puro vector used for in-frame in situ tagging of TbeRF1 contains a tandem purification tag composed of protein C and two protein A open reading frames separated by TEV cleavage site. The C-terminal part (nt 844 – 1357 bp) of TbeRF1 ORF was amplified with specific primers (TbeRF1-PTP fw&rv) and inserted to pC-PTP with ApaI and NotI restriction sites. The sequenced construct was linearized with NruI restriction endonuclease with its site naturally present in the TbeRF1 fragment, and the final construct was transfected into BF 427 and dKO TbMTQ1 parental cell lines. After selection with

PART I

0.1 µg/ml puromycin, resulting stable cell lines were verified for constitutive expression of TbeRF1-PTP tagged protein (of expected size 70 kDa).

For the RNAi TbeRF1 cell line, we employed a head-to-head T7 promoter driven plasmid p2T7-TA Blue¹⁵⁸. A fragment spanning 485 bp of TbeRF1 ORF (primers TbeRF1-KD fw&rv) was inserted with BamHI and XhoI, the final construct was sequenced, linearized with NotI and transfected into parental BF SM cell line. Stable transfectants were selected with 5 µg/ml hygromycin and the decreased level of TbeRF1 transcript in induced cells was verified by qPCR (primers TbeRF1-qPCR fw&rv). The growth rate of induced and uninduced cells was recorded for nine days.

To construct the double knockout (dKO) TbMTQ1 cell line, we replaced the two endogenous *TbMTQ1* alleles (Tb927.10.9860) with neomycin and hygromycin resistance gene cassettes using pLEW13 and pLEW90 vectors, respectively¹⁵⁹. Specific 464 bp long 5' and 495 long 3' untranslated region (UTR) sequences of the *TbMTQ1* gene were derived from TritrypDB³³. Desired regions were amplified from BF 427 gDNA using PCR with specific oligonucleotides (5'UTR_fw&rv and 3'UTR_fw&rv). The neomycin-resistance cassette containing the gene for T7 polymerase was flanked sequentially with TbMTQ1 5' and 3' UTRs using endonucleases NotI and MluI, and XbaI and StuI, respectively. The resulting construct pLEW13_TbMTQ1_3'/5'UTRs_neomycin was digested with NotI and this single knockout (sKO) cassette was transfected to parental BF 427. The stably transfected cell line was created by limiting dilution after 2 weeks of selection with neomycin at 2.5 µg/ml. The genomic DNA was isolated from selected transfectants by phenol/chloroform extraction, and the successful replacement of *TbMTQ1* allele with the sKO cassette was verified by PCR with specific primers: 5'UTR_ext_fw and sKO_rv; sKO_fw and 3'UTR_ext_rv. The hygromycin-resistance cassette containing the TetR was excised from the pLEW90 vector with XhoI and StuI endonucleases. This cassette was then used to replace the neomycin-resistance cassette from

pLEW13_TbMTQ1_3'/5'UTRs_neomycin vector, using XhoI and SmaI restriction enzymes. The resulting construct pLEW13_TbMTQ1_3'/5'UTRs_hygromycin was digested with NotI and the dKO cassette was transfected to the verified TbMTQ1 sKO cell line. The selection was performed using 25 µg/ml of hygromycin. To verify successful replacement of the second TbMTQ1 allele, the gDNA was isolated from stably transfected cell line termed dKO TbMTQ1 and used for PCR reaction with two pairs of specific primers (5'UTR_ext_fw and dKO_rv; dKO_fw and 3'UTR_ext_rv). The loss of the TbMTQ1 open reading frame was confirmed by ORF-specific primers (TbMTQ1_fw and rv). All sequences of used oligonucleotides are summarized in Supplementary table 1.

1.2.2 Native electrophoresis

High resolution clear native electrophoresis was used to test the structural integrity of F₀F₁ ATPase in mt lysates which were prepared by treatment with digitonin at the concentration ratio of 4 mg of digitonin per 1 mg of protein. The 10 µg of mt protein was loaded on the 3 – 12% gradient Tricine PAGE gel, separated for three hours at 100V with anode buffer (125 mM imidazole, pH 7.0) and cathode buffer (250 mM Tricine, 37.5 mM imidazole, pH 7.0, 0.02% dodecylmaltoside, 0.05% deoxycholine). Separated proteins were transferred on the nitrocellulose membrane and signals corresponding to F₀F₁ ATPase moieties and sub-complexes were detected with polyclonal anti-subunit β antibody (1:5000), polyclonal anti-ATPaseTb2 antibody (1:1000), and polyclonal antibody anti-p18 (1:1000).

1.2.3 Sucrose gradient with dot blot analysis

Changes in the quantity and stability of mt ribosomes were investigated using sucrose gradient sedimentation of whole cell lysates followed by dot blot analysis of 12S and 9S RNAs levels in individual gradient fractions, as described in ⁸⁶. Specifically, 1x10⁸ cells were freshly harvested and lysed with 1%

PART I

dodecylmaltoside in the presence of RNase inhibitor on ice. The lysate was cleared by centrifugation and loaded on 12 ml 5 – 30% sucrose gradient prepared with Gradient Makers Station (Biocomp). The material was sedimented for 16 hours at 36 000g in 4°C. Approximately 500 µl fractions were tapped using GMST (Biocomp) and immediately flash frozen in liquid nitrogen. Total RNA was isolated from individual fractions with TrizolLS (ThermoFisher Scientific) according to manufacturer's recommendation, and loaded onto the pre-wetted nitrocellulose membrane mounted into the Bio-Dot apparatus (Bio-Rad). Loaded RNA was crosslinked with UV, the membrane was washed with 2xSSC and pre-hybridized at 42°C for an hour in the hybridization solution. Gamma-ATP labeled oligo probe against 9S and 12S rRNA (Supplementary table) was added directly into the pre-hybridized membrane and further incubated for 16 hours. The membrane was washed twice with 5x SSC, and the phosphor-Imager screen was used to accumulate the radioactive signal for 24 hours. The screen was scanned on Typhoon scanner (GE Healthcare) and the quantification was performed with ImageQuant software.

1.2.4 Isolation of total RNA and Northern blot

Total RNA from 1×10^9 BF cells was extracted with acid guanidinium thiocyanate and phenol-chloroform solutions based on published protocol ¹⁶⁰. Briefly, harvested cells were resuspended in 400 µl of ice cold solution D (4 M guanidine isothiocyanate, 25 mM sodium citrate, pH 7.0; 0.5% sodium lauroyl sarcosine, 0.1 M mercaptoethanol) supplemented with 200 mM sodium acetate, subjected to phenol/chloroform extraction using Phase-lock tubes (5PRIME) and finally precipitated with isopropanol. Purified total RNA was separated by electrophoresis on either a 1.8 % agarose gel (A6 analysis) or a 5% acrylamide gel (RPS12 and Murf5 analysis). Resolved RNA was transferred to a BrighStar plus hybridization membrane (Ambion) and crosslinked with UV. PCR DNA probes complementary to the rare never-edited, pre-edited or edited transcripts (Murf5,

RPS12 and A6) were prepared with specific primer pairs (Table S1) that annealed to either gDNA or total cDNA templates. The reverse primers were 5' labeled with [γ - 32 P] ATP using T4 Polynucleotide kinase (Ambion) as outlined in the manufacturer's protocol. The more abundant transcripts (18S, 12S and 9S rRNAs) were probed with a transcript-specific oligo that was also 5' end-labeled with [γ - 32 P] ATP. In accordance with the manufacturer's guidelines, the membranes were first pre-hybridized for 1 hour at 42° C with either the ULTRAhyb Ultrasensitive hybridization buffer (PCR based probes, ThermoScientific) or the ULTRAhyb Oligo hybridization buffer (oligo-based probes, ThermoScientific) before the specific probes were added and allowed to incubate overnight at 42° C. Next, the Northern blots were washed (2xSSPE, 0.1% SDS) three times at 42° C, exposed to a phosphor-imager screen for various periods of time specifically determined for each transcript (i.e. 5 min for 18S rRNA, 10 min for 9S and 12S, 3 days for RPS12 and 5 days for A6) and then scanned using a Typhoon FLA 7000 instrument (GE Healthcare). Scanning densitometry was performed using the ImageJ software and the determined values were normalized to an 18S rRNA loading control signal.

I.3. RESULTS & DISCUSSIONS

I.3.1 Cultured bloodstream *Trypanosoma brucei* adapt to life without TbMrf1 [Publication]

SCIENTIFIC REPORTS

OPEN

Cultured bloodstream *Trypanosoma brucei* adapt to life without mitochondrial translation release factor 1

Michaela Procházková^{1,2,3}, Brian Panicucci¹ & Alena Zíková^{1,2}

Trypanosoma brucei is an extracellular parasite that alternates between an insect vector (procyclic form) and the bloodstream of a mammalian host (bloodstream form). While it was previously reported that mitochondrial release factor 1 (TbMrf1) is essential in cultured procyclic form cells, we demonstrate here that *in vitro* bloodstream form cells can tolerate the elimination of TbMrf1. Therefore, we explored if this discrepancy is due to the unique bioenergetics of the parasite since procyclic form cells rely on oxidative phosphorylation; whereas bloodstream form cells utilize glycolysis for ATP production and F₀F₁-ATPase to maintain the essential mitochondrial membrane potential. The observed disruption of intact bloodstream form F₀F₁-ATPases serves as a proxy to indicate that the translation of its mitochondrially encoded subunit A6 is impaired without TbMrf1. While these null mutants have a decreased mitochondrial membrane potential, they have adapted by increasing their dependence on the electrogenic contributions of the ADP/ATP carrier to maintain the mitochondrial membrane potential above the minimum threshold required for *T. brucei* viability *in vitro*. However, this inefficient compensatory mechanism results in avirulent mutants in mice. Finally, the depletion of the codon-independent release factor TbPth4 in the TbMrf1 knockouts further exacerbates the characterized mitochondrial phenotypes.

Not only are *Trypanosoma brucei* medically and economically important parasites that cause disease in humans and livestock, but these flagellated protists are also an excellent model to address fundamental questions within eukaryotic cell biology¹. One of the most prominent areas of research over the last three decades has focused on the mitochondrial (mt) gene expression of this early divergent eukaryote. Its mt DNA is arranged in an immense network of concatenated large (maxi-) and small (mini-) circular DNA molecules that are condensed into a disc-like structure termed the kinetoplast². Transcription of the maxicircle DNA generates polycistronic precursors that are processed into two ribosomal RNAs and 18 mRNAs that encode subunits of the mitoribosome and the oxidative phosphorylation complexes. However, to generate functional open reading frames, 12 of these protein-encoding transcripts require further maturation by an RNA editing process that specifically directs the insertion or deletion of uridylyl nucleotides (nt)³ with the help of short guide RNAs transcribed from the minicircles^{4,5}. While much of the editing process has been elucidated, little is known about how the *T. brucei* mitoribosome selectively translates only correctly edited transcripts^{6,7}.

Although mitoribosomes are more closely related to bacterial ribosomes than their eukaryotic cytosolic counterparts, they nonetheless possess shorter mt ribosomal RNA (rRNA) and have acquired additional mitochondrial-specific proteins. The *T. brucei* mitoribosome represents an extreme example of this evolutionary divergence as it consists of 133 subunits, 56 of which do not have any recognizable homology to components of known mitoribosomes outside the Kinetoplastida group⁸. Furthermore, the 611 nt 9S rRNA of the mitoribosomal small subunit (SSU) and the 1149 nt 12S rRNA of the large subunit (LSU) are extremely short^{9,10}. The cryo-EM map of a kinetoplastid mitoribosome illustrates that proteins have replaced the loss of key functional rRNA helices¹¹. While the overall size and morphology is comparable to the bacterial ribosome, the structure on average

¹Institute of Parasitology, Biology Centre ASCR, Ceske Budejovice, Czech Republic. ²Faculty of Science, University of South Bohemia, Ceske Budejovice, Czech Republic. ³Present address: Central European Institute of Technology, Masaryk University, Brno, Czech Republic. Correspondence and requests for materials should be addressed to A.Z. (email: azikova@paru.cas.cz)

is more porous and the topology of the intersubunit space is remodeled. Furthermore, since the mRNA channel, the tRNA corridors and the nascent polypeptide exit tunnel are all predominantly lined with unique kinetoplastid proteins, it suggests that the specific translational mechanisms employed by the kinetoplastid mitoribosome will vary from the ribosomes examined in other model organisms¹¹.

Noticeably, the *T. brucei* mt DNA does not encode for any tRNAs; instead, the full complement must be imported from nuclear encoded genes^{12,13}. However, the mt genome does contain a cryptogene for a single ribosomal protein, a homolog of the highly conserved bacterial S12, designated RPS12¹⁴. The transcript is extensively edited throughout the open reading frame before it is translated. In the bacterial ribosome, S12 is incorporated into the shoulder of the SSU, near the subunit interface and extends into the decoding center of the SSU aminoacyl tRNA site (A site), where it binds 16S rRNA and plays a critical role in the fidelity of tRNA selection^{15–17}. In addition, through its interaction with elongation factors, it acts as a control element in the translocation of the mRNA-tRNA through the ribosome¹⁸. A similar indispensable role is assumed for the *T. brucei* RPS12 because the inactivation of RNA editing leads to the reduction of the 45S SSU-related complex and the 80S mRNA-bound monosome⁷. Furthermore, while only a few (cytochrome b, cytochrome oxidase subunit 1, F₀F₁-ATP synthase subunit A6) of the highly hydrophobic proteins translated from the maxicircle transcripts can be reliably detected in just procyclic form parasites^{19,20}, the disruption of RNA editing severely impairs mitochondrial translation. Therefore, it is proposed that RPS12 acts as a functional link between RNA editing and translation in *T. brucei*⁷.

Remarkably, due to their complex mt gene expression, several hundreds of proteins are required to synthesize the only two mt encoded proteins (RPS12 and F₀F₁-ATPase subunit A6) deemed to be essential for the extracellular pathogen to reside in the bloodstream of its mammalian host^{7,21}. While the insect stage (procyclic form, PF) of the parasite depends on the oxidative phosphorylation pathway to generate sufficient quantities of cellular ATP, the bloodstream form (BF) exploits the high glucose content of its surroundings to synthesize ATP through glycolysis²². This bioenergetics adaptation to the varied nutrients available throughout its life cycle results in a dramatic remodeling of the singular mitochondrion. The tubular BF mitochondrion lacks a functional cytochrome-mediated respiratory chain and thus respire through the trypanosome alternative oxidase^{23,24}. Therefore, the F₀F₁-ATP synthase reverses direction and hydrolyzes ATP to pump protons into the mt inner membrane space, maintaining the essential mt membrane potential ($\Delta\psi_m$)²⁵. This rotary molecular machine is comprised of a catalytic F₁ moiety and the membrane embedded F₀ domain that contains the proton pore. Proton translocation occurs via interactions between the F₀ c-ring and the only mt encoded component of F₀F₁-ATPase, subunit A6. The A6 transcript of this maxicircle gene is pan-edited in both life cycle stages, but it is only in the reduced BF mitochondrion that a single point mutation in the γ subunit of the F₁ central stalk permits the parasite to become mt DNA independent²¹. Naturally occurring dyskinetoplastic (Dk) trypanosomes that lack a complete mt genome²⁶, have also obtained compensatory mutations that allow the parasite to escape their dependency on the proton pumping function of the F₀F₁-ATPase. While the hydrolytic function of this enzyme is still essential, there is a greater reliance on the ADP/ATP carrier (TbAAC)^{27,28} to not only provide ATP substrate, but to also maintain the $\Delta\psi_m$ through the electrogenic exchange of cytosolic ATP⁴⁻ for mt ADP^{3-21,29}.

Mt translation is a complex process that can be divided into four steps: initiation, elongation, termination and ribosome recycling. Here we focus on translation termination, which occurs when a mt release factor (RF), containing two decoding motifs (α -5 helix and PXT), determines that a mRNA stop codon occupies the ribosomal A site^{30,31}. Upon recognition, the conserved GGQ loop of the RF shifts into the LSU peptidyl-transferase center (PTC) and hydrolyzes the ester bond between the tRNA in the peptidyl tRNA site (P site) and the terminal amino acid of the nascent peptide, thus releasing the protein from the translational apparatus^{32,33}. Most mitochondrial translation systems have a reduced number of termination codons (UAA and UAG) that can be recognized by a single mt release factor (yeast – Mrf1)³⁴. The depletion of Mrf1 in *S. cerevisiae*, a petite-positive yeast, results in respiratory dysfunction and rapid mt genomic instability, indicating that Mrf1 is essential for mitochondrial translation³⁵. However, the depletion of this ortholog in either mammalian cells or *S. pombe*, a petite-negative yeast, only leads to a partial respiratory defect because mt protein synthesis is not completely eliminated³⁴. This outcome suggests that another member of the RF family can compensate for the loss of the Mrf1. Indeed, while the depletion of the peptidyl-tRNA hydrolase, Pth4 in *S. pombe*, does not result in any phenotype, its ablation significantly exacerbates the Δ mrf1 phenotype³⁶. Pth4 retains the highly conserved GGQ motif, but it is smaller than standard RFs because it lacks the codon recognition domains³⁷. Instead, it has an unstructured basic residue-rich tail at the C-terminus that is required for ribosomal binding. Unlike other members of the RF family that transiently interact with the ribosomal A site, Pth4 is an integral member of the LSU^{37,38}. Therefore, it has been proposed that Pth4 acts as a codon-independent, mitoribosome-dependent RF that can rescue stalled ribosomes.

Mt translation is required for BF *T. brucei* viability³⁹, but it presumably serves only to synthesize the essential F₀F₁-ATPase subunit A6. While TbMrf1 is indispensable in PF *T. brucei*⁴⁰, where translation of most of the mt genome is required to generate sufficient ATP via an active oxidative phosphorylation pathway, we determined that the BF parasites grown in culture are able to adapt to life without TbMrf1.

Results

Cultured BF *T. brucei* tolerate the loss of TbMrf1, displaying only a mild growth phenotype.

Due to the limitations of RNAi to wholly silence a gene product, we eliminated both alleles of TbMrf1 (Tb927.03.1070) by homologous recombination. The generation of a viable double knockout TbMrf1 (dKO TbMrf1) cell line indicates that this release factor is not essential for the reduced mitochondrion of BF *T. brucei*. Lacking a TbMrf1 antibody, we verified the null cells by PCR analysis, incorporating primers designed to bridge each of the integration sites of the selectable markers that replaced both alleles (Fig. 1a). The single knockout (sKO) TbMrf1 cell line contained amplicons of the expected size for the TbMrf1 coding sequence (cds), as well as the 5' and 3' integration sites for the T7 polymerase/neomycin cassette (Fig. 1b). Noticeably, the TbMrf1 cds

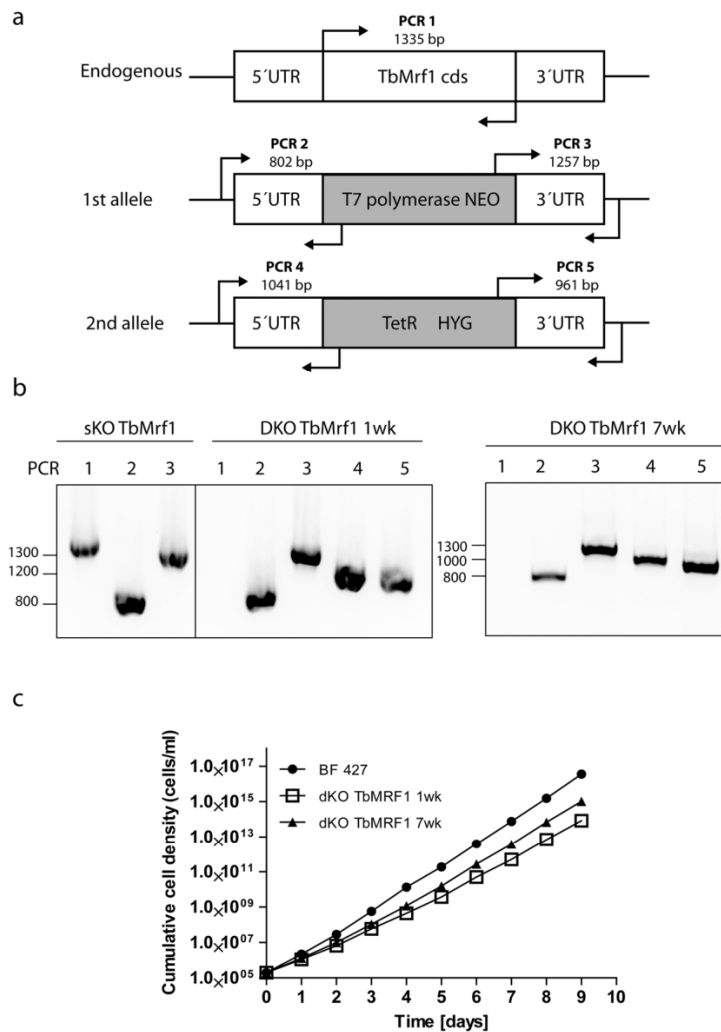


Figure 1. *T. brucei* BF dKO TbMrf1 parasites are viable in culture. **(a)** Schematic representation of the TbMrf1 gene knockout strategy based on homology recombination. To verify the correct integration of both allelic exchange cassettes by PCR, different primers sets were used to amplify PCR amplicons 1 to 5, with the expected sizes indicated. **(b)** PCR verification for the first TbMrf1 allelic replacement (sKO TbMrf1) and for the elimination of both TbMrf1 alleles in a dKO cell line grown in culture for one or seven weeks (dKO TbMrf1 1wk and 7wk). **(c)** Growth of dKO_TbMRf1 1wk and 7wk cell lines was monitored daily for nine days and compared to parental BF 427 cells. Cumulative cell density was plotted on a log scale.

Cell line	Doubling time [hours]
BF 427	5.5 ± 0.3
dKO TbMrf1 1wk	7.1 ± 0.7
dKO TbMrf1 7wk	6.4 ± 0.6

Table 1. Doubling time of *T. brucei* BF 427, dKO TbMrf1 1wk and 7wk cell lines. The values represent the average and SD of three independent experiments. The P value of an unpaired Student's t-test comparing the doubling time values for BF 427 and dKO TbMrf1 1wk, BF 427 and dKO TbMrf1 7wk and dKO TbMrf1 1wk and 7wk are as follows: $p < 0.001$, $p = 0.001$ and $p = 0.02$, respectively.

amplicon is not detected in the dKO cell line, while the replacement of both alleles was confirmed. Even though the dKO TbMrf1 cell line is certainly viable, it does have a reduced doubling time compared to the parental cell line (Fig. 1c, Table 1). Furthermore, we observed that dKO Mrf1 cells maintained in culture for 7 weeks had a modified rate of cell proliferation that reverted back towards the values of the wild-type (WT) BF 427 cells. Since

these parasites appeared better adjusted to life without TbMrf1, we included this dKO TbMrf1 7wk cell line throughout our phenotypic analyses so they could be compared with the dKO TbMrf1 1wk cell line, which were the first cells to arise during the selection of transfected cells.

The absence of TbMrf1 significantly alters the structural integrity of the protein complexes containing mt encoded subunits. While de novo mt synthesis of cytochrome b, cytochrome oxidase subunit 1 and F_0F_1 -ATP synthase subunit A6 can be observed in PF parasites, none of the highly hydrophobic mt encoded proteins have ever been detected in the BF mitochondrion²⁰. Therefore, to circumvent the dearth of direct assays to measure mt translation in the dKO TbMrf1 cell line, we opted to investigate the structural integrity of the mitoribosomes and F_0F_1 -ATPase. Both of these large molecular complexes contain just a single gene product (RPS12 and A6, respectively) that is synthesized from the mt genome after extensive post-transcriptional editing in BF parasites. To determine how the loss of TbMrf1 affects the mitoribosomes, equal numbers of cells from the parental and dKO TbMrf1 cultures were lysed with 1% Nonidet NP40 and fractionated on a 10–30% glycerol gradient. Total RNA isolated from equal volumes of each fraction was resolved on a 5% polyacrylamide/8 M urea gel and visualized with 9S and 12S rRNA probes (Fig. 2a). To verify that each glycerol gradient created on the Gradient Master from BioComp Instruments produced reproducible sedimentation profiles, the total RNA samples from each fraction were also analyzed with a cytosolic LSU 18S rRNA probe. To compare the amount of rRNA in each fraction between the various cell lines, 8 μ g of BF 427 total RNA was included for each northern blot. After normalization to this input, the relative intensity of 9S and 12S rRNA was plotted (Fig. 2b). The drastic decrease in both rRNA molecules throughout the gradient fractions of the dKO TbMrf1 1wk cell line indicates that the translational apparatus has been impaired, as both the LSU and SSU become unstable. Interestingly, it appears that the sedimentation profile has generally been restored in the dKO TbMrf1 7wk cell line, even though the recovery of the 9S rRNA trails that of the 12S rRNA.

The supramolecular organization of the F_0F_1 -ATPase can be visualized when hypotonically isolated mitochondria are lysed with n-dodecyl- β -D-maltoside (DDM), resolved by light blue native (BN) electrophoresis and then transferred to a PVDF blot that is probed with serum that recognizes components of either the F_0 or F_1 moieties. In the absence of subunit A6, the higher molecular weight structures of the intact F_0F_1 -ATPase are destabilized under the aforementioned conditions^{41,42}. Strikingly, the dKO TbMrf1 1wk F_0F_1 -ATPase monomers and oligomers are drastically reduced compared to the parental enzyme, whereas F_1 accumulates (Fig. 2c). In addition, there is a recovery of the ATPase monomers in the dKO TbMrf1 7wk cell line. To demonstrate equal loading between the different cell lines, the same DDM-lysed mitochondria were also resolved by SDS-PAGE and transferred to membranes that were immunodecorated with a mtHSP70 monoclonal antibody (Fig. 2d). Furthermore, the decreased steady state expression of specific F_0 subunits (Fig. 2d) in these denatured samples correlates with the loss of ATPase monomers and dimers visualized by BN westerns. On the other hand, components of the F_1 catalytic moiety and the TbAAC transporter responsible for supplying this enzyme with its ATP substrate remain unchanged.

Despite reduced ATPase monomers, dKO TbMrf1 cells still rely on the proton pumping activity of the remaining intact enzymes. While the stability of the F_0F_1 -ATPase monomers and oligomers is greatly reduced in the dKO TbMrf1 1wk culture, these structures are still detected. To determine if these DDM-resistant complexes contribute to cell viability, an Alamar Blue assay was performed to calculate the EC_{50} of oligomycin. This potent inhibitor binds at the interface of subunit c and A6, thereby blocking the proton translocation of intact F_0F_1 -ATPase⁴³. Even though BF 427 parasites are highly sensitive to oligomycin because they depend on the F_0F_1 -ATPase activity to pump protons that maintain the $\Delta\psi_m$, the dKO TbMrf1 1wk cells are several orders of magnitude more sensitive to this antibiotic (Fig. 3, Table 2). Once again, the dKO TbMrf1 7wk culture demonstrates an intermediate phenotype as the oligomycin EC_{50} increases towards the values measured in the parental cell line.

Destabilization of intact F_0F_1 -ATPase complexes only partially diminishes the $\Delta\psi_m$. In BF *T. brucei* mitochondria, the intact F_0F_1 -ATPase hydrolyzes ATP and pumps protons into the mt intermembrane space to maintain the essential $\Delta\psi_m$. Since the absence of TbMrf1 leads to the partial destabilization of F_0F_1 -ATPase monomers and dimers, the relative $\Delta\psi_m$ was determined by staining these cell lines with TMRE and measuring the fluorescence produced from the $\Delta\psi_m$ dependent probe. Compared to BF 427 cells, the $\Delta\psi_m$ was diminished ~35% in the dKO TbMrf1 1wk cells (Fig. 4a), which most likely contributed to the mild growth phenotype seen in these cells. Furthermore, the $\Delta\psi_m$ of the dKO TbMrf1 7wk cells returned to within ~15% of BF 427 values, which correlates with the increased stability observed in the F_0F_1 -ATPase monomers in these parasites (Fig. 2c).

While there were dramatically fewer intact F_0F_1 -ATPases to maintain the $\Delta\psi_m$ in the dKO TbMrf1 1wk cell line (Fig. 2c), the depolarization of the inner mt membrane was not as drastic as when a subunit of the catalytic F_1 moiety is depleted^{25,44}. Therefore, we hypothesized that the mt bioenergetics of dKO TbMrf1 1wk cells might more closely resemble Dk trypanosomes, where the dependence on the electrogenic exchange of cytosolic ATP^{4-} for mt ADP^{3-} by TbAAC becomes magnified. To assess this possibility, we employed an Alamar Blue assay to measure the EC_{50} of carboxyatractyloside (CATR), an inhibitor of AAC, in BF 427 cells, dyskinetoplastic *T. evansi* and the dKO TbMrf1 cell lines. While there is no significant change in the steady state levels of TbAAC expression when the parasite lacks TbMrf1 (Fig. 2d), the sensitivity to CATR is drastically increased in the dKO TbMrf1 1wk cells to almost the same levels observed in *T. evansi* (Fig. 4b, Table 2). Furthermore, the intermediate CATR EC_{50} values measured in the dKO TbMrf1 7wk cells correlates with the observed increased levels of intact F_0F_1 -ATPase monomers in these parasites.

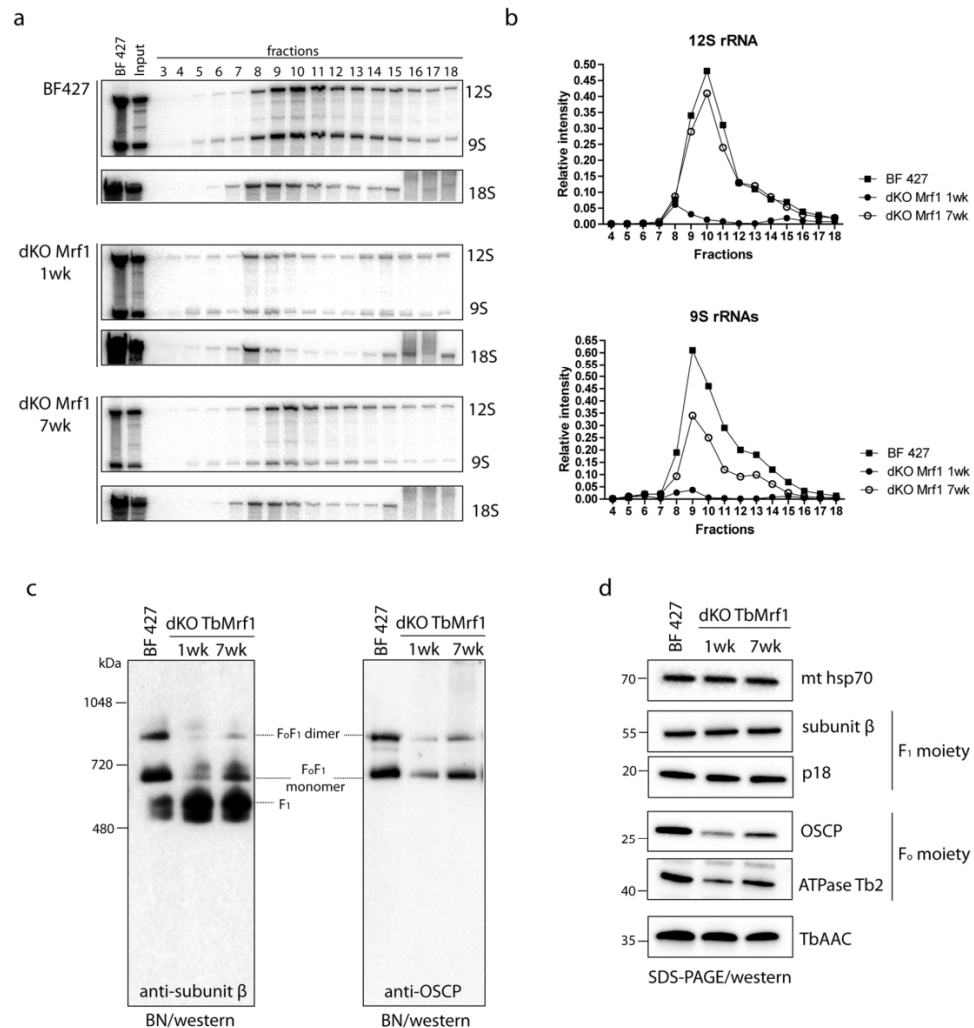


Figure 2. Loss of TbMrf1 affects the structural integrity of protein complexes that contain mt encoded subunits. **(a)** The sedimentation pattern of 12S and 9S rRNAs in BF 427 and dKO TbMrf1 1wk and 7wk cell lines. Whole cell lysates from 5×10^8 parasites were resolved on a 10–30% glycerol gradient. RNA was extracted from each fraction and separated on 5% polyacrylamide/8 M urea gels that were blotted and probed for 12S and 9S mitochondrial rRNAs and 18S cytosolic rRNA (sedimentation control). BF 427—8 μ g of total RNA from BF 427. Input—3 μ g of total RNA isolated from the remaining material that was loaded on a gradient. **(b)** After normalization to BF 427 RNA, the relative intensities of 9S and 12S rRNA signals from each sample were plotted. **(c)** The native F₁- and F_oF₁-ATPase complexes were visualized using light blue native electrophoresis. Purified mitochondria from BF 427 and dKO TbMrf1 1wk and 7wk cultures were lysed with dodecyl maltoside, fractionated on 3–12% BisTris gel and blotted on a PVDF membrane. The F₁-ATPase (F₁) and the F_oF₁-ATPase monomer and dimer were all visualized using specific polyclonal antibodies against F₁-ATPase subunit β and F_o-ATPase subunit OSCP. **(d)** SDS-PAGE Western blot analyses of the same mitochondrial lysates as in **(c)**. The steady state abundance of mt hsp70, TbAAC, F₁-ATPase subunits β and p18 and F_o-ATPase subunits OSCP and ATPaseTb2 were determined using specific antibodies.

Dk trypanosomes are able to lose their mt genomes because they contain compensatory mutations within specific F₁-ATPase subunits. However, when we sequenced the γ subunit from dKO TbMrf1 7wk culture, no mutations including the ones known for Dk cells²⁶ were observed (data not shown). Furthermore, the completed genome of the dyskinetoplastic *T. evansi* strain STIB805 revealed that there are only two notable amino acid substitutions in the α (G510C) and β (N395S) subunits⁴⁵, but neither one was detected in our sequencing data from the dKO TbMrf1 7wk cell line. In fact, unlike yeast Mrf1 mutants that display a rapid loss of mt DNA, the DAPI staining of fixed *T. brucei* lacking TbMrf1 did not result in cells without kinetoplast DNA (Supplementary Fig. S1). Furthermore, the dKO TbMrf1 cell lines are slightly more sensitive than BF 427 cells to acriflavin, a lethal DNA intercalator that predominantly accumulates in the mt DNA (Table 2). Finally, the calculated oligomycin

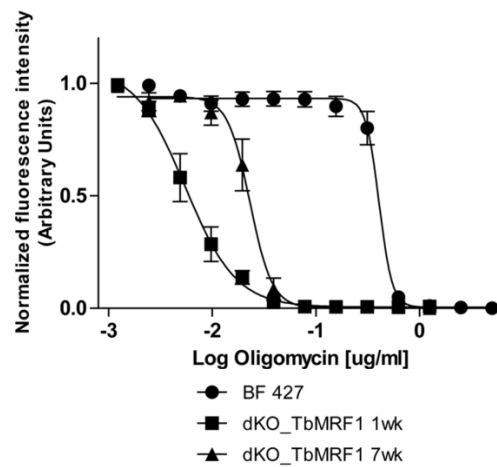


Figure 3. dKO TbMrf1 1wk and 7wk cell lines are significantly more sensitive to oligomycin than BF 427 cells. The oligomycin sensitivity of BF427, dKO TbMrf1 1wk and 7wk cells was determined by an Alamar Blue assay. The oligomycin dose-response curves were calculated using GraphPad Prism. Error bars represent the standard deviation calculated from three independent experimental replicates.

Cell line	Oligomycin [ug/ml]	Carboxyatractyl-loside [mM]	Acriflavin [nM]
BF 427	0.403 ± 0.03	>0.369	6.02 ± 0.52
dKO TbMrf1 1wk	0.006 ± 0.006	0.017 ± 0.02	2.68 ± 0.26
dKO TbMrf1 7wk	0.022 ± 0.005	0.076 ± 0.02	3.55 ± 0.17
cKO TbMrf1 7wk (+tet)	0.13 ± 0.05	0.125 ± 0.01	n.d.
<i>T. evansi</i> Antat 3/3	>2.657	0.009 ± 0.002	n.d.
dKO TbMrf1 7wk + V5 TbPth4 (- tet)	0.013 ± 0.03	0.027 ± 0.05	n.d.
dKO TbMrf1 7wk + V5 TbPth4 (+tet)	0.027 ± 0.01	0.06 ± 0.09	n.d.

Table 2. EC₅₀ values for oligomycin, carboxyatractyl-loside and acriflavin for BF 427, dKO TbMrf1 1wk and 7wk and dKO TbMrf1 + V5 TbPth4 cells that were either noninduced (-tet) or induced with tetracycline (+tet) for 2 days. n.d. – not determined. The values represent the average and SEM of three independent experimental replicates.

EC₅₀ value of the dyskinetoplastic *T. evansi* (Table 2) indicates that unlike the dKO TbMrf1 1wk cell line, these parasites are even less sensitive to oligomycin than BF 427. Altogether, this would suggest that the dKO TbMrf1 mutants are still dependent on their mt genome expression.

To confirm that the observed phenotypes measured were truly due to the loss of TbMrf1, we generated a conditional knockout (cKO) TbMrf1 7wk cell line with heterologous expression of a C-terminally V5-tagged TbMrf1 that was verified by western blot analysis with a V5 antibody (Supplementary Fig. S2a). This cell line demonstrated that despite the epitope tag, tetracycline induced ectopic TbMrf1 expression largely restored the oligomycin and carboxyatractyl-loside EC₅₀ values to BF 427 levels (Supplementary Fig. S2b, Table 2).

TbMrf1 deficient parasites are avirulent in the mouse model. While dKO TbMrf1 cell lines are able to cope with a significant loss of intact F₀F₁-ATPase complexes and remain viable when grown in culture, we questioned whether these parasites would be virulent when introduced into an animal model with an active immune system. Therefore, we infected 3 groups of 5 BALB/c mice with 1 × 10⁵ BF 427 or dKO TbMrf1 1wk or 7wk parasites. The survival rate was monitored and parasitemia levels were calculated from blood samples obtained via tail pricks. While none of the mice infected with BF 427 trypanosomes survived past day 6, neither set of mice infected with either dKO TbMrf1 cell line succumbed to disease after 30 days (Fig. 5a). This discrepancy was further illustrated in the parasitemia levels, where BF 427 cells were quickly able to reach lethal levels (>1 × 10⁸ trypanosomes/ml blood), while only very low levels of dKO TbMrf1 parasites were sporadically detected throughout the length of the experiment (Fig. 5b). Thus, while convenient, measuring the growth phenotypes of genetically modified trypanosomes in culture does not always depict the true importance of a protein function, especially in the case of gene products that can potentially disrupt bioenergetic processes of the cell.

Overexpression of release factor TbPth4 partially alleviates the dKO TbMrf1 phenotypes. The viability of the dKO TbMrf1 cell line in culture suggests the presence of another factor that is able to compensate for the loss of TbMrf1 and ensure some mt translation termination. In *S. pombe*, it has been demonstrated that the peptidyl-tRNA hydrolase Pth4 plays an overlapping role with Mrf1³⁶. A protein BLAST search on TriTrypDB

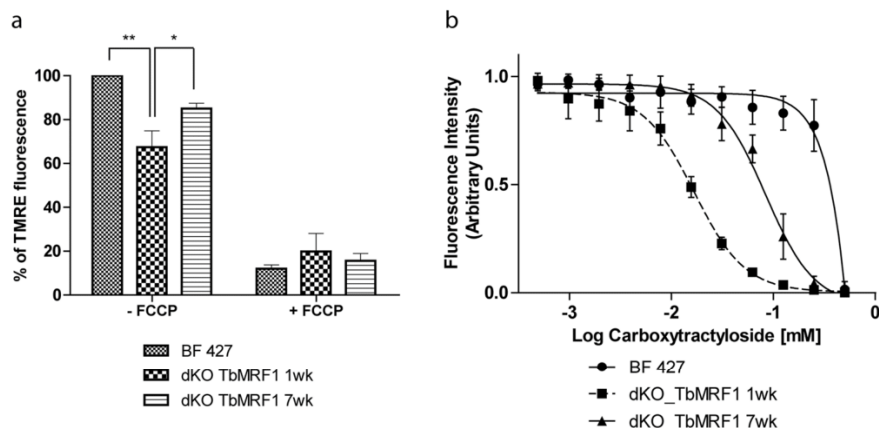


Figure 4. $\Delta\psi_m$ is only partially diminished in dKO TbMrf1 1wk and 7wk cells. (a) The $\Delta\psi_m$ of cells stained with TMRE was measured by flow cytometry. The median fluorescence for each sample is depicted on the y-axis of the column graph. The results are means \pm s.d. (n = 5). **p < 0.002, *p < 0.02, Student's t test. (b) Carboxyatractyloside sensitivity of BF 427 and dKO TbMrf1 1wk and 7wk cells was assessed using an Alamar Blue assay. The dose-response curves were calculated using GrapPad Prism. Error bars represent the standard deviation calculated from three independent experimental replicates.

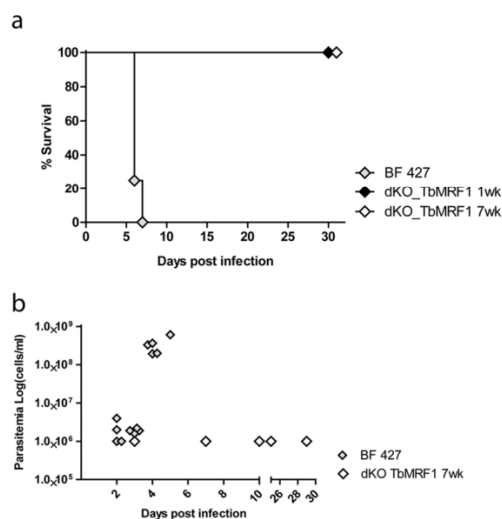


Figure 5. dKO TbMrf1 parasites are avirulent in a mouse model. (a) Groups of five female BALB/c mice were intraperitoneally infected with 1×10^5 BF 427 and dKO TbMrf1 1wk and 7wk trypanosomes. The survival rate of infected mice was monitored for 30 days. (b) Mouse parasitemia levels were calculated daily post-infection.

revealed that TbPth4 (Tb927.6.2500), which contains a release factor domain, is the most obvious *T. brucei* ortholog of the yeast protein as they share 36% similarity and 21% identity (MUSCLE alignment). To ascertain if the function of TbPth4 becomes more important when the mt translation apparatus becomes impaired, we monitored its gene expression in the dKO TbMrf1 cell lines. Since we lack an antibody that recognizes TbPth4, we employed qPCR to analyze the levels of mRNA in the dKO TbMrf1 cell lines compared to BF 427. Using β -tubulin as an internal control, a very modest increase of TbPth4 mRNA was observed in the absence of TbMrf1 (Fig. 6a). However, compared to the considerable Pth4 mRNA expression observed in the tetracycline induced dKO TbMrf1 cell line overexpressing a V5-tagged ectopic TbPth4, this slight uptick may not translate into any biological significance in the dKO TbMrf1 parasites.

Since the overexpression of the *S. pombe* Pth4 helps to alleviate the phenotypes induced by the loss of Mrf1³⁶, we explored if the same could be true in *T. brucei*. While the dKO TbMrf1 1wk cell line demonstrates the largest phenotypic changes compared to BF 427, we have demonstrated that the severity of these measured outcomes reduces over time as the cells are maintained in culture. Therefore, due to the length of time involved in selecting transfected *T. brucei* and verifying positive clonal cell lines, it was not feasible to generate the ectopic V5-tagged

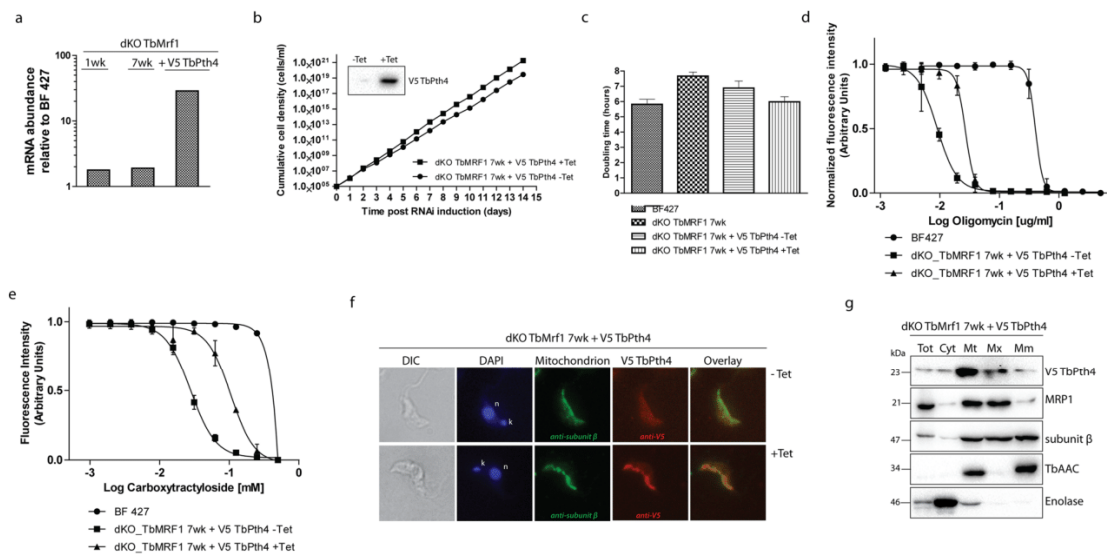


Figure 6. Overexpression of mitochondrially localized TbPth4 abates the dKO TbMrf1 phenotype. **(a)** RT-qPCR analysis of TbPth4 transcript levels in dKO TbMrf1 1wk, 7wk and dKO TbMrf1 + V5 TbPth4 cells compared to BF 427 trypanosomes. The relative changes in transcript abundance were plotted on a log scale. Transcript levels of β -tubulin were used as internal controls. **(b)** Growth curves spanning 14 days were generated for tetracycline induced (+tet) and noninduced (-tet) dKO TbMrf1 + V5 TbPth4 cells. The figure is representative of three independent experimental tetracycline inductions. Inset: Whole cell lysates from cultures either noninduced (-tet) or induced (+tet) with tetracycline for 48 hours were probed with a specific anti-V5 antibody. **(c)** Plot of doubling times calculated from the linear growth of BF 427, dKO TbMrf1 7wk and tetracycline induced (+tet) and noninduced (-tet) dKO TbMrf1 + V5 TbPth4 cells. **(d)** & **(e)** Alamar Blue assays determined either the oligomycin **(c)** or carboxyatractylamide **(d)** sensitivity of induced (+tet) and noninduced (-tet) dKO TbMrf1 + V5 TbPth4 cells compared to BF 427 cells. Error bars represent the standard deviations calculated from three independent experimental replicates. **(f)** Immunofluorescence assays verify that V5-tagged TbPth4 is targeted to the mitochondrion in BF dKO TbMrf1 + V5 TbPth4 cells induced for 48 hours (+Tet). The ectopic TbPth4 was visualized with a Texas Red-conjugated secondary antibody that recognizes a primary monoclonal anti-V5 antibody. Noninduced (-Tet) BF BF dKO TbMrf1 + V5 TbPth4 cells were included as a control, while the single tubular mitochondrion was visualized with a fluorescein isothiocyanate (FITC)-conjugated secondary antibody that recognizes a polyclonal primary antibody detecting F_1 -ATPase subunit β . The DNA contents were visualized using DAPI (4,6-diamidino-2-phenylindole). The overall cell morphology is depicted in the differential interference contrast (DIC) microscopy images. **(g)** Subcellular localization of TbPth4 was determined in dKO TbMrf1 cells expressing V5-tagged TbPth4. Harvested parasites (Tot) were lysed under hypotonic conditions to obtain cytosolic (Cyt) and mitochondrial (Mt) fractions. Mt pellets treated with Na_2CO_3 underwent differential centrifugation to produce matrix (Mx) and mt membrane (Mm) fractions. Purified fractions were analyzed by Western blot with the following antibodies: anti-V5 (V5-TbPth4), anti-MRP1 (mt matrix), subunit β (mt matrix and membranes), anti-AAC (mt membranes), anti-enolase (cytosol).

TbPth4 in the dKO TbMrf1 1wk cell line. However, when the V5-tagged TbPth4 is overexpressed in the dKO TbMrf1 7wk background, the doubling time continues to return towards WT values (Fig. 6b,c). We also determined from additional Alamar Blue assays that the increased sensitivity to oligomycin and carboxyatractylamide observed in the dKO TbMrf1 cell lines is reduced when the ectopic TbPth4 is induced (Fig. 6d,e, Table 2).

Since TbPth4 has not been characterized previously, we analyzed the subcellular localization of the release factor. An immunofluorescence assay determined that the dKO TbMrf1 + V5 TbPth4 is colocalized with the F_1 -ATPase subunit β in the mitochondrion (Fig. 6f). Furthermore, the tagged TbPth4 was tracked in a Western blot analysis of fractions generated from a carbonate extraction of enriched mitochondria isolated by hypotonic lysis of the parasite. The specificity of the resulting subcellular fractions was verified using enolase as a cytosolic marker; while MRP1, ATPase subunit β and TbAAC represented mt proteins with various propensities for either the mt inner membrane or the matrix. This analysis reveals that TbPth4 is largely localized in the mt matrix (Fig. 6g).

Depletion of TbPth4 exacerbates the phenotypes identified in BFT. brucei lacking TbMrf1. To determine if TbPth4 is involved in the rescue of an impaired mt translation system missing TbMrf1, we depleted this release factor in both BF 427 single marker (SM) and dKO TbMrf1 7wk cells using a stem loop RNAi vector. While there was a very modest increase in the doubling time observed in the RNAi induced BF 427 SM cells (Fig. 7a), there was a striking growth phenotype when TbPth4 is abated in the dKO TbMrf1 7wk cell line

(Fig. 7b). A qPCR analysis verified that the TbPth4 transcript is similarly reduced in both cell lines. Typical of the RNAi system in *T. brucei*, the dKO TbMrfl + RNAi TbPth4 culture escaped the RNAi regulation around day 10 of tetracycline induction.

We further characterized the dKO TbMrfl + RNAi TbPth4 cell line by once again observing what happens to the structural integrity of the mitoribosomes. Since the parental cell line is the dKO TbMrfl 7wk culture, the unduced RNAi cells display a fairly normal and broad sedimentation profile of the 9S and 12S rRNA on a glycerol gradient (Fig. 7c,d). By day 3 of the TbPth4 RNAi induction, the levels of both rRNAs are reduced, with a greater impact on the RPS12 associated 9S SSU peak. There are also two distinct rRNA peaks that presumably represent the individual SSU and LSU subcomplexes (45S) and the higher S-value (80S) monosome fraction associated with mRNA. However, after depleting TbPth4 for 5 days, the 80S rRNA peak is largely reduced and all that remains is a diminished broad peak centered around the lower 45S fractions. These results would suggest that the partially restored WT-like mitoribosome profile observed in the dKO TbMrfl 7wk cell line has been eliminated with the loss of TbPth4.

To understand how an impeded mt translation system could result in a cytostatic dKO TbMrfl + RNAi TbPth4 cell line, we observed the supramolecular organization of the F_0F_1 -ATPase by probing Western blots generated from light blue native gels with serum that recognize distinct ATPase moieties. Unlike the dKO TbMrfl 7wk cells that had recovered some of the F_0F_1 -ATPase monomers, the monomers and dimers of this proton pumping enzyme are virtually undetectable by day 3 and 5 of TbPth4 RNAi induction (Fig. 7e). This result is further exemplified by the steady-state Western analysis of these same DDM-lysed mitochondria resolved on SDS-PAGE, which demonstrate that the F_0 subunit OSCP that couples the catalytic activity of the F_1 region to the proton pumping activity is not visualized upon the induction of TbPth4 RNAi (Fig. 7f). With little to no intact F_0F_1 -ATPase with a functional proton pore that can directly contribute to the $\Delta\psi_m$, the measured relative $\Delta\psi_m$ of the induced dKO TbMrfl + RNAi TbPth4 cells drops to 50% of wildtype levels (Fig. 7g).

Discussion

Despite the severe growth phenotype previously observed in cultured PF *T. brucei* depleted of TbMrfl⁴⁰, we were able to generate *in vitro* BF parasites without this release factor. Confronted with an intriguing BF cell line that can tolerate the elimination of TbMrfl, but without any direct means of ascertaining how mt translation termination was affected, we chose to characterize mitochondrial phenotypes that could rationally be attributed to the loss of a release factor. In fact, it was indirect evidence that originally assigned the expected function of TbMrfl when it was shown that oxidative phosphorylation (OXPHOS) is disturbed upon TbMrfl RNAi induction⁴⁰. Unfortunately, even this assay is impractical when working with BF trypanosomes, so we decided to look at the integrity of two essential complexes in the BF mitochondrion that contain a solitary mt encoded subunit. Indeed, this is not unprecedented as the stability and composition of the mitoribosomes and F_0F_1 -ATPase has been extensively characterized when mt gene expression is impeded^{7,42}.

With this rationale, we interpreted the significant disruption of intact mitoribosomes and F_0F_1 -ATPases in the dKO TbMrfl 1wk cell line to indirectly indicate that mt translation has been impaired. The instability of the F_0F_1 -ATPase monomer and dimers is most likely due to the abated protein expression of the F_0 integral membrane subunit A6, which causes the complex to become more labile in the presence of detergent^{41,42,46}. However, since the dKO TbMrfl parasites are hypersensitive to oligomycin and thus still depend on the proton pumping function of the remaining intact F_0F_1 -ATPase enzymes, we believe that mt translation is not completely blocked. This analysis is further supported by the observations that the dKO TbMrfl cells retain some intact F_0F_1 -ATPases, do not lose their mt DNA, display increased sensitivity to acriflavin and do not possess any of the required γ mutations previously catalogued in dyskinetoplasmic trypanosomes²⁶.

The ability of the dKO TbMrfl 1wk cells to continue to synthesize some amount of subunit A6 in the absence of TbMrfl presumably allows the parasite to adapt its bioenergetics by relying more heavily on TbAAC to produce an electrogenic exchange of cytosolic ATP^{4-} for mt ADP^{3-} , which can compensate for the decrease in intact F_0F_1 -ATPase complexes containing a functioning proton pore. Indeed, it appears that there is a delicate equilibrium that is maintained between the amount of proton pumping F_0F_1 -ATPase enzymes and the activity levels of TbAAC to maintain the $\Delta\psi_m$, as evidenced by the increased levels of intact F_0F_1 -ATPase monomers in the dKO TbMrfl 7wk cells and the intermediate CATR EC_{50} values observed for these parasites.

This unique compensatory mechanism can occur in the BF trypanosoma mitochondrion because of the unusual dependence on the F_0F_1 -ATPase to continually hydrolyze ATP to maintain the essential $\Delta\psi_m$ required for mt protein import⁴⁷. However, this comes at a large energetic cost to the parasite. Therefore, it is pertinent to understand how much of a $\Delta\psi_m$ is needed to maintain sufficient protein and metabolite (e.g. pyruvate) import for key mt processes⁴⁸. By thoroughly characterizing these dKO TbMrfl cell lines, we propose that *in vitro* BF trypanosoma cell cultures can tolerate a substantial decrease in their $\Delta\psi_m$ as long as it remains above a minimal threshold, which we predict is between 50–65% of WT $\Delta\psi_m$ values. While this allows the parasite to survive in culture, it is no longer a viable option when the *T. brucei* dKO TbMrfl is introduced into an animal model, probably because the parasite has greater energetic requirements when it needs to evade the host's immune system⁴⁹. Under these conditions, even the dKO TbMrfl 7wk parasites, observed to possess 85% of the WT $\Delta\psi_m$ when grown *in vitro*, are unable to establish a lethal infection in a mouse.

Canonical translation termination occurs when Mrfl recognizes a stop codon in the A site and hydrolyzes the ester bond between the P site tRNA and the nascent polypeptide. However, ribosomes can become stalled when they encounter truncated mRNA or transcripts that contain nonstop mutations or rare codons⁵⁰. Pth4 is a yeast codon-independent release factor that is described as a versatile mitoribosome rescue factor that is involved in recycling these stalled ribosomes. The observed phenotypes in both the induced dKO TbMrfl + V5 Pth4 and dKO TbMrfl + RNAi TbPth4 cell lines provide tantalizing evidence that TbPth4 is able to recognize that the dKO

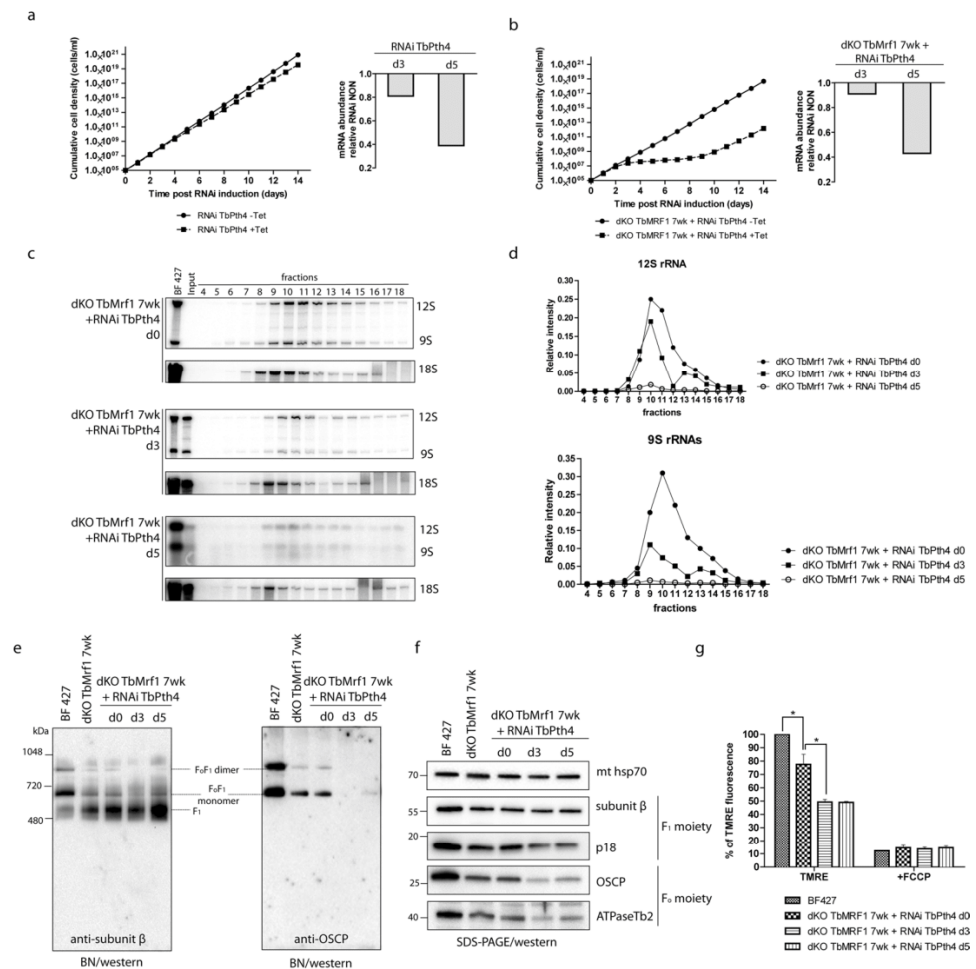


Figure 7. TbPth4 RNAi silencing in the dKO TbMrf1 background generates more severe phenotypes than the loss of TbMrf1 alone. **(a,b)** Growth curves of the noninduced (-tet) and induced (+tet) RNAi TbPth4 in either SM BF 427 **(a)** or dKO TbMrf1 cells **(b)** were measured for 14 days. Right panels: RT-qPCR analysis of the TbPth4 transcript levels after 3 (d3) or 5 (d5) days of tetracycline induction compared to noninduced RNAi cells. The relative changes in transcript abundance are plotted on a linear scale. β -tubulin transcript levels were used as internal controls. **(c)** The sedimentation profile of 12S and 9S rRNAs in dKO TbMrf1 + RNAi TbPth4 cells that were either never induced (d0) or induced with tetracycline for 3 (d3) or 5 (d5) days. BF427–8 μ g of total RNA from BF 427. Input – 3 μ g of total RNA isolated from the remaining material (if available) that was loaded on a gradient. **(d)** After normalization to a BF 427 RNA, the relative intensities of 9S and 12S rRNA signals from each sample were plotted. **(e)** The native F_1 - and F_0F_1 -ATPase complexes were visualized using light blue native electrophoresis. dKO TbMrf1 7wk and dKO TbMrf1 + RNAi TbPth4 cells were either never induced (d0) or induced with tetracycline for 3 (d3) or 5 (d5) days. The F_1 -ATPase (F_1) and the F_0F_1 -ATPase monomer and dimer were all visualized using specific polyclonal antibodies against either F_1 -ATPase subunit β or F_0 -ATPase subunit OSCP. **(f)** SDS-PAGE Western blot analyses of the same mitochondrial lysates as in **(e)**. The steady state abundance of mt hsp70, F_1 -ATPase subunits β and p18 and F_0 -ATPase subunits OSCP and ATPaseTb2 were determined using specific antibodies. **(g)** The $\Delta\psi_m$ of TMRE stained BF 427 and dKO TbMrf1 + RNAi TbPth4 cells that were either never induced (d0) or induced with tetracycline for 3 (d3) or 5 (d5) days was measured by flow cytometry. The median fluorescence for each sample is depicted on the y-axis of the column graph. The results are means \pm s.d. (n = 5). *p < 0.02, Student's t test.

TbMrf1 mitoribosome has become stalled at the UAG stop codon and is able to release the completed polypeptide to create a sufficient amount of RPS12 and subunit A6.

While Pth4 homologs are found throughout bacteria and eukaryotic mitochondria^{36,37,51}, it appears that they probably function via different molecular mechanisms. For example, it has been demonstrated that upon RNAi depletion of the Pth4 mammalian ortholog (ICT1), cell viability is greatly affected as well as the stability of mt encoded subunits of OXPHOS complexes, in particular cytochrome c oxidase³⁷. However, the deletion of Pth4 in

S. pombe caused no reduction in cell proliferation even when grown on media containing only non-fermentable carbon sources. Similarly, the silencing of TbPth4 in BF 427 *T. brucei* did not generate a significant growth effect.

It is currently unclear how this ribosome integrated release factor is able to gain access to the distant PTC and become catalytically active. The LSU bound ICT1 may be restricted to an architectural role, while soluble forms of the protein are able to bind the mitoribosomal A site and perform peptidyl-tRNA hydrolysis⁵⁰. While no free pool of the ICT1 has yet to be detected in the mammalian mt matrix, ectopic expression of TbPth4 in *T. brucei* is predominantly localized in the soluble mt fraction. This would suggest that the mechanism of TbPth4 will be more similar to yeast, which also has a fraction of the release factor that is unassociated with the mitoribosome. The overexpression of TbPth4 in the dKO TbMrf1 background likely increased the overall amount of the protein, most of which probably contributed to a pool of unbound release factor that was available to bind the empty A site of stalled mitoribosomes. However, this only produced mild decreases in the observed dKO TbMrf1 phenotypes, suggesting that this emergency release factor is not overly efficient at rescuing stalled ribosomes. This would perhaps explain why TbPth4 was not able to replace the loss of TbMrf1 in the procyclic stage of the parasite, where the bioenergetic needs of the active mitochondrion requires robust translation of nearly all 18 mt encoded transcripts. Additional studies are being pursued to determine the molecular mechanism in which TbPth4, a release factor without a codon recognition domain, is able to terminate translation at a stop codon.

Methods

Transgenic *T. brucei* cell cultures. The bloodstream form *T. brucei brucei* Lister 427 strain (information about the identity and genealogy of this strain is available at <http://tryps.rockefeller.edu>) and the dyskinetoplastic strain *T. b. evansi* Antat 3/3⁵² were cultured in HMI-9 media containing 10% FBS and incubated in a 37 °C incubator with 5% CO₂. The BF 427 single marker (SM) cell line, constitutively expressing the ectopic copy of T7 RNA polymerase and tetracycline repressor, was used for the tetracycline inducible expression of dsRNA and V5-tagged proteins⁵³. This expression system was induced by the addition of 1 µg/ml of tetracycline into the media. Cell densities were monitored using the Z2 Cell Counter (Beckman Coulter Inc.) and maintained in the mid-log phase (between 1 × 10⁵ to 1 × 10⁶ cells/ml). Growth curves depicting the cumulative cell number of the cultures were calculated from the measured cell densities that were adjusted by the dilution factor needed to seed the cultures at 1 × 10⁵ cells/ml each day.

The generation of a TbMrf1 double knockout (dKO) cell line involved replacing both alleles of the *TbMrf1* gene (Tb927.3.1070) with either a neomycin or hygromycin resistance gene cassette derived from the pLEW13 and pLEW90 vectors, respectively⁵³. To direct the homologous recombination to the *TbMrf1* alleles, these knockout (KO) cassettes were flanked by short sequences of the *TbMrf1* 5' (469 nt) and 3' (540nt) untranslated region (UTR) that were identified with TritypDB (version Tb927_3_V5.1). These UTR fragments were PCR amplified from BF 427 genomic DNA (gDNA) with either the 5'UTR_fw&rv or the 3'UTR_fw&rv primer pairs (Supplementary Table S1). The amplicons were then digested either with NotI and MluI endonucleases (5' UTR) or XbaI and StuI (3' UTR) before sequentially being ligated into the neomycin-resistance cassette containing the T7 polymerase gene. The final pLEW13_TbMrf1_3'/5'UTRs_neomycin construct was linearized with NotI and electroporated with human T cell nucleofactor solution (AMAXA) into BF 427 to generate a single knockout (sKO) cell line. To create near-clonal cell lines, the transfected cells were serially diluted after 16 hours of recovery and selected with 2.5 µg/ml neomycin. The gDNA from stable transgenic cell lines that arose after ~2 weeks of selection was isolated using the GenElute Mammalian Genomic DNA Miniprep Kits from Sigma. The correct integration of the sKO cassette into the *TbMrf1* allele was verified by PCR with the following primer pairs that bridge either the 5' or 3' integration sites: 5'UTR_ext_fw and sKO_rv; sKO_fw and 3'UTR_ext_rv (Fig. 1a,b, Supplementary Table S1).

The hygromycin-resistance cassette containing the tetracycline repressor was excised from the pLEW90 vector with XhoI and StuI endonucleases. This cassette was then used to replace the neomycin-resistance cassette from the pLEW13_TbMrf1_3'/5'UTRs_neomycin vector, which was digested with XhoI and SmaI restriction enzymes. The resulting construct pLEW13_TbMrf1_3'/5'UTRs_hygromycin was linearized with NotI and the dKO cassette was transfected into the verified TbMrf1_sKO cell line. Selection with 25 µg/ml of hygromycin resulted in stably transfected cell lines termed TbMrf1_dKO. To verify that both *TbMrf1* alleles had been replaced, isolated gDNA served as a PCR template to produce amplicons with primer pairs that bridge the 5' and 3' integration sites of both selectable markers (5'UTR_ext_fw and dKO_rv; dKO_fw and 3'UTR_ext_rv) (Fig. 1a,b, Supplementary Table S1). The elimination of the *TbMrf1* open reading frame (ORF) from the genome was confirmed by PCR using ORF-specific primers (TbMrf1_fw and rv).

A conditional knockout (cKO) cell line with heterologous expression of a C-terminal 3xV5-tagged TbMrf1 in the dKO TbMrf1 7wk background was also generated. The TbMrf1 ORF was amplified from gDNA with the primers TbMrf1 cKO_fw and TbMrf1 cKO_rv (Supplementary Table S1). The resulting amplicon was digested with BamHI and HindIII before being ligated into a similarly digested pT7-3V5-PAC vector containing the puromycin resistance gene (PAC)⁵⁴. The sequenced-verified construct was transfected into the dKO TbMrf1 7wk cell line and the transgenic trypanosomes were selected with 0.1 µg/ml of puromycin. These selected transgenic parasites were termed cKO TbMrf1 once it was verified by Western blot that tetracycline induced cells displayed the ectopic V5 TbMrf1 protein. This regulatable expression system is possible due to the previous TbMrf1 allelic replacements with the T7 polymerase and the tetracycline repressor.

In a similar manner, a dKO TbMrf1 + V5 TbPth4 (Tb927.6.2500) transgenic cell line was generated using the following forward (fw) and reverse (rv) primers: TbPth4V5_fw and TbPth4V5_rv (Supplementary Table S1).

To silence the expression of the *TbPth4* gene by double stranded RNA interference (RNAi), we employed a construct that inducibly expresses a stem loop RNA with T7 RNA polymerase. The original pRPhyg-iSL vector (courtesy of Sam Alford) was adapted to our needs by replacing the hygromycin resistance gene with the ble gene that provides resistance to phleomycin. A 501 nt fragment of *TbPth4* that includes a portion of the 5'UTR

and CDS (−55 nt to 446 nt) was amplified with a primer pair containing the restrictions sites SmaI and XhoI on the forward oligonucleotide, while the reverse contained BamHI and HindIII sites (TbPth4iSL_fw and rv). By digesting the same amplicon with either SmaI and BamHI or XhoI and HindIII, it could be sequentially ligated into the vector so that it was inserted twice in a head-to-head orientation, which would create a hairpin structure upon tetracycline-induced transcription. The transfection of the™ NotI-linearized pRPphleo_TbPth4-iSL construct into SM BF cells and the dKO TbMrf1 7wk cell line resulted in the RNAi TbPth4 and dKO TbMrf1 + RNAi TbPth4 cell lines, respectively. Both of these transgenic cell lines were actively selected using 2.5 µg/ml of phleomycin.

Subcellular fractionation followed by carbonate extraction. Na₂CO₃ extraction of mt membranes was adapted from a previously published protocols^{29,55}.

Briefly, mt vesicles from 5 × 10⁸ cells were isolated by hypotonic lysis. The mt pellet was further treated with digitonin (80 µg/ml) for 15 min on ice to disrupt the mt outer membrane. The material was then cleared by centrifugation (12,000 g, 20 min, 4 °C) and the pelleted mitoplasts were resuspended in 0.1 M Na₂CO₃ buffer (pH 11.5) and incubated for 30 min on ice. A final ultracentrifugation step (100,000 g, 4 °C for 1 hr, SW50Ti rotor) resulted in a supernatant comprised of proteins from the mt matrix, including stripped peripheral membrane proteins, and a pellet containing integral proteins isolated from the mt membrane fraction.

Glycerol gradient fractionation. Whole cell lysates were prepared by resuspending 5 × 10⁸ BF cells in 300 µl of lysis buffer (30 mM HEPES pH 7.3, 12 mM MgCl₂, 120 mM KCl, 1% Nonidet NP40, 1 mM DTT) supplemented with 2 × EDTA-free protease inhibitors (Roche) and RNaseOUT RNase inhibitor. Lysed cells were treated with TURBO DNase for 15 minutes on ice and pelleted (21,000 g for 15 min at 4 °C). In the meantime, linear 10–30% glycerol gradients were prepared in thin-wall tubes (Beckman) using a Gradient Station (BioComp) according to the manufacturer's protocol. The cleared supernatant (200 µl) was loaded onto the glycerol gradient and centrifuged (38,000 g for 4 hours at 4 °C) in a SW 41 Ti rotor (Beckman Coulter). The Gradient Station was then used to collect 500 µl fractions that were used to isolate total RNA using a standard phenol-chloroform extraction protocol.

Isolation of total RNA, reverse transcription, and qPCR. Quantitative reverse transcription PCR (RT-qPCR) was performed using a Light Cycler[®] 480 system (Roche) according to the manufacturer's recommendations. Briefly, total RNA from 1 × 10⁷ BF cells was extracted as described earlier and 10 µg were treated with TURBO DNase (Ambion). The excess DNase was then removed using an RNAeasy kit (Qiagen). Following the manufacturer's instructions, two micrograms of total RNA was reverse transcribed using the TaqMan Reverse Transcription kit (ABI). 100 ng of the resulting cDNA (2 µl) was mixed with SYBR Green (Applied Biosystems) and specific primers for either the TbPth4 transcript or the internal control transcripts that included 18S rDNA and β-tubulin (Supplementary Table S1). The samples were analyzed on a Light Cycler 480 (Roche) and the relative fold changes in the target amplicons were determined using the Pfaffl method, with the PCR efficiencies calculated by linear regression⁵⁶.

SDS-PAGE and Western blot analysis. Protein samples were separated by SDS-PAGE on a 12% Tri-Glycine acrylamide gel, blotted onto a PVDF membrane (BioRad) and probed with the appropriate monoclonal (mAb) or polyclonal (pAb) antibody. This was followed by incubation with a secondary HRP-conjugated anti-rabbit or anti-mouse antibody (1:2000, BioRad). Proteins were visualized using the Clarity ECL system (Bio-Rad) on a ChemiDoc instrument (BioRad). The Page Ruler pre-stained protein ladder (Thermo Scientific) was used to determine the size of detected bands. Primary antibodies used in this study included the mAb anti-V5 epitope tag (1:2000, Invitrogen), mAb anti-mtHsp70 (1:2000)⁵⁷, pAb anti-MRP1 (1:1000)⁵⁸, pAb anti-AAC (1:2000)⁵⁹, and pAb anti-enolase (1:1000)⁶⁰. Additionally, the following pAbs were produced in our laboratory: anti-APRT (1:500), anti-ATPaseTb2 (1:1000), anti-OSCP (1:500), anti-β subunit (1:2000) and anti-p18 (1:1000)²⁹.

Light blue native electrophoresis (BN PAGE). Hypotonically isolated crude mt vesicles from 5 × 10⁸ BF trypanosomes were resuspended in 1 M aminocaproic acid (ACA) and lysed with 2% dodecyl-maltoside for one hour on ice. The samples were pelleted at 16,000 g for 30 min and the protein concentrations were determined by a Bradford assay. Equal amounts of protein for each sample were mixed with loading dye (0.5 M ACA, 5% w/v comassie G-250) and loaded onto a 3%–12% BisTris native gradient acrylamide gel. Two different native running buffers were used, a cathode buffer (50 mM tricine, 15 mM BisTris, 0.002% of Coomassie Blue) and an anode buffer (50 mM BisTris), both at pH 7. After electrophoresis (3 hr, 100 V, 4 °C), the resolved mt proteins were transferred onto a nitrocellulose membrane (90 min, 90 V, 4 °C, stirring) and probed with specific pAbs against F₁F₀-ATPase subunits: β, OSCP, ATPaseTb2, and p18.

Mt membrane potential (Δψ_m) measurement. The Δψ_m was determined utilizing the red-fluorescent stain tetramethylrhodamine ethyl ester (TMRE, Invitrogen). Cells in the exponential growth phase were stained with 60 nM of the dye for 30 min at 37 °C. Each time, 1 × 10⁵ cells were pelleted (1,300 g, 10 min, room temperature), resuspended in 1 ml of PBS (pH 7.4) and immediately analyzed by flow cytometry (BD FACSCanto II Instrument). For each sample, 10,000 fluorescent events were collected. Treatment with the protonophore FCCP (20 µM) for 10 min was used as a control for mt membrane depolarization. Data were evaluated using BD FACSDiva (BD Company) software.

Drug sensitivity assay. Drug sensitivity assays using the resazurin sodium salt dye (Alamar Blue assay) were performed according to a published protocol⁶¹. Tested inhibitors dissolved in HMI-9 media (i.e. oligomycin

and carboxyatractyloside, SIGMA) were serially diluted 2 fold across each column of a 96-well plate. Individual wells were then seeded with either 5×10^3 BF 427 cells or 1×10^4 dKO TbMrfl1wk/7wk cells, resulting in a total volume of 200 μ l of HMI-9 media. The plates were incubated for 72 hours at 37 °C with 5% CO₂. Finally, 20 μ l of resazurin (0.125 mg/ml in 1xPBS, pH 7.4) was added to each well and the plate was further incubated for 8 hours. Fluorescence was measured on the Infinite M100 plate reader (Tecan) at excitation and emission wavelengths of 560 and 590 nm, respectively. Using GraphPad Prism 5.0, data were analyzed by non-linear regression with a variable slope.

Survival analysis in an animal model. Three groups of 5 female BALB/c mice were infected via a 200 μ l intraperitoneal injection of 1×10^5 BF 427, dKO TbMrfl1wk or 7wk trypanosomes. Parasitemia levels of individual animals were monitored daily for 7 days. Blood samples from a tail prick were diluted 100 times in TrypFix solution (1X SSC, 3.7% formaldehyde) and the number of parasites were quantified using an improved Neubauer haemocytometer. Mice displaying impaired health and/or a parasite load $>10^8$ cells/ml of blood were euthanized. Survival of the experimental group was visually monitored for up to 30 days. The data were analyzed with the built in survival analysis on GraphPad Prism 5.0.

All data generated or analyzed during this study are included in this published article (and its Supplementary Information file).

References

1. Matthews, K. R. 25 years of African trypanosome research: From description to molecular dissection and new drug discovery. *Mol Biochem Parasitol* **200**, 30–40, <https://doi.org/10.1016/j.molbiopara.2015.01.006> (2015).
2. Jensen, R. E. & Englund, P. T. Network news: the replication of kinetoplast DNA. *Annu Rev Microbiol* **66**, 473–491, <https://doi.org/10.1146/annurev-micro-092611-150057> (2012).
3. Read, L. K., Lukes, J. & Hashimi, H. Trypanosome RNA editing: the complexity of getting U in and taking U out. *Wiley interdisciplinary reviews. RNA* **7**, 33–51, <https://doi.org/10.1002/wrna.1313> (2016).
4. Blum, B., Bakalara, N. & Simpson, L. A model for RNA editing in kinetoplastid mitochondria: “guide” RNA molecules transcribed from maxicircle DNA provide the edited information. *Cell* **60**, 189–198 (1990).
5. Seiwert, S. D., Heidmann, S. & Stuart, K. Direct visualization of uridylyate deletion *in vitro* suggests a mechanism for kinetoplastid RNA editing. *Cell* **84**, 831–841 (1996).
6. Aphasizheva, I. *et al.* Ribosome-associated pentatricopeptide repeat proteins function as translational activators in mitochondria of trypanosomes. *Mol Microbiol* **99**, 1043–1058, <https://doi.org/10.1111/mmi.13287> (2016).
7. Aphasizheva, I., Maslov, D. A. & Aphasizhev, R. Kinetoplast DNA-encoded ribosomal protein S12: A possible functional link between mitochondrial RNA editing and translation in *Trypanosoma brucei*. *RNA Biol* **10**, 1679–1688, <https://doi.org/10.4161/rna.26733> (2013).
8. Zikova, A. *et al.* *Trypanosoma brucei* mitochondrial ribosomes: affinity purification and component identification by mass spectrometry. *Mol Cell Proteomics* **7**, 1286–1296, <https://doi.org/10.1074/mcp.M700490-MCP200> (2008).
9. de la Cruz, V. F., Lake, J. A., Simpson, A. M. & Simpson, L. A minimal ribosomal RNA: sequence and secondary structure of the 9S kinetoplast ribosomal RNA from *Leishmania tarentolae*. *Proc Natl Acad Sci USA* **82**, 1401–1405 (1985).
10. de la Cruz, V. F., Simpson, A. M., Lake, J. A. & Simpson, L. Primary sequence and partial secondary structure of the 12S kinetoplast (mitochondrial) ribosomal RNA from *Leishmania tarentolae*: conservation of peptidyl-transferase structural elements. *Nucleic Acids Res* **13**, 2337–2356 (1985).
11. Sharma, M. R., Booth, T. M., Simpson, L., Maslov, D. A. & Agrawal, R. K. Structure of a mitochondrial ribosome with minimal RNA. *Proc Natl Acad Sci USA* **106**, 9637–9642, <https://doi.org/10.1073/pnas.0901631106> (2009).
12. Hancock, K. & Hajduk, S. L. The mitochondrial tRNAs of *Trypanosoma brucei* are nuclear encoded. *J Biol Chem* **265**, 19208–19215 (1990).
13. Schneider, A. Mitochondrial tRNA import and its consequences for mitochondrial translation. *Annu Rev Biochem* **80**, 1033–1053, <https://doi.org/10.1146/annurev-biochem-060109-092838> (2011).
14. Maslov, D. A. *et al.* An intergenic G-rich region in *Leishmania tarentolae* kinetoplast maxicircle DNA is a pan-edited cryptogene encoding ribosomal protein S12. *Mol Cell Biol* **12**, 56–67 (1992).
15. Ogle, J. M. *et al.* Recognition of cognate transfer RNA by the 30S ribosomal subunit. *Science* **292**, 897–902, <https://doi.org/10.1126/science.1060612> (2001).
16. Ogle, J. M. & Ramakrishnan, V. Structural insights into translational fidelity. *Annu Rev Biochem* **74**, 129–177, <https://doi.org/10.1146/annurev-biochem.74.061903.155440> (2005).
17. Schmeing, T. M. *et al.* The crystal structure of the ribosome bound to EF-Tu and aminoacyl-tRNA. *Science* **326**, 688–694, <https://doi.org/10.1126/science.1179700> (2009).
18. Cukras, A. R., Southworth, D. R., Brunelle, J. L., Culver, G. M. & Green, R. Ribosomal proteins S12 and S13 function as control elements for translocation of the mRNA:tRNA complex. *Mol Cell* **12**, 321–328 (2003).
19. Horvath, A., Nebohacova, M., Lukes, J. & Maslov, D. A. Unusual polypeptide synthesis in the kinetoplast-mitochondria from *Leishmania tarentolae*. Identification of individual de novo translation products. *J Biol Chem* **277**, 7222–7230, <https://doi.org/10.1074/jbc.M109715200> (2002).
20. Skodova-Sverakova, I., Horvath, A. & Maslov, D. A. Identification of the mitochondrially encoded subunit 6 of FF ATPase in *Trypanosoma brucei*. *Mol Biochem Parasitol* **201**, 135–138, <https://doi.org/10.1016/j.molbiopara.2015.08.002> (2015).
21. Dean, S., Gould, M. K., Dewar, C. E. & Schnauffer, A. C. Single point mutations in ATP synthase compensate for mitochondrial genome loss in trypanosomes. *Proc Natl Acad Sci USA* **110**, 14741–14746, <https://doi.org/10.1073/pnas.1305404110> (2013).
22. Tielens, A. G. & van Hellemond, J. J. Surprising variety in energy metabolism within Trypanosomatidae. *Trends Parasitol* **25**, 482–490, <https://doi.org/10.1016/j.pt.2009.07.007> (2009).
23. Clarkson, A. B. Jr., Bienen, E. J., Pollakis, G. & Grady, R. W. Respiration of bloodstream forms of the parasite *Trypanosoma brucei* is dependent on a plant-like alternative oxidase. *J Biol Chem* **264**, 17770–17776 (1989).
24. Chaudhuri, M., Ajayi, W. & Hill, G. C. Biochemical and molecular properties of the *Trypanosoma brucei* alternative oxidase. *Mol Biochem Parasitol* **95**, 53–68, [https://doi.org/10.1016/S0166-6851\(98\)00091-7](https://doi.org/10.1016/S0166-6851(98)00091-7) (1998).
25. Schnauffer, A., Clark-Walker, G. D., Steinberg, A. G. & Stuart, K. The F1-ATP synthase complex in bloodstream stage trypanosomes has an unusual and essential function. *EMBO J* **24**, 4029–4040, <https://doi.org/10.1038/sj.emboj.7600862> (2005).
26. Lai, D. H., Hashimi, H., Lun, Z. R., Ayala, F. J. & Lukes, J. Adaptations of *Trypanosoma brucei* to gradual loss of kinetoplast DNA: *Trypanosoma equiperdum* and *Trypanosoma evansi* are petite mutants of *T. brucei*. *Proc Natl Acad Sci USA* **105**, 1999–2004, <https://doi.org/10.1073/pnas.0711799105> (2008).
27. Pena-Diaz, P. *et al.* Functional Characterisation of TbMCP5, a Conserved and Essential ADP/ATP Carrier Present in the Mitochondrion of the Human Pathogen *Trypanosoma brucei*. *J Biol Chem*. <https://doi.org/10.1074/jbc.M112.404699> (2012).

28. Gnipova, A. *et al.* The ADP/ATP carrier and its relationship to oxidative phosphorylation in ancestral protist trypanosoma brucei. *Eukaryot Cell* **14**, 297–310, <https://doi.org/10.1128/EC.00238-14> (2015).
29. Subrtova, K., Panicucci, B. & Zikova, A. ATPaseTb2, a unique membrane-bound FoF1-ATPase component, is essential in bloodstream and dyskinetoplastic trypanosomes. *PLoS Pathog* **11**, e1004660, <https://doi.org/10.1371/journal.ppat.1004660> (2015).
30. Ito, K., Uno, M. & Nakamura, Y. A tripeptide 'anticodon' deciphers stop codons in messenger RNA. *Nature* **403**, 680–684, <https://doi.org/10.1038/35001115> (2000).
31. Nakamura, Y., Ito, K. & Ehrenberg, M. Mimicry grasps reality in translation termination. *Cell* **101**, 349–352 (2000).
32. Frolova, L. Y., Merkulova, T. I. & Kisselev, L. L. Translation termination in eukaryotes: polypeptide release factor eRF1 is composed of functionally and structurally distinct domains. *RNA* **6**, 381–390 (2000).
33. Seit-Nebi, A., Frolova, L., Justesen, J. & Kisselev, L. Class-1 translation termination factors: invariant GGQ minidomain is essential for release activity and ribosome binding but not for stop codon recognition. *Nucleic Acids Res* **29**, 3982–3987 (2001).
34. Soleimanpour-Lichaei, H. R. *et al.* mTRF1a is a human mitochondrial translation release factor decoding the major termination codons UAA and UAG. *Mol Cell* **27**, 745–757, <https://doi.org/10.1016/j.molcel.2007.06.031> (2007).
35. Pel, H. J., Maat, C., Rep, M. & Grivell, L. A. The yeast nuclear gene MRF1 encodes a mitochondrial peptide chain release factor and cures several mitochondrial RNA splicing defects. *Nucleic Acids Res* **20**, 6339–6346 (1992).
36. Dujeancourt, L., Richter, R., Chrzanowska-Lightowler, Z. M., Bonnefoy, N. & Herbert, C. J. Interactions between peptidyl tRNA hydrolase homologs and the ribosomal release factor Mrf1 in *S. pombe* mitochondria. *Mitochondrion* **13**, 871–880, <https://doi.org/10.1016/j.mito.2013.07.115> (2013).
37. Richter, R. *et al.* A functional peptidyl-tRNA hydrolase, ICT1, has been recruited into the human mitochondrial ribosome. *EMBO J* **29**, 1116–1125, <https://doi.org/10.1038/emboj.2010.14> (2010).
38. Kehrein, K. *et al.* Organization of Mitochondrial Gene Expression in Two Distinct Ribosome-Containing Assemblies. *Cell reports*. <https://doi.org/10.1016/j.celrep.2015.01.012> (2015).
39. Cristodero, M., Seebeck, T. & Schneider, A. Mitochondrial translation is essential in bloodstream forms of *Trypanosoma brucei*. *Mol Microbiol* **78**, 757–769, <https://doi.org/10.1111/j.1365-2958.2010.07368.x> (2010).
40. Cristodero, M. *et al.* Mitochondrial translation factors of *Trypanosoma brucei*: elongation factor-Tu has a unique subdomain that is essential for its function. *Mol Microbiol* **90**, 744–755, <https://doi.org/10.1111/mmi.12397> (2013).
41. Wittig, I. *et al.* Assembly and oligomerization of human ATP synthase lacking mitochondrial subunits a and A6L. *Biochim Biophys Acta* **1797**, 1004–1011, <https://doi.org/10.1016/j.bbabi.2010.02.021> (2010).
42. Hashimi, H. *et al.* The assembly of F(1)F(O)-ATP synthase is disrupted upon interference of RNA editing in *Trypanosoma brucei*. *Int J Parasitol* **40**, 45–54, <https://doi.org/10.1016/j.ijpara.2009.07.005> (2010).
43. Symersky, J., Osowski, D., Walters, D. E. & Mueller, D. M. Oligomycin frames a common drug-binding site in the ATP synthase. *Proc Natl Acad Sci USA* **109**, 13961–13965, <https://doi.org/10.1073/pnas.1207912109> (2012).
44. Gahura, O. *et al.* The F1 -ATPase from *Trypanosoma brucei* is elaborated by three copies of an additional p18-subunit. *FEBS J*, <https://doi.org/10.1111/febs.14364> (2017).
45. Carnes, J. *et al.* Genome and Phylogenetic Analyses of *Trypanosoma evansi* Reveal Extensive Similarity to *T. brucei* and Multiple Independent Origins for Dyskinetoplasty. *PLoS Negl Trop Dis* **9**, e3404, <https://doi.org/10.1371/journal.pntd.0003404> (2015).
46. He, J. *et al.* Persistence of the mitochondrial permeability transition in the absence of subunit c of human ATP synthase. *Proc Natl Acad Sci USA*, <https://doi.org/10.1073/pnas.1702357114> (2017).
47. Martin, J., Mahlke, K. & Pfanner, N. Role of an energized inner membrane in mitochondrial protein import. Delta psi drives the movement of presequences. *J Biol Chem* **266**, 18051–18057 (1991).
48. Mazet, M. *et al.* Revisiting the central metabolism of the bloodstream forms of *Trypanosoma brucei*: production of acetate in the mitochondrion is essential for parasite viability. *PLoS Negl Trop Dis* **7**, e2587, <https://doi.org/10.1371/journal.pntd.0002587> (2013).
49. Engstler, M. *et al.* Hydrodynamic flow-mediated protein sorting on the cell surface of trypanosomes. *Cell* **131**, 505–515, <https://doi.org/10.1016/j.cell.2007.08.046> (2007).
50. Akabane, S., Ueda, T., Nierhaus, K. H. & Takeuchi, N. Ribosome rescue and translation termination at non-standard stop codons by ICT1 in mammalian mitochondria. *PLoS genetics* **10**, e1004616, <https://doi.org/10.1371/journal.pgen.1004616> (2014).
51. Handa, Y., Inaho, N. & Nameki, N. YaeJ is a novel ribosome-associated protein in *Escherichia coli* that can hydrolyze peptidyl-tRNA on stalled ribosomes. *Nucleic Acids Res* **39**, 1739–1748, <https://doi.org/10.1093/nar/gkq1097> (2011).
52. Borst, P., Fase-Fowler, F. & Gibson, W. C. Kinetoplast DNA of *Trypanosoma evansi*. *Mol Biochem Parasitol* **23**, 31–38 (1987).
53. Wirtz, E., Leal, S., Ochatt, C. & Cross, G. A. A tightly regulated inducible expression system for conditional gene knock-outs and dominant-negative genetics in *Trypanosoma brucei*. *Mol Biochem Parasitol* **99**, 89–101 (1999).
54. Flaspohler, J. A., Jensen, B. C., Saveria, T., Kifer, C. T. & Parsons, M. A novel protein kinase localized to lipid droplets is required for droplet biogenesis in trypanosomes. *Eukaryot Cell* **9**, 1702–1710, <https://doi.org/10.1128/EC.00106-10> (2010).
55. Acestor, N., Panigrahi, A. K., Ogata, Y., Anupama, A. & Stuart, K. D. Protein composition of *Trypanosoma brucei* mitochondrial membranes. *Proteomics* **9**, 5497–5508, <https://doi.org/10.1002/pmic.200900354> (2009).
56. Pfaffl, M. W. A new mathematical model for relative quantification in real-time RT-PCR. *Nucleic Acids Res* **29**, e45 (2001).
57. Panigrahi, A. K. *et al.* Mitochondrial complexes in *Trypanosoma brucei*: a novel complex and a unique oxidoreductase complex. *Mol Cell Proteomics* **7**, 534–545, <https://doi.org/10.1074/mcp.M700430-MCP200> (2008).
58. Vondruskova, E. *et al.* RNA interference analyses suggest a transcript-specific regulatory role for mitochondrial RNA-binding proteins MRP1 and MRP2 in RNA editing and other RNA processing in *Trypanosoma brucei*. *J Biol Chem* **280**, 2429–2438, <https://doi.org/10.1074/jbc.M405933200> (2005).
59. Singha, U. K. *et al.* Characterization of the mitochondrial inner membrane protein translocator Tim17 from *Trypanosoma brucei*. *Mol Biochem Parasitol* **159**, 30–43, <https://doi.org/10.1016/j.molbiopara.2008.01.003> (2008).
60. Hannaert, V. *et al.* Kinetic characterization, structure modelling studies and crystallization of *Trypanosoma brucei* enolase. *Eur J Biochem* **270**, 3205–3213 (2003).
61. Raz, B., Iten, M., Grether-Buhler, Y., Kaminsky, R. & Brun, R. The Alamar Blue assay to determine drug sensitivity of African trypanosomes (*T.b. rhodesiense* and *T.b. gambiense*) *in vitro*. *Acta Trop* **68**, 139–147 (1997).

Acknowledgements

This work was funded by Ministry of Education ERC CZ grant LL1205, the EMBO Installation grant no. 1965 to AZ and ERD Fund (No. CZ.02.1.01/0.0/0.0/16_019/0000759). The funders had no role in study design, data collection and analysis, decision to publish, or preparation of the manuscript. We would like to thank Ruslan Aphasizhev and Inna Aphasizheva (Boston University) for hosting Michaela Procházková in their labs so she could fulfill the research abroad requirement for her PhD studies.

Author Contributions

M.P., B.P. and A.Z. performed the experiments, analyzed data, participated in experiment design. B.P. and A.Z. prepared and edited the manuscript.

Additional Information

Supplementary information accompanies this paper at <https://doi.org/10.1038/s41598-018-23472-6>.

Competing Interests: The authors declare no competing interests.

Publisher's note: Springer Nature remains neutral with regard to jurisdictional claims in published maps and institutional affiliations.



Open Access This article is licensed under a Creative Commons Attribution 4.0 International License, which permits use, sharing, adaptation, distribution and reproduction in any medium or format, as long as you give appropriate credit to the original author(s) and the source, provide a link to the Creative Commons license, and indicate if changes were made. The images or other third party material in this article are included in the article's Creative Commons license, unless indicated otherwise in a credit line to the material. If material is not included in the article's Creative Commons license and your intended use is not permitted by statutory regulation or exceeds the permitted use, you will need to obtain permission directly from the copyright holder. To view a copy of this license, visit <http://creativecommons.org/licenses/by/4.0/>.

© The Author(s) 2018

1.3.1.1 Additional unpublished data

Loss of TbMrf1 decreases mt transcript levels.

To complement published results, I explored how missing TbMrf1 affects mt transcription and RNA processing. Northern blots of total RNA were probed with end-labeled PCR probes generated against either the pre-edited or edited transcripts of RPS12 and A6. After normalization to the 18S cytosolic rRNA, the amounts of each transcript in the dKO TbMrf1 cell lines were compared to the parental BF 427 cells. The abundance of the pre-edited RPS12 and A6 are significantly reduced in the dKO TbMrf1 1wk cells compared to the BF 427 (Figure 6, A). While the Murf5 never-edited transcript is also decreased in these cells, indicating that the loss of TbMrf1 has a global effect on the steady state levels of mt mRNA, the RPS12 transcript appears to be depleted the most (Figure 6, B). Since there is still some pre-edited transcript detected for RPS12 and A6, we examined the 3' untranslated tail lengths of these edited transcripts to determine if they had become translationally competent. The population of RPS12 and A6 mRNA with a short A-tail, which stabilizes the transcript once editing begins, is drastically reduced in the dKO TbMrf1 1wk cell line. Furthermore, transcripts with a long A/U-tail that promotes the loading of completely edited transcripts onto mitoribosomes, are almost undetectable in the cells lacking TbMrf1 (Figure 6, C). As observed previously, the dKO TbMrf1 7wk cell line has adapted to the loss of the release factor and a marked increase is observed in the steady state pre-edited and short-tailed edited mRNA of RPS12 and A6. Finally, the decreased steady state levels of total 12S and 9S rRNA in the dKO TbMrf1 1wk cells and their recovery in the 7wk cells corroborate the alterations observed in the sedimentation profile of the mitoribosomes (Figure 6, D).

PART I

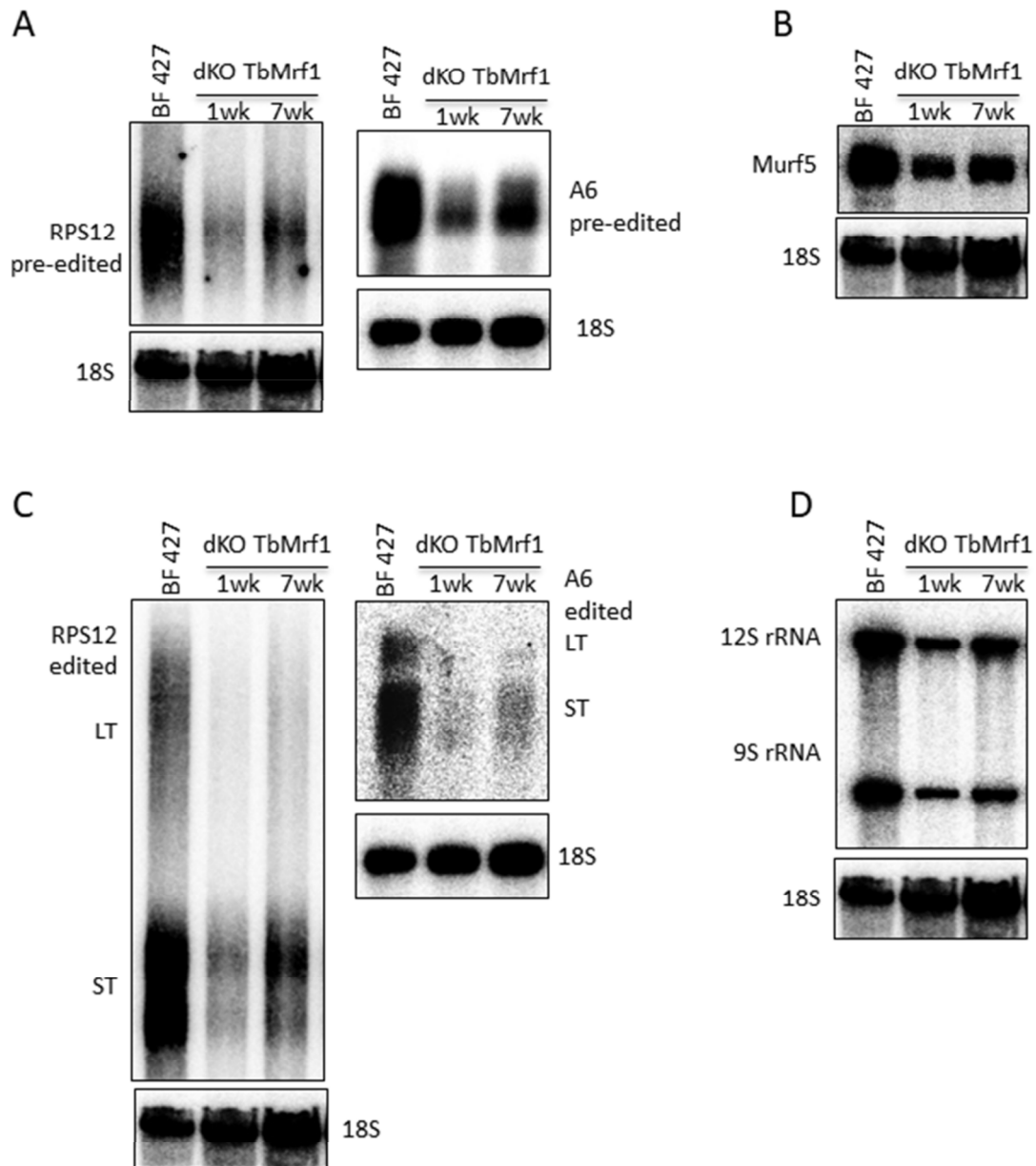


Figure 6: Elimination of TbMrf1 causes a decrease in mt transcript levels. Northern blot analysis of BF 427 and dKO TbMrf1 1wk and 7wk cells reveals the steady state abundance of key mt transcripts. Total RNA was resolved on either a 1.8% agarose-formaldehyde gel (A6 mRNA) or a 5% polyacrylamide/8M urea gel (all other transcripts), transferred to a membrane and probed with either an oligo probe (rRNAs) or a PCR probe (maxicircle transcripts). 18S rRNA served as a loading control. A. Pre-edited A6 and RPS12 B. Never-edited Murf5 C. Edited A6 and RPS12 depicting long-tailed (LT) and short-tailed (ST) mRNA D. 9S and 12S rRNA.

Mt transcripts accumulate when TbPth4 is down-regulated in the dKO TbMrf1 cell line

Without the aid of a depleted TbPth4 to rescue the protein synthetic machinery lacking TbMrf1, we analyzed how impaired translation in these cells affects the mt transcripts. Northern blots containing total RNA from the parental cell line and dKO TbMrf1 + RNAi TbPth4 were probed with end-labeled PCR products that were complementary to either pre-edited or edited RPS12 and A6. Using the cytosolic 18S to normalize the output between samples, both pre-edited and edited mRNAs accumulate throughout the time course of the RNAi induction (Figure 7). This is in dramatic contrast to the dKO TbMrf1 cell lines that exhibit a decrease in mt mRNA. Furthermore, while the recovery observed in the dKO TbMrf1 7wk cells was largely due to the increased stability of short A-tailed edited transcripts, there is also a significant accumulation of the long A/U-tailed edited transcripts in the induced dKO TbMrf1 + TbPth4 RNAi cells. As has been shown previously, these transcripts associate with the 70S monosomes⁷⁹. Perhaps the observed mRNAs are being stabilized due to an increased proportion of stalled mitoribosomes that are unable to terminate translation and recycle in the absence of both TbMrf1 and TbPth4.

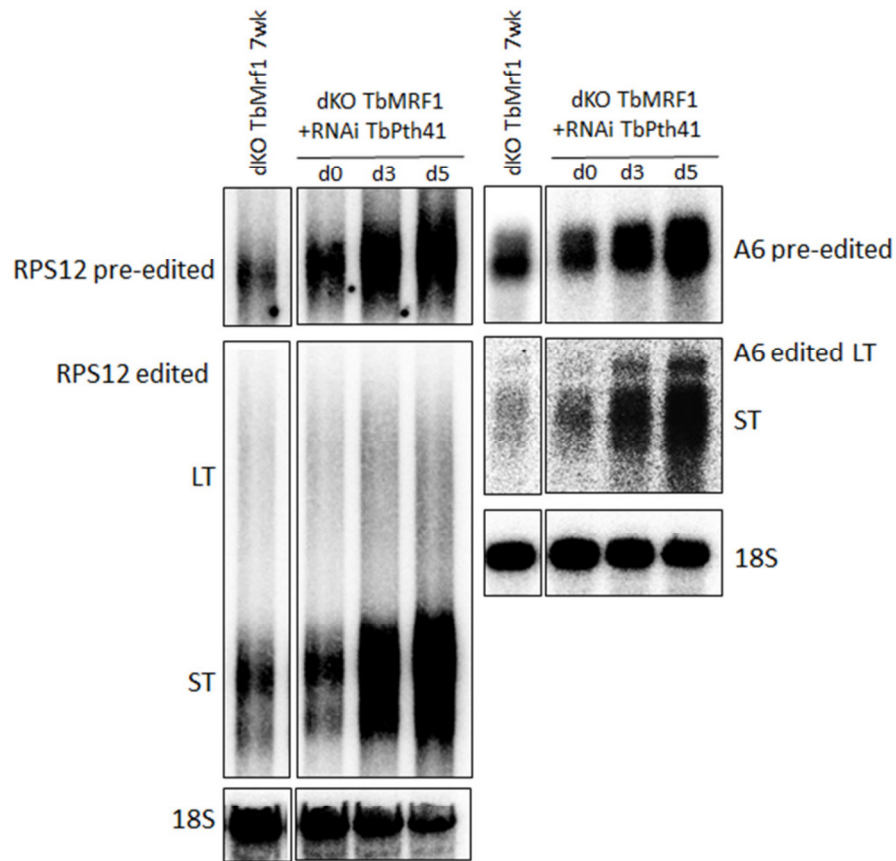


Figure 7: A6 and RPS12 transcripts accumulate upon RNAi induction of TbPth4 in dKO TbMrf1 cells. Northern blot analysis determined the steady state abundance of pre-edited and short-tailed (ST) or long-tailed (LT) edited mt transcripts A6 and RPS12 in dKO TbMrf1 7wk and dKO TbMrf1 + RNAi TbPth4 cells that were either never induced (d0) or induced with tetracycline for 3 (d3) or 5 (d5) days. Total RNA was resolved on either a 1.8% agarose-formaldehyde gel (A6) or a 5% polyacrylamide/8M urea gel (RPS12), transferred to a membrane and probed with a PCR probe. 18S rRNA served as a loading control.

1.3.2 Identification of cytosolic class 1 release factor - TbeRF1

An initial bioinformatic search of the trypanosome genome using yeast release factor Sup45p as a bait returned two significant hits: Tb927.3.1070 (peptide chain release factor 1, mitochondrial, TbMrf1) and Tb927.11.2300 (eukaryotic peptide chain release factor subunit 1, putative, TbeRF1). The mt candidate was described in the previous chapter. To investigate cellular localization of the second hit, putative TbeRF1, I employed in situ PTP tagging of the corresponding gene to prepare two cell lines: TbeRF1-PTP tagged in the wild-type BF 427 cells and TbeRF1 PTP in the TbMTQ1 dKO cells (Figure 8, A). The TbeRF1-PTP dKO TbMTQ1 cell line was supposed to serve later as a negative control for the experiment in which the methylation of TbeRF1 would not be affected due to the absence of TbMTQ1 – the mt methyltransferase described in depth in part III of this thesis. I expected to show that in TbMrf1-PTP dKO TbMTQ1 cell line the methylation of the mitochondrial TbMrf1, but not cytosolic TbeRF1, is diminished. Unfortunately, I encountered technical difficulties such as low endogenous expression of the TbMrf-PTP protein and thus inefficient purification. For these reasons the planned experiment was not finalized.

In order to verify cytosolic localization of TbeRF1-PTP, the cells were treated with digitonin to separate cytosolic and organelle fractions. The subsequent immunoblotting analyses of extracted fractions established sufficient separation as the cytosolic enolase and mitochondrial Hsp70 proteins were confined within their respective subcellular fractions. The constitutively expressed TbeRF1-PTP protein was exclusively localized in the cytosolic fraction in both cell lines (Figure 8, B). To confirm the expected essential nature of TbeRF1, we generated an RNAi cell line. Silencing of TbeRF1 caused severe growth phenotype which was apparent as early as two days after the RNAi induction (Figure 8, C). The specific decrease of TbeRF1 transcript upon RNAi induction was confirmed by RT-PCR (Figure 8, D).

PART I

Based on the sequence homology and observed cellular localization, I concluded that TbeRF1 is the cytosolic termination factor essential for viability of the parasite. Since then, the gene was additionally annotated as such by another research group ³³.

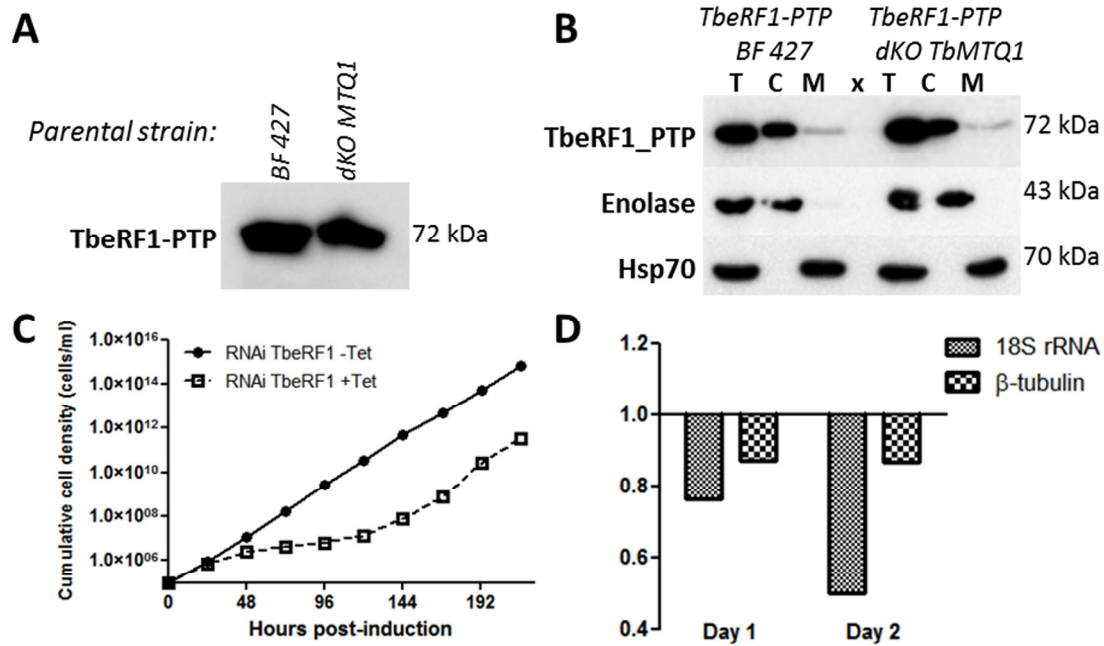


Figure 8: A - TbeRF1-PTP construct is expressed in wild-type and dKO TbMTQ1 background. Cell lysate corresponding to 5x10⁶ cells was analyzed by western blot. The PAP reagent recognizing protein A, part of PTP tag, was used. **B - TbeRF1 is localized to cytosol.** The TbeRF1-PTP tagged cell lines were treated with digitonin. T – whole cell lysate, C – cytosolic fraction, M – organellar fraction. Detection of cytosolic enolase and mt heat-shock protein 70 (Hsp70) served as markers for subcellular compartments. **C - Growth curve.** The growth of RNAi TbeRF1 cell line induced with tetracycline was monitored for nine days. The cumulative cell density of induced cell line was compared to uninduced cells. **D - RT-PCR analysis of TbeRF1 knockdown cell line.** Total RNA from cells induced for one and two days was isolated and level of the TbeRF1 transcript was compared to that of the uninduced cell.

I.3.3 Characterization of mt MTase TbMTQ1

Based on the bioinformatic analysis, the TbMTQ1 (Tb927.10.9860) belongs to the N5-glutamine MTases from PrmC/HemK superfamily^{135,140,162,163} as it contains the conserved motif Asn-Pro-Pro-Tyr (NPPY) positioned between residues 311 – 314, and a non-canonical AdoMet binding site represented by conserved residues Gly220 and Gly222. Initially, we planned to detect the activity of TbMTQ1 *in vitro*, however, I was not able to produce either the enzyme or the substrate (TbMrf1) in native form in sufficient quantities for the experiment. Consequently, I abandoned this approach and resorted to *in vivo* methods using transgenic trypanosome cell lines. Two strategies were employed. First, I endogenously tagged TbMrf1 gene in BF 427 and dKO TbMTQ1 cell lines in order to purify the TbMrf1 protein and detect the methylation by mass spectrometry. Here again, I encountered technical difficulties. The web-based tool PeptideCutter¹⁶³ for prediction of protease cleavage sites was used to estimate if the size of the peptide fragment containing methylated GGQ motif would fit the preferred mass range for MS analysis. The *in silico* tryptic digest produced a peptide of 26 amino acids, which is, upon a consultation with a mass spectrometry expert, too long to be efficiently identified. Alternative protease chymotrypsin was suggested, but as I did not have enough material to test it I was not able to verify function on TbMTQ1 as exclusive mt TbMrf1 methylase.

Consequently, I decided to functionally characterize a cell line, in which TbMTQ1 is knocked out in order to decipher the physiological role of this enzyme. For this purpose, a null background dKO TbMTQ1 BF cell line was generated. I expected the cell line to be viable because we previously showed that RNAi silencing of TbMTQ1 did not produce a growth phenotype in BF trypanosomes¹⁵⁶. The replacement of TbMTQ1 endogenous alleles with antibiotic markers and the absence of TbMTQ1 open reading frame were verified by PCR

PART I

using specific primers (Figure 9, A). Growth rate and doubling time of dKO TbMTQ1 were recorded for twelve days (Figure 9, B & C). Observed mild growth phenotype was apparent after the fifth day from the start of the measurements and calculated doubling time values show approximately one hour difference between dKO TbMTQ1 and parental BF 427 cell growth rate. Further experiments were performed in parallel with analyses of TbMrf1 and TbeRF1 using the same methods as described in research paper unless stated otherwise in Part I - Methods section. To evaluate the impact of presumably missing methylation at the GGQ motif of TbMrf1, I determined the level of mmp, levels of 9S and 12S rRNAs, the quantity of assembled mt F₀F₁ ATPase, and sensitivity of cells to specific inhibitors. In addition, I observed virulence of dKO TbMTQ1 cell line in an animal model.

The mmp was measured by FACS using a fluorescent dye TMRE, which specifically stains the energized mitochondria. A 20% decrease in signal was detected when compared to the parental BF 427 in the independent triplicate experiment (Figure 9, D). The modest decrease in the proton gradient may correspond to the prolonged doubling time however, 20% decrease does not limit cell proliferation¹⁶⁴. To observe if the F₀F₁ ATPase complex is fully assembled I analyzed mt lysate using native electrophoresis followed by immunoblotting. Hypotonically purified mitochondria were lysed with digitonin and cleared lysate was separated on 3-12% hrCNE native gel and transferred onto the nitrocellulose membrane. The membrane was then incubated with specific antibodies against subunit β , ATPaseTb2, and p18. The pattern of detected F₀F₁ ATPase complexes and sub-complexes and their band intensities were comparable between dKO TbMTQ1 and parental BF 427 (Figure 9, E) suggesting that no significant changes occur during the complex assembly. Furthermore, the dKO cells retained the same sensitivity to azide as expected because the BF does not contain functional complex IV⁶². However, the observed sensitivity to oligomycin (F₀ moiety binding inhibitor of proton pore) was comparable to

parental BF SM cells, which implies that presumable lack of TbMrf1 methylation does not have a direct effect on translation of A6 (Figure 10, A & B).

To evaluate mt ribosome profile in the dKO TbMTQ1 cell, the mt rRNAs levels were examined. Mt extracts were subjected to sedimentation on 10-30% sucrose gradient (described in the Methods section) and RNA isolated from individual fractions was applied to dot blot. The radioactive signal corresponding to the levels of 9S and 12S rRNA in individual fractions was quantified. Comparison with the likewise treated sample of parental strain showed that even though the overall signal for mitoribosomes is lower in dKO TbMTQ1, the global peak profile is retained (Figure 10, C & D). The profile indicates that the ratio of individual intermediate mitoribosome sub-complexes remains unchanged upon knockdown of methylase.

Finally, we did not observe a difference in parasitemia levels (Figure 10, E) or survival rate (Figure 10, F) in mice infected with BF 427 and dKO TbMTQ1 cells. Unchanged parasite virulence shows that if indeed the TbMrf1 GGQ motif is not methylated, this post-translation modification has no effect on TbMrf1 function and thus the translation efficiency of A6 and RPS12 proteins in BF.

In *E. coli*, the presence of methylation at Gln252 in GGQ motif of RF2 correlates with an increased translation termination efficiency¹⁶⁵. In addition, the absence of methylation causes a growth arrest in bacteria kept on poor carbon sources¹³³. In bacterium *Thermus thermophilus*, the effect of RF1 methylation on stop codon recognition was investigated in detail. The results from bacterial reconstituted expression system demonstrated a direct relationship between the termination rate and levels of RF1 methylation. The study showed that methylation of GGQ significantly increases release efficiency of peptides ending with proline and glycine. When the RF1 methylation was missing, peptides ending with proline or glycine displayed slow release rate perhaps due to a natural hindrance of an amino acid with position of a coordinated water molecule, which can be alleviated by a presence of an amino acid with larger side

PART I

chain or a methyl group ¹⁶⁶. Therefore, terminal amino acids with aliphatic side chains do not significantly benefit from the presence of methylation on the release factor GGQ motif.

In yeast, mass spectrometry analysis showed that only 50% of the endogenous Mrf1 pool is methylated, pointing to a fact that presence of GGQ methylation is perhaps not required for release of every nascent peptide. The deletion of the corresponding yeast MTase, Mtt1p, had no consequences on mt metabolism however, the mutant cells grew slower in nonfermentable media (ethanol, YPE) ¹²³. In human tissue culture, the absence of MTase HMPmC methylating the GGQ motif in HMRF1L causes 60% decrease of mt translation activity in cells on galactose medium with streptomycin, which affects the translation fidelity ¹⁴⁴.

Despite the universal presence of N5-glutamine methylation of mt release factor 1, trypanosomes seem to be able to cope with missing mRF1 GGQ methylation. As the BF mitochondrion likely requires expression of only two proteins encoded in its genome, the F₀F₁ ATPase subunit A6 with the final amino acid being Asn, and mitoribosome SSU subunit RPS12 ending with Phe, the unmethylated release factor appears to be able to perform the reaction without observable lag. Additionally, no appreciable growth defect was observed in induced PF RNAi TbMTQ1 cells ¹⁵⁶ that depend largely on oxidative phosphorylation requiring translation of mt-encoded proteins. Among essential proteins expressed in PF cell are cytochrome b (UniProt entry P00164: ends with Asp), cytochrome oxidase subunits I (P04371: Ile) and II (P04372: Ile), and NADH dehydrogenase subunits e.g. ND5 (P04540: ending with Val), all medium size side chains. Alternatively, the missing growth phenotype of PF RNAi TbMTQ1 cells results from glucose-rich cultivation media insufficiently activating oxidative phosphorylation pathway as the cells can still supply the ATP consumption through glycolysis. It was shown that the decrease of glucose in PF media significantly upregulated levels of F₁ ATPase moiety subunits and

increased sensitivity to oligomycin¹⁶⁷. Perhaps a growth analysis in glucose-depleted conditions would allow us to observe the effect of the TbMrf1 methylation in PF trypanosome.

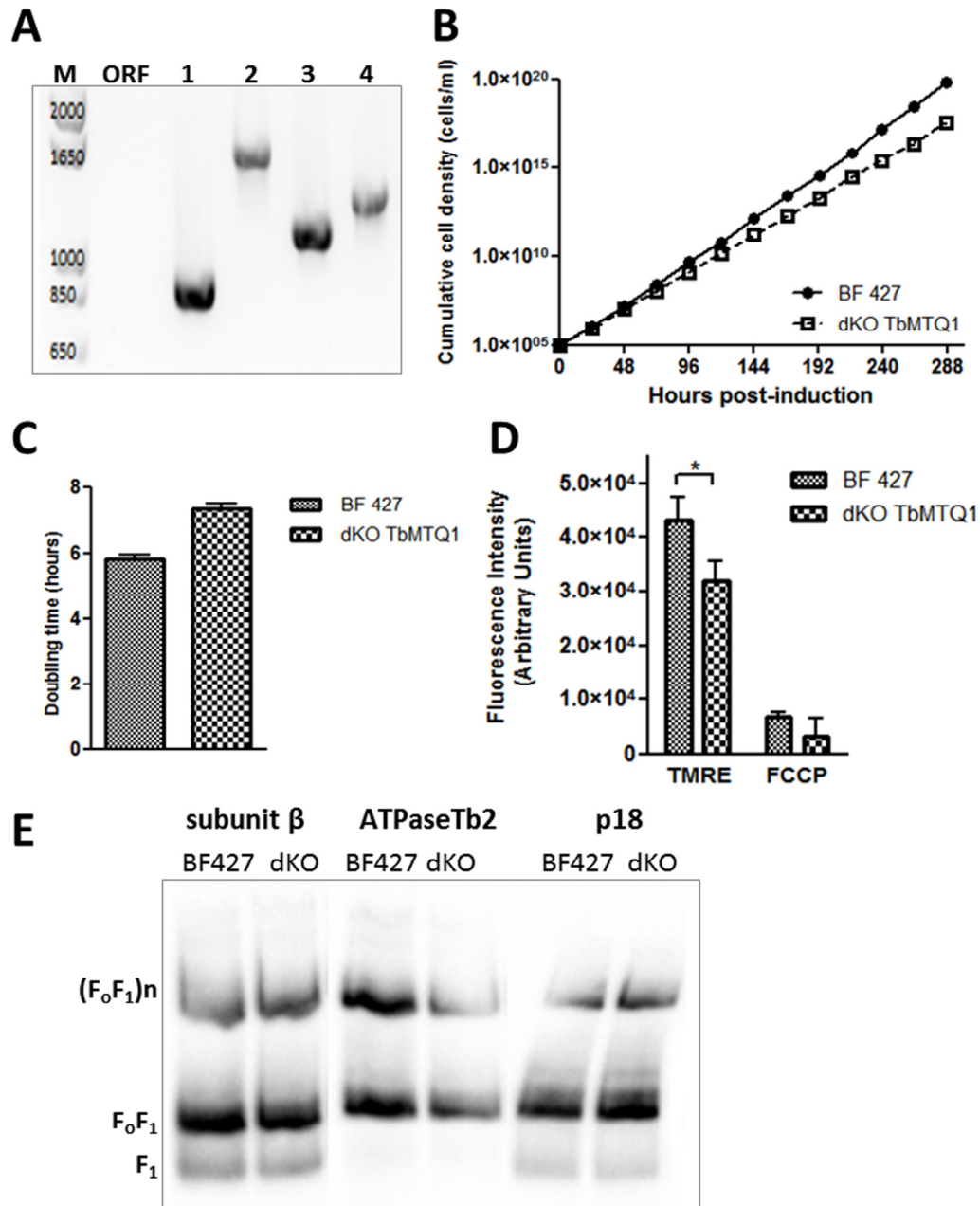


Figure 9: **A** – Verification of dKO TbMTQ1 knockout of coding sequence. M – marker, 1 – 5' flanking region of the first allele, 2 – 3' flanking region of the first allele, 3 – 5' flanking region of the second allele, 4 – 3' flanking region of the second allele. **B** - **Growth curve.** The growth of a double knockout cell line dKO TbMTQ1 was monitored for twelve days. The cumulative cell density of dKO cells was compared to parental cell line BF427. **C** - **Doubling time.** The growth of double knockout cell line dKO TbMTQ1 induced with tetracycline was monitored for twelve days. The doubling time of induced

PART I

cell line was calculated and compared to parental cell line BF427. **D - Mitochondrial membrane potential.** Level of mmp was measured as a fluorescence intensity of TMRE. Treatment with FCCP was used as a control for membrane depolarization. **E - Level of mt F_oF₁ ATPase moieties in dKO TbMTQ1 compared to BF 427.** Mt lysate was extracted from BF cells. The hrCNE followed by immunostaining was used to visualize F₁ and F_oF₁ ATPase complexes. The free F₁ moiety was detected with antibodies against subunit β and p18, assembled complex and oligomers were detected additionally with an antibody against ATPaseTb2.

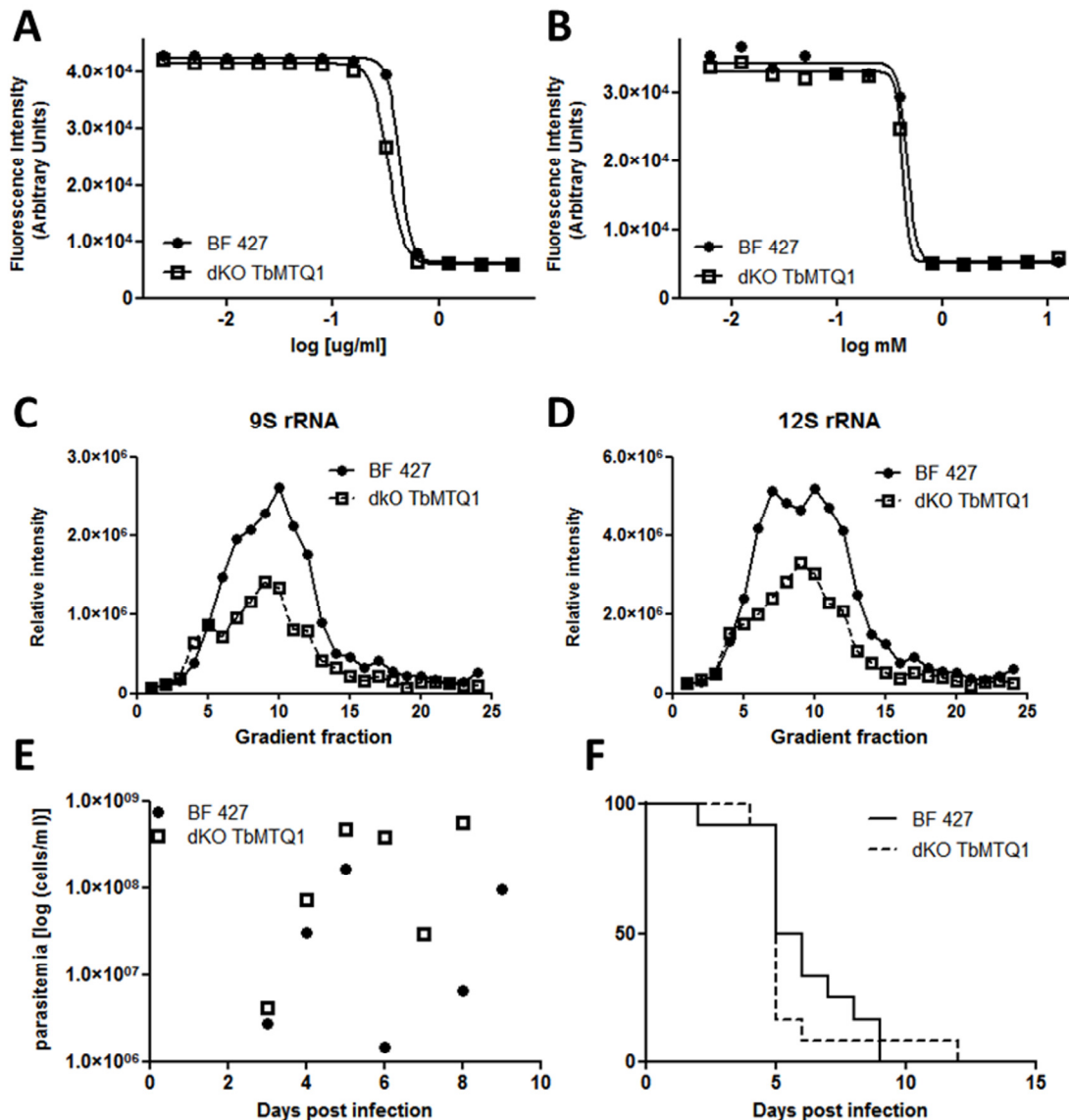


Figure 10: A, B - Sensitivity to specific inhibitors. Oligomycin (A) and azide (B) treated cells were subjected to Alamar blue assay. Measured fluorescence readings were plotted against the log of the final concentration of inhibitor. **C, D - Level of individual ribosomal RNAs.** Total RNA from the same amount of parental cells and dKO TbMTQ1 cells was isolated and resolved on a glycerol gradient. Resulting fractions were analyzed with dot blot. The signal of gamma-ATP³² corresponding to 9S and 12S rRNA was recorded and quantified with Typhoon reader. **E - Parasitemia in the blood of infected animals.** The blood of individual animals was fixed and parasitemia was calculated every day. Average values of parasitemia in each day are plotted. **F - Survival curve of the mice infected with wild-type BF 427 and dKO TbMTQ1 cells.** Group of five female BALB/c mice was injected i.p. with 1×10^4 parasites and observed for 15 days. The survival was recorded and plotted using GraphPad Prism built-in survival analysis.

PART II OPTIMIZATION OF THE SAFRANINE O

ASSAY FOR MEASUREMENT OF F₀F₁

ATPASE ACTIVITY

II.1 INTRODUCTION

The mmp, a gradient of hydrogens across an mt inner membrane, is generated by three out of the four ETC complexes (complex I, III and IV). In mitochondrion, the electrochemical force pulling hydrogens back into the matrix consists of two components, the electric charge ($\Delta\psi_m$) and pH gradient also expressed as a concentration of hydrogen ions (ΔpH_m). The mmp level was experimentally determined to be in 180 - 220 mV range, with five times higher contribution of the electrical component in comparison to the chemical component ¹⁶⁸⁻¹⁷⁰. The mmp is a driving force for a number of essential processes in the mitochondrion and directly influences the fitness of the cell.

In living cells, relative levels of mmp can be detected by flow cytometry-based assays using fluorescent rhodamine derivatives such as tetramethylrhodamine ethylester (TMRE) ¹⁷¹. In permeabilized cells or in isolated mitochondria a quantitative approach yielding value of mmp in mV was developed using azonium compound safranine O ¹⁷². It was shown that energization of the mt membrane by respiration or ATP hydrolysis gives rise to a spectral shift in safranine O fluorescence. This spectral shift results in loss of fluorescent signal at 511 - 533 nm, which is linearly related to generated membrane potential ¹⁷³. Safranine O quenching assay is sensitive, fast and

reproducible and can be performed in 96-well plate format which is compatible with most plate readers equipped with a suitable filter set (excitation from 496 nm, emission detection to 586 nm) and accessory injectors.

II.1.1 F_oF₁ ATPase composition and function in BF trypanosomes

In mitochondrion, the F_oF₁ ATPase complex consists of a matrix facing F₁ subcomplex (subunits β , α) responsible for binding of ADP + Pi for ATP synthesis, a central stalk (subunits γ , δ , ϵ)¹⁷⁴, and a membrane-anchored F_o moiety composed of several copies of subunit *c* and single subunit *a*. Subunit *c* forms homo-multimeric ring submerged in the inner mt membrane, with a single subunit *a* closely associated at one side. The proton is translocated from the intermembrane space through the proton pore at the interface of the *c*-ring and subunit *a*. The translocation process drives the rotation of the *c*-ring and central stalk (rotor). Through a long-distance steric movement, the three states in F₁ moiety corresponding to binding of ADP+Pi, generation of ATP, and ATP release, are induced¹⁷⁵. To ensure the stationary position of the alpha/beta headpiece, the peripheral stalk (subunits OSCP, *b*, *d*, F6) is in place to tether the F₁ moiety to the inner mt membrane¹⁷⁵.

From an NMR model of *E. coli* subunit *c* and set of structures of *ac*₁₂, the mechanism of proton release is proposed to be dependent on deprotonation of residue Asp61 in subunit *c* in proximity to Arg210 of subunit *a*. The deprotonated Asp61 is re-protonated by hydrogen traveling down the concentration gradient thus driving the rotational movement of *c*-ring¹⁷⁶. In green alga *Polytomella*, the proton path was deduced from the cryoEM structure of solubilized ATP synthase at resolution 7.0 Å. The structural analysis uncovered two half-channels through the inner mt membrane with subunit *a* residue Arg239 and subunit *c* residue Gln295 playing an essential role in proton translocation by driving the movement of F_oF₁ ATPase rotor¹⁷⁷.

PART II

The trypanosome F_oF₁ ATPase complex contains 14 extra subunits identified through a series of tandem affinity purifications and mass spectrometry analyses. Interestingly, the BLAST searches of the extra subunits show no homology outside *Euglenozoa*¹⁷⁸. In addition to extra subunit p18 in F₁ moiety^{179,180}, two unique subunits, ATPaseTb1 and ATPaseTb2, were shown to be essential for structural integrity of the F_o moiety^{181,182}. The ATPaseTb1 subunit is essential for BF cell, even a moderate (40%) decrease in ATPaseTb1 level had a drastic effect on cell viability, levels of mmp and assembly of the F_oF₁ ATPase complex¹⁸². The proposed function of ATPaseTb1 in stabilization and assembly of subunit *a* (referred to as A6 in trypanosome field) called for further investigation. However, *in vitro* analysis of subunit A6 is complicated by its extreme hydrophobicity rendering the protein refractory to conventional analytical methods. In mt lysates from PF trypanosome, an anomalous electrophoretic migration assay¹⁸³ was used to observe the subunit A6 but in BF trypanosome the A6 has not been detected yet. However, the indirect method could be employed to indirectly detect the activity of the proton pore. In the light of the fact that in BF the mmp is generated by a reverse function of F_oF₁ ATPase at the expense of cytosolic ATP, the assembly and activity of the F_oF₁ ATPase complex directly correlates with levels of mmp and *vice versa*, changes in mmp measured *in vitro* can be attributed to structural integrity and activity of F_oF₁ ATPase^{64,184}. Consequently, any changes in A6 level will be measured as a variation of the mmp⁶⁴. We adapted the safranin O quenching assay originally developed to investigate a calcium transport in *Leishmania* to measure changes in mmp in permeabilized BF trypanosome cells^{67,185}.

II.2 PROTOCOL

For safranin O quenching assay, freshly harvested log phase BF cells at the quantity of 8.2×10^6 per 100 μl reaction/well (in 96-well plate format) are required. Care should be taken to use cells in good condition within 30 minutes from harvest, as frozen material or isolated mitochondria do not yield reproducible results. In addition to that, it is not recommended to keep the cells on ice during the experiment. Mixture of BF cells in final concentration $8.2 \times 10^7/\text{ml}$ in reaction buffer (125 mM sucrose, 65 mM KCl, 10 mM HEPES-KOH pH 7.2, 1 mM MgCl_2 , 2.5 mM KH_2PO_4 , 20 μM EGTA, 500 μM $\text{Na}_3\text{O}_4\text{V}$) is suitable for one experiment spanning approximately 30 min. Additional reagents are 12.5 μM safranin O, 40 μM digitonin, and 10 μM FCCP. Specific inhibitors are prepared in a respective solvent and use in final concentrations 2.5 $\mu\text{g}/\text{ml}$ oligomycin, 43 μM carboxyatractyloside. Safranin and ATP are added to the cell mixture and immediately distributed into the 96-well plate. The baseline is measured in the plate reader (Tecan Infinite Pro), and then digitonin is added to start the measurements. The presented representative experiment was programmed as follows: 10 s/a cycle, 75 cycles in total. The injection of inhibitor was programmed either at cycle 20, 25 or 30 (marked with an arrow in respective figures), depending on the condition of cells.

II.3 RESULTS WITH DISCUSSION

An initial safranin O quenching profile of untreated BF cell was acquired (Figure 11, A – no inhibitor). At approximately 200 seconds after the digitonin addition, the quenching reached its limits and the curve slowly turned back towards the initial levels. Thus, the time point for inhibitor injection was set to

PART II

200 s. The FCCP uncoupler was injected at the cycle 60 to fully depolarize the membranes.

The effect of common inhibitor solvents (DMSO, 70% ethanol) was tested to exclude depolarization of the membrane due to the effect of solvents (Figure 11, A). DMSO and 70% ethanol seem to dissipate the mmp as efficiently as FCCP, whereas a lower concentration of ethanol (20%) influences the level of mmp less than oligomycin or atractyloside (compare Figure 11, A and B). Measured quenching curves show that DMSO is not a suitable solvent and ethanol, if needed, should be used at a final concentration lower than 20%. The inhibitors used in subsequent experiments (carboxyatractyloside, oligomycin) were dissolved in the reaction buffer or reaction buffer supplemented with 20% ethanol (FCCP).

The sensitivity of BF 427 cell mmp to specific inhibitors of F_0F_1 ATPase (oligomycin) and AAC (carboxyatractyloside) was also evaluated. Both inhibitors fully dissipated mmp levels in BF 427 permeabilized cell, with oligomycin having a moderately faster effect than carboxyatractyloside (Figure 11, B). We assume that blockade of proton pore by oligomycin has an immediate effect, whereas the pool of ATP imported by AAC has to be first depleted for the effect of carboxyatractyloside to be observed. Nevertheless, the speed of signal formation points to a relatively small amount of ATP stored in an mt matrix.

Finally, the RNAi ATPaseTb1 cell line was investigated by safranin O quenching measurement to test the ATPaseTb1 putative role as an A6 assembly factor (Figure 11, C). The RNAi ATPaseTb1 cells were induced for 6 hours (time point before a growth phenotype), 12 hours (after the observed growth phenotype first appeared), and 24 hours. Harvested cells were solubilized with digitonin and at cycle 30 the oligomycin was injected. The quenching profile was compared to the parental strain BF SM and uninduced RNAi ATPaseTb1 cells. Calculated quenching curves show that at 6 hours after induction, the cells are still capable of producing a wild-type level of mmp, whereas after 12 hours of

RNAi induction the overall mmp is significantly decreased with the negligible sensitivity to oligomycin. As previously suggested, in the absence of ATPaseTb1 the stability of the F_0 pore is compromised, or alternatively, the pore is not completely formed as a result of misassembled subunit A6.

In summary, the safranin quenching assay proved to be a fast and reproducible method to measure mmp levels in permeabilized BF cells. It is recommended to use reaction buffer as a solvent for all additives. For organic compounds, we advocate ethanol in less than 20% final concentration as a solvent.

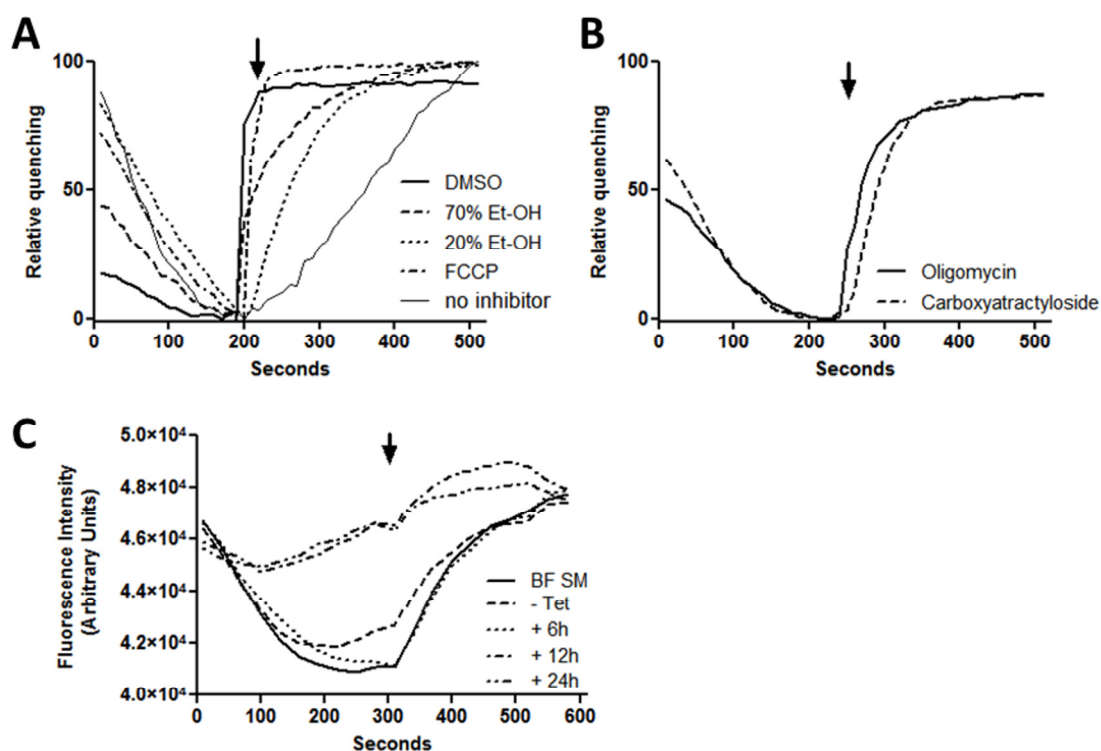


Figure 11: A - Solvent controls. Common solvents DMSO, 70% and 20% ethanol were added to BF 427 cells at 200 s to test the background quenching of signal. Uncoupler FCCP served as depolarization control. **B - Relative quenching of safranin fluorescent signal by addition of specific inhibitors.** Oligomycin and carboxyatractyloside were added at 240 s to BF 427 cells. **C - ATPaseTb1 RNAi cell line analysis with safranin quenching.** The level of fluorescence quenching in parental cell line BF SM and uninduced control was compared to RNAi cells induced for 6, 12 and 24 hours.

PART III DESTABILIZATION DOMAIN TECHNIQUE IN MITOCHONDRION

III.1 INTRODUCTION

To identify and verify novel targets for either vaccine or drug development, we require tools that can help us study essential genes in *Leishmania* species. However, the *Leishmania* genetic toolkit is limited to homologous recombination that only allows us to prepare overexpressing strains or deletion mutants for non-essential genes. In the most extensively studied *Leishmania* models, *L. major*, and *L. donovani*, we lack the most widely used tool for essential gene silencing, the RNAi pathway¹⁸⁶. Database searches of the current *Leishmania* genome sequence databases have not identified convincing homologs of genes specifically implicated in the RNAi pathway in other organisms. Recently, the RNAi activity was demonstrated in *L. braziliensis*¹⁸⁷. The authors showed that RNAi pathway was lost after the *Leishmania* species diverged to *L. major* and *L. donovani* and thus the RNAi enzymes are only preserved in subgenus *Viannia* that includes *L. braziliensis* and *L. guyanensis*¹⁸⁸. In spite of *L. major* lacking the RNAi machinery, it is possible to directly regulate cytosolic proteins expression with the destabilization domain technique^{156,189}.

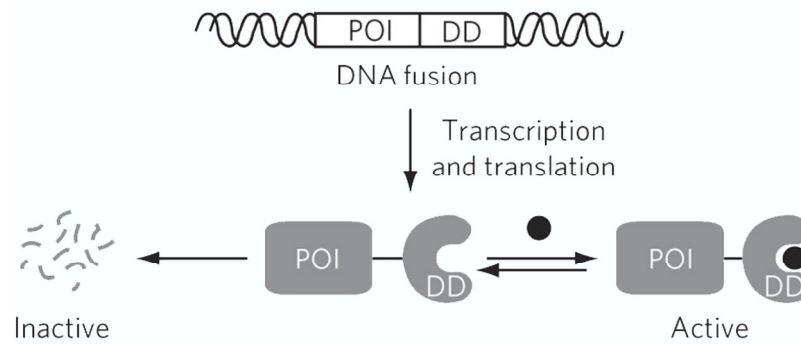


Figure 12: Schematic overview of destabilization domain technique. POI – protein of interest; DD – destabilization domain. The stabilization ligand is depicted as a black dot. Adapted from ¹⁹⁰.

A protein-based regulatable system offers a great potential to overcome the lack of tools in *Leishmania*. This methodology utilizes a mutated version of human FK506 binding protein 12 (FKBP12) as a destabilization domain (dd) fused to a protein of interest. In the absence of small molecule ligand (rapamycin or FK506), the improper folding of the dd domain leads to the rapid degradation of the whole fusion protein through the proteasome pathway. Conversely, the addition of FK506 stabilizes the dd domain and allows the protein of interest to acquire its proper folding and function (Figure 12).

FK506 (under commercial name Tacrolimus) is used in human medicine for immune system suppression in patients after transplantation. Binding of FK506 to FKBP12 affects the PPIase activity of the protein which then binds together TOR kinase and calcineurin into a tripod complex that stops downstream signal transduction. The TOR signaling in control of cell division is inhibited, which leads to decrease of mature T-lymphocytes numbers and suppression of immune response ¹⁹¹. In trypanosome, TbFKBP12 homolog is a cytoskeleton-associated factor specific for BF flagellar pocket area ¹⁹². Genetic knockdown of TbFKBP12 show phenotype connected to the cytoskeleton in both stages; affected motility in PF and disrupted cytokinesis and cytoskeletal architecture in BF. Any adverse effects of supplemented FK506 ligand in trypanosome or *Leishmania* were not observed.

PART III

The dd methodology has been applied to study various genes in *L. major*¹⁹³, and some other protozoan parasites: *Toxoplasma gondii*¹⁹⁴ and *Plasmodium falciparum*¹⁵⁶. The tested protein targets were of different size, folding, function (kinases, GTPases), various stability throughout the cell cycle (p21, securin) and cell localization (trans-membrane glycoprotein). Instability was conferred in case of N-terminal as well as C-terminal fusion, although the N-terminal fusions appear to exhibit stronger destabilizing effect on some fusion proteins¹⁹⁵. To date, there has been no report of mitochondrial, ER or any other compartmentally localized protein used as a target for destabilization by dd domain¹⁹³. To further develop this powerful technique, we decided to test its efficiency on a protein targeted to the mitochondrion.

Potential difficulties in implementing this system to study essential proteins of various organelles might arise from the inability of FK506 to penetrate the organellar membranes, which frequently functions as an effective barrier to various small molecules, although FK506 is obviously able to pass through the plasma membrane or enter the cytoplasm via active transport mechanism. The other potential hazard involves the mechanism of protein degradation of these organelle localized proteins where it is generally thought that the proteasome does not function. Beside one mammalian mt inner membrane protein rapidly degraded by the cytosolic ubiquitin proteasome system¹⁹⁶, The bulk of mammalian mt protein degradation relies on three major ATP-dependent oligomeric proteases, Lon, Clp-like and AAA proteases. Clp-like and AAA proteases are hetero-subunit oligomeric complexes located in the matrix and inner mt membrane¹⁹⁷, respectively. Lon on the other hand is a homo-oligomeric complex located within the mt matrix¹⁹⁸. The specific mechanism of protein degradation in the *Leishmania* mitochondrion remains to be elucidated¹⁹⁹. In this part of my research, I attempted to adapt the dd technique to study mitochondrial proteins and aimed to open the door for investigations of essential mt targets in organisms lacking RNAi pathway such as *L. major*.

The *Leishmania* mitochondrion harbor important metabolic functions such as the oxidative phosphorylation pathway for the production of cellular ATP. It is clear that disrupting its function would have detrimental effects for both, the promastigote and amastigote forms of *Leishmania*, and may serve as a therapeutic approach. A promising candidate for novel drug or vaccine development was identified in *Leishmania major* on the basis of the Hidden Markov model targeting motifs of known mitochondrial proteins as a tool to search the *L. major* genome²⁰⁰. The mitochondrial protein X (MIX) is a kinetoplastid-specific mitochondrial inner membrane protein that has an influence on cell morphology, mitochondrial segregation, cell division, and importantly, on parasite virulence. Published data suggest that MIX has a role in regulating mitochondrial membrane dynamics²⁰⁰, although the exact mechanism remains to be elucidated. The phenotypes of $\Delta mix/MIX$ *L. major* cell line included compromised growth, morphologically abnormal elongated posterior end of the cell, and occurrence of N2K1 and N(n+2)K1 multinucleate-single kinetoplast parasites pointing at disrupted mitochondrial fission. Furthermore, the LmMIX structure at resolution 2.4 Å revealed 14-3-3 architecture with HEAT repeats with additional reference to tetratricopeptide structure suggesting a function in mediating protein-protein interactions as a scaffold protein²⁰¹.

III.2 METHODS

As a reporter system for initial testing, I used eGFP fused to the dd domain. To incorporate alien DNA into the SSU rRNA locus in *L. major* genome, the SSU rDNA fragments were amplified with specific primers (Lm_5'SSU_fw&rv and Lm_3'SSU_fw&rv) and introduced as a flanking regions of expression cassette comprising: eGFP reporter gene (primers eGFP_fw&rv, ML-eGFP_fw), the downstream intergenic region of DHFR containing

PART III

polyadenylation signal (primers DST-IR_fw&rv), mitochondrial localization signal (ML, incorporated in individual primers) derived from LmMIX protein (LmjF08.1200, nt 1-27)²⁰⁰, and FKBP12 protein (dd_fw&rv, dd_rv (no STOP)). The individual sections of the cassette were assembled in four different arrangements and then inserted into the carrier vector (pIR_phleo_dd), which is described in¹⁹³. As a result, four constructs were designed; the dd fused to eGFP on its C or N-terminus, and either cytosolic or localized to mitochondrion with use of LmMIX mt localization signal. The sequenced constructs eGFP-dd, ML-eGFP-dd, dd-eGFP, and ML-dd-eGFP were stably transfected into parental *L. major* (Friedlin strain) to test and compare dd-domain destabilization efficiency by western blot analysis (described earlier) with use of the anti-eGFP polyclonal antibody.

For an alternative approach, additional constructs were prepared to place protein of interest (LmMIX) into transcriptionally silent position in *Leishmania* genome, the LD1 locus²⁰², under control of a T7 promoter. The T7 RNAP was in turn introduced into SSU rDNA locus and regulated by the dd domain. Initially, T7 RNAP construct with N-terminal dd domain was prepared with phleomycin selection marker. Stably transfected clones were tested with PCR to verify correct incorporation of the cassette. Subsequently, the dd_T7 RNAP expression in response to FK506 ligand presence was investigated with western blot analysis. A selected clone was further transfected with the construct containing LD1 locus homologous sequences flanking LmMIX-His under control of T7 promoter (100%) and hygromycin selection marker. Obtained clones were again tested using the same approaches as described for the paternal cell line.

III.3 RESULTS WITH DISCUSSION

To show that the selected strain of *L. major* is responsive to dd domain stabilization, I cultivated stably transfected reporter cell lines for 24 hours in

presence of 50 - 2000 nM of FK506 ligand. The eGFP reporter was detected with SDS-PAGE and immunoblotting. A representative result is presented, showing dose-dependent stabilization of reporter eGFP after 24 hours (Figure 13, A). Based on this titration experiment, the 1 μ M FK506 concentration was selected for further experiments as a sufficient concentration to stabilize the reporter protein. Next, the time-dependence of reporter stabilization and destabilization upon withdrawal of ligand was tested. Cells were treated with 1 μ M FK506 and harvested at 0, 6, 12 and 24 hours after induction. The remaining cells were washed and transferred to fresh media without FK506. Additional samples were harvested at 6, 12 and 24 hours after removal of FK506. Cell lysates were again tested with SDS-PAGE and immunoblotting (Figure 13, B).

Stabilization of the eGFP was observed in all four cell lines after 6 hours of FK506 treatment albeit the detected signals varied in their intensities. The destabilization of the reporter protein eGFP was more efficient in the two cell lines in which the eGFP protein is dd-tagged on its N-terminal end. This is in agreement with the published results showing that the N-terminal dd-tag was more efficient for some proteins ¹⁹⁵. The C-terminal construct was stabilized stronger when fused to ML (Figure 13, B).

All four cell lines treated for 6 hours with FK506 were further fractionated using digitonin in order to detect the subcellular localization of the stabilized eGFP. The position of eGFP was compared to position of marker proteins for individual compartments (enolase – cytosol, Hsp70 – mitochondrion). Importantly, the eGFP signal was detected in all four cases in the cytosolic fractions suggesting that regardless of the dd position, the ML-eGFP was not targeted to the mitochondrion. (Figure 13, C).

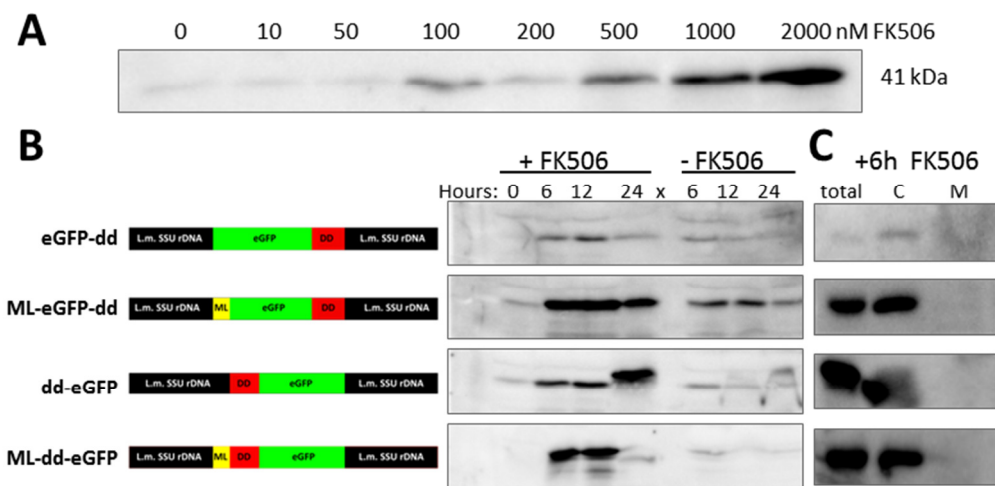


Figure 13: A - Titration of stabilization ligand FK506. Expression of cytosolic eGFP was induced for 24 hours by addition of FK506 in increasing concentrations. Lysates were probed by anti GFP polyclonal antibody. **B - Detection of stabilized eGFP in individual reporter cells lines.** Respective cell lines (eGFP-dd, ML-eGFP-dd, dd-eGFP, ML-dd-eGFP) were monitored for eGFP expression upon addition or withdrawal of FK506. **C - Subcellular fractionation.** Total, cytosolic (C) and mitochondrial (M) fractions of cell incubated 6 hours with FK506 were analyzed for enrichment of eGFP. L.m. SSU rDNA – ribosomal locus flanking regions for incorporation to transcriptionally active site of L. major genome; ML – mitochondrial localization signal; DD – destabilization domain, eGFP – enhanced green fluorescent protein reporter gene.

It was shown that to enter the mitochondrion, the imported protein has to unfold and pass through a relatively narrow passage formed by TOM/TIM import complexes (reviewed in ²⁰³). To explain the unsuccessful targeting of ML-eGFP-dd and ML-dd-eGFP into the mitochondrion, two possible scenarios are at hand. First, the unfolding process releases the non-covalently bound FK506 from dd and the imported protein is not able to re-fold to its stable conformation in the mitochondrion. Second, the binding of FK506 is strong enough to interfere with the protein import process. Additionally, the dd domain was shown to induce the formation of dimer upon interaction with its ligand. This trait is employed commercially as an artificial dimer formation tool ²⁰⁴ but it is not advantageous in connection with mt transport as the dimeric reporter protein might not be able to enter the organelle.

To circumvent some of these issues, we tried to implement a regulation of T7 RNA polymerase (T7 RNAP) expression using the dd. In this case, stabilized dd_T7 RNAP would drive an expression of the T7-controlled copy of a protein of interest from transcriptionally silent locus while both alleles of the endogenous gene would be knocked out. Then upon the removal of FK506, the dd_T7 RNAP expression would be eliminated and thus also the expression of the protein of interest.

The dd_T7RNA construct (Figure 14, A) was transfected to *L. major* and selected clones were analyzed by PCR (Figure 14, B). The N-terminally fused dd_T7 RNAP was expressed from transcriptionally active SSU rDNA locus in response to induction by the FK506 ligand for 24 hours. The removal of the ligand for additional 24 hours significantly decreased the dd_T7 RNAP levels as shown by western blot analysis (Figure 14, C). A selected clone of dd_T7 RNAP was used as a parental cell line to experimentally test the regulation of LmMIX expression. Integration of His-tagged version LmMIX-His (Figure 15, A) into LD1 locus (schematically in Figure 15, B and C) was verified by PCR (data not shown). The immunoblotting analysis of five clones of dd-T7 RNAP_LmMIX-His stable transfectants identified two clones (Figure 15, D – lower panel, clone 4 and 5) with a FK506-dependent expression of dd-T7 similar to parental cell line. However, only clone 5 expressed also LmMIX-His protein, unfortunately in T7 RNAP-independent manner (Figure 15, D – upper panel). It can be concluded that LmMIX is expressed independently on the presence of FK506 ligand either due to an unforeseen genetic recombination event, which is common in *Leishmania*²⁰⁵, or the leaky dd-T7 RNAP expression.

Presumably transcriptionally silent LD1 locus (27.5 kb) was previously thoroughly described in various *Leishmania* species and was shown to occur in several genomic organizations. In a majority of analyzed samples, LD1 is located on chromosome 35, close to telomere region, and appears to be multiplied. In some isolates, smaller chromosomes (550 bp) carrying LD1 were observed.

PART III

Additionally, small circular DNA molecules were also detected to carry parts of LD1 locus, predominantly in isolates with LD1 also present in the original position on megabase chromosome. In *L. major*, only strain 252 (Iran), which served as a parental strain for methotrexate-resistant experimental lineages, contains small chromosome carrying LD1 locus²⁰⁶⁻²⁰⁸. However, the body of this evidence suggests that LD1 locus undergo natural rearrangements and can regularly occur in multiple copies. This could potentially increase the level of transcription to a point when dd domain cannot regulate expression of a protein of interest. After a significant effort, we concluded that the dd method in its current form is not suitable for organellar, especially mt, targets expression regulation.

Recently, novel approach represented by CRISPR/Cas9 system was shown to be an effective tool in many model organisms (*Plasmodium sp.*^{209,210}, *Toxoplasma gondii*²¹¹, *T. cruzi*²¹², *L. donovani*²¹³, *L. mexicana*²¹⁴, and *L. major*²¹⁵). As the originally prokaryotic CRISPR/Cas9 system operates directly on the level of genomic DNA, regulation of targets localized in organelles will not suffer the issues connected with transmembrane import as in dd domain technique and consequently, it could facilitate investigation of organellar targets in *Leishmania*.

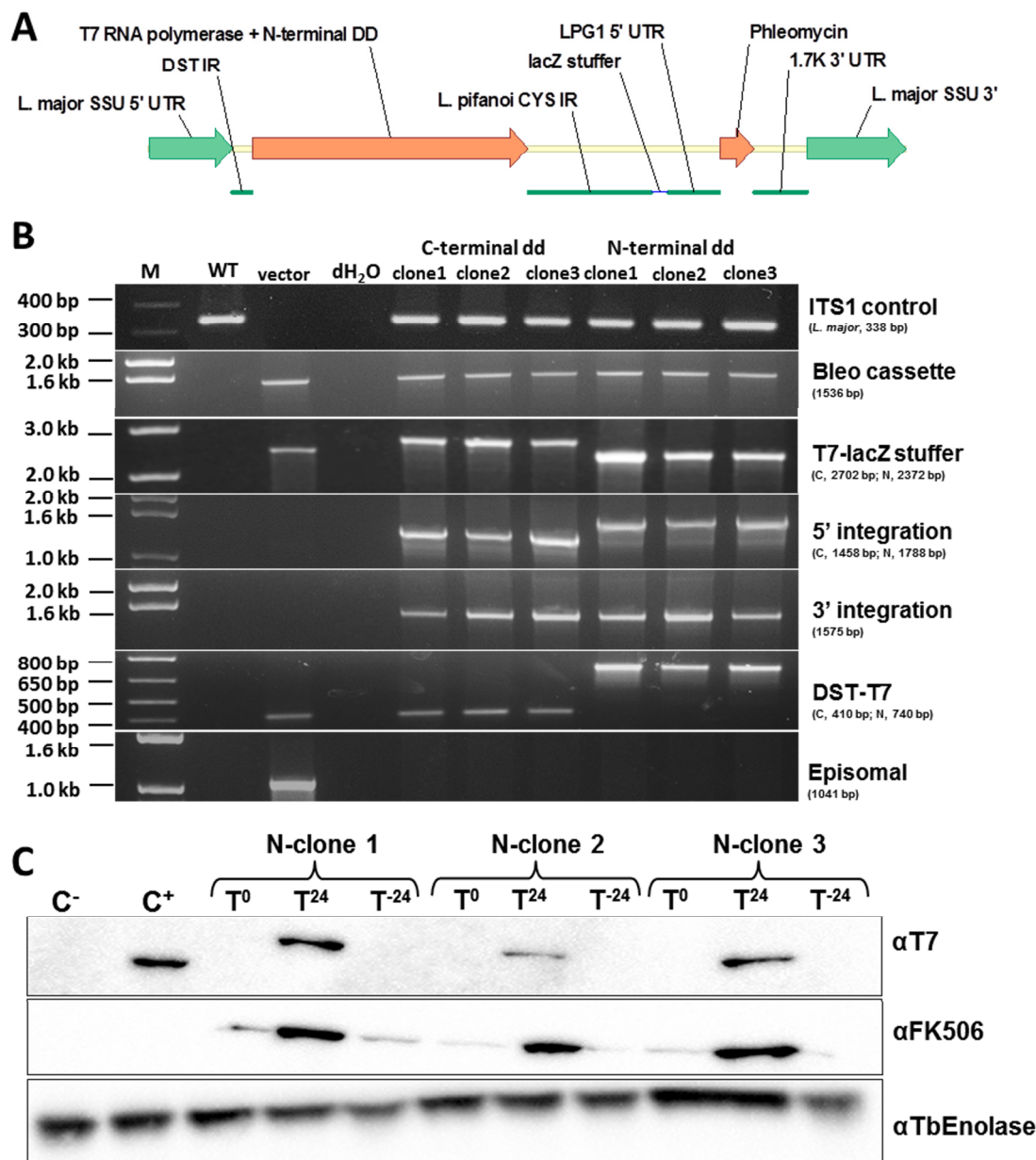


Figure 14: A – Schematic of dd_T7 polymerase construct for incorporation in the SSU rDNA. Homologous regions for incorporation into SSU locus are depicted in green. **B - Verification of correctly incorporated dd domain by PCR.** Three clones for each transfected construct, N and C-terminal dd domain, were verified for the presence of T7 polymerase cassette at the ribosomal locus. Individual segments of cassette were tested with a specific pair of primers. The ITS was used as a control for *Leishmania* gDNA. **C - Stabilization of the T7 RNA polymerase with N-terminal dd domain fusion in response to the addition of FK506 ligand.** Three clones were analyzed by western blot for stabilization and destabilization of dd_T7 polymerase (α T7) and binding of ligand FK506 (α FK506). The α TbEnolase was used as a loading control.

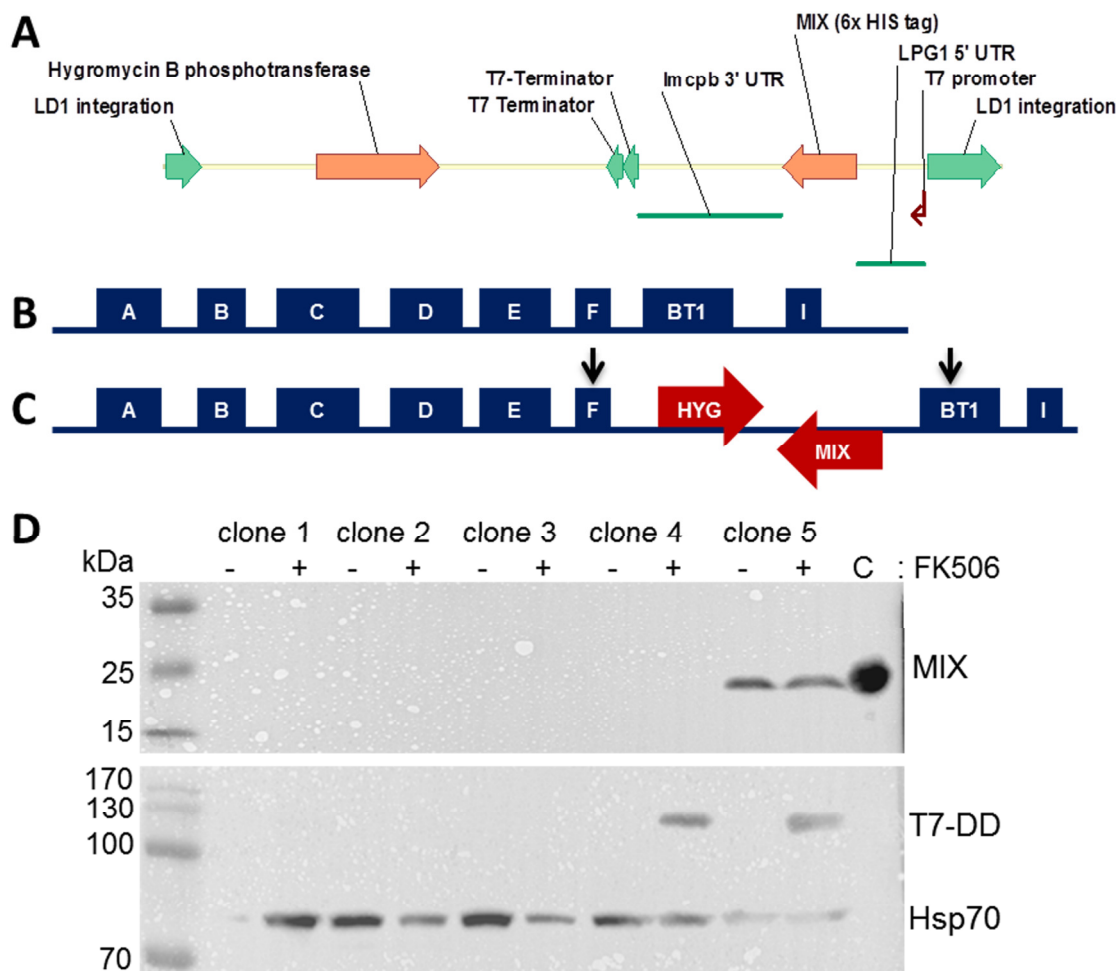


Figure 15: A – Scheme of the cassette for genomic integration to the LD1 locus containing MIX with C-terminal His tag for detection. B – The endogenous LD1 locus. C – Protein MIX integration scheme. Arrows indicate the site of integration between gene F (*LmjF.35.5140*) and Biopterin Transporter 1 (BT1). D – Immunoblotting analysis of cassette expression. Expression of MIX-His and T7 polymerase in five clones induced for 24 hours in comparison with uninduced control.

PART IV RESPIRATORY COMPLEX IV- ASSOCIATED PROTEIN MIX IN BLOODSTREAM FORM TRYPANOSOME

IV.1 INTRODUCTION

In the previous chapter I mentioned mitochondrial protein, LmMIX, which plays an important role in virulence of *L. major*. Intriguingly, this protein was also found to be associated with respiratory complex IV in the PF *T. brucei* and its decrease affected cell growth rate and activity of the complex IV. The Complex IV, or cytochrome *c* oxidase, is the fourth complex of electron transport chain (ETC) embedded in mt inner membrane. By transferring electrons from reduced cytochrome *c* to water, complex IV concludes the process of cellular respiration. Transferred electrons still possess enough energy to drive translocation of hydrogens to the intermembrane space. Consequently, Complex IV also participates on the generation of mmp for the synthesis of ATP, essential processes for the survival of PF cells. Unexpectedly, TbMIX was identified by two independent studies ^{216,217} using mass spectrometry also in BF parasites, where complex IV is not active and it is thought to be completely absent as the mmp is maintained by F₀F₁ ATPase. The presence of TbMIX in BF opened a possibility that additional functions are performed by TbMIX in *T. brucei*.

IV.2 METHODS

Two different strategies for TbMIX downregulation in BF were considered: knockdown of TbMIX with RNAi, and a complete gene knockout with homology recombination.

For the RNAi knockdown of TbMIX, a fragment spanning 476 bp from 148 bp upstream of TbMIX start codon to nucleotide 328 of ORF was introduced into head-to-head T7 RNAi vector p2T7-177 targeting the construct into transcriptionally silent minichromosome 177²¹⁸ (primers TbMIX_KD fw&rv). A non-overlapping pair of primers was also designed for qPCR evaluation of knockdown level (TbMIX_qPCR fw&rv). The resulting construct was transfected into BF SM parental cell line¹⁵⁹, and clones emerging from phleomycin selection were further characterized. The growth rate of RNAi TbMIX in presence of tetracycline observed for eleven days was compared to uninduced and parental cell line. A similar strategy was employed to re-construct published PF RNAi TbMIX cell line serving as a control. For verification of protein knockdown, immunoblotting with newly produced anti TbMIX_PAbII (described below) was performed.

For the complete knockout strategy, fragments of upstream 5'UTR (TbMIX_5'UTR fw&rv) and downstream 3'UTR (TbMIX_3'UTR fw&rv) untranslated regions were used as in¹⁵⁹ and previously described for TbMrf1 and TbMTQ1, in the respective Methods sections. As viable clones emerged from combined phleomycin and hygromycin selection, the growth rate of dKO TbMIX cell line was measured.

His-tagged TbMIX_PAbII (17 kDa) was inserted into pSKB3 expression vector (primers TbMIX_PAbII fw&rv) and expressed in BL21(DE3) *E. coli*. The cells were lysed in the native lysis buffer (50 mM Tris-HCl pH 7.5, 150 mM NaCl, 1 mg/ml lysozyme, 100U/ml DNaseI, and protease inhibitors). The pellet with

insoluble inclusion bodies containing protein was further solubilized in solubilization buffer (50 mM Tris-HCl pH 7.5, 150 mM NaCl, 1.5% sarkosyl, 1 mM EDTA pH 8, 100U/ml DNaseI) at 4 °C for 30 min. The solubilized material was cleared by centrifugation at 20 000 g for 20 min at 4 °C and directly purified using Ni-NTA affinity chromatography. Purified His-TbMIX_PAbII antigen was dialyzed against storage buffer suitable for antibody preparation (50 mM Tris-HCl pH 7.5, 150 mM NaCl, 0.1% sarkosyl) and submitted for commercial antibody preparation. Resulting antisera and purified antibody were tested against PF, BF and *Leishmania* cell lysates (1×10^7 cells per well) by western blot analysis. The cross-reactivity with anti-LmMIX antibody used in ²⁰⁰ was tested.

IV.3 RESULTS WITH DISCUSSION

To examine the role of MIX in BF parasites we attempted to decrease TbMIX expression in BF cells by two methods, RNAi, and genetic knockout. Results on previously studied RNAi TbMIX in PF trypanosome revealed a decreased growth rate within 48 hours after induction. The published cell line was re-created in our conditions and phenotype was verified by growth rate analysis and immunoblotting (Figure 16, A with inlay). In contrast to PF, no growth retardation was observed in BF upon induction of RNAi. A similar result was obtained for genetic knockout dKO TbMIX BF cell line where the correct incorporation of knockout cassettes replacing respective alleles was verified by PCR (Figure 16, B – inlay). The growth rates of dKO TbMIX together with induced and uninduced RNAi TbMIX were compared to wild-type BF 427 (Figure 16, B). The generally slower growth of RNAi TbMIX ($T_d = 6.3$ hours) compared to BF 427 ($T_d = 5.8$ hours) could be attributed to the presence of antibiotic selection rather than the effect of TbMIX downregulation. The viable and stable dKO TbMIX cell line ($T_d = 6.7$ hours) without significantly impaired

PART IV

growth rate shows that TbMIX is probably dispensable in this life cycle stage similarly to complex IV, to which it is associated. To conclude, TbMIX is not essential for BF cell survival *in vitro*. However, I cannot exclude the possibility that *in vivo* in the animal model the TbMIX can exhibit essential function, as observed in TbMrf1.

To facilitate further analysis of TbMIX role in the mitochondrion, I endeavored to produce TbMIX antigen for commercial antibody production. The *in silico* analysis of TbMIX protein sequence with a semi-empirical method for prediction of antigenic determinants ²¹⁹ uncovered presence of five potential antigenic regions regularly covering the length of protein and suitable for antibody preparation. At the same time, structural analysis of LmMIX shown presence of structurally distinct 14-3-3 motif ²⁰¹ found in a large group of proteins. To ensure sufficient specificity of resulting antibody, I truncated originally 198 residues long TbMIX to avoid initial mt targeting sequence (residue 1 – 24), predicted transmembrane region (residue 26 – 48), and two predicted 14-3-3 motives (residue 44 – 53 and 168 – 180). Resulting fragment used for antigen preparation was the N and C-terminally truncated TbMIX_PAbII (A54 – R167). Expressed in *E.coli*, the antigen was insoluble in all tested expression conditions. To circumvent this issue, I employed solubilization effect of the ionic surfactant N-Lauroylsarcosine in optimized purification protocol. Briefly, the harvested culture was lysed and pelleted insoluble inclusion bodies containing TbMIX_PAbII were solubilized with solubilization buffer containing 1.5% sarkosyl. The resulting material was cleared, purified efficiently with Ni-NTA affinity chromatography under native conditions (Figure 16, C) and dialyzed against buffer more suitable for animal immunization (see methods). Resulting antigen (containing less than 0.1% sarkosyl) was submitted for commercial preparation of rabbit polyclonal antibody (Davids Biotechnologie).

Purified antibody was tested against cell lysates from PF and BF cells. A clear signal at the expected size (23 kDa) was detected in PF. Moreover, this band

was not detected in induced PF TbMIX RNAi cells, confirming targets identity as MIX. Unfortunately, no band corresponding to MIX protein was visible in BF sample (Figure 16, D). Further attempts to detect this protein were performed, e.g. loading more material and decreasing the antibody dilution, with no success. Without a potent antibody, it would be extremely difficult to track TbMIX in BF cell during subsequent functional studies and thus the project was discontinued. However, in the frame of this project, I was able to introduce and optimize the sarkosyl-based purification protocol, which is widely used by other team members to purify hydrophobic proteins under native conditions.

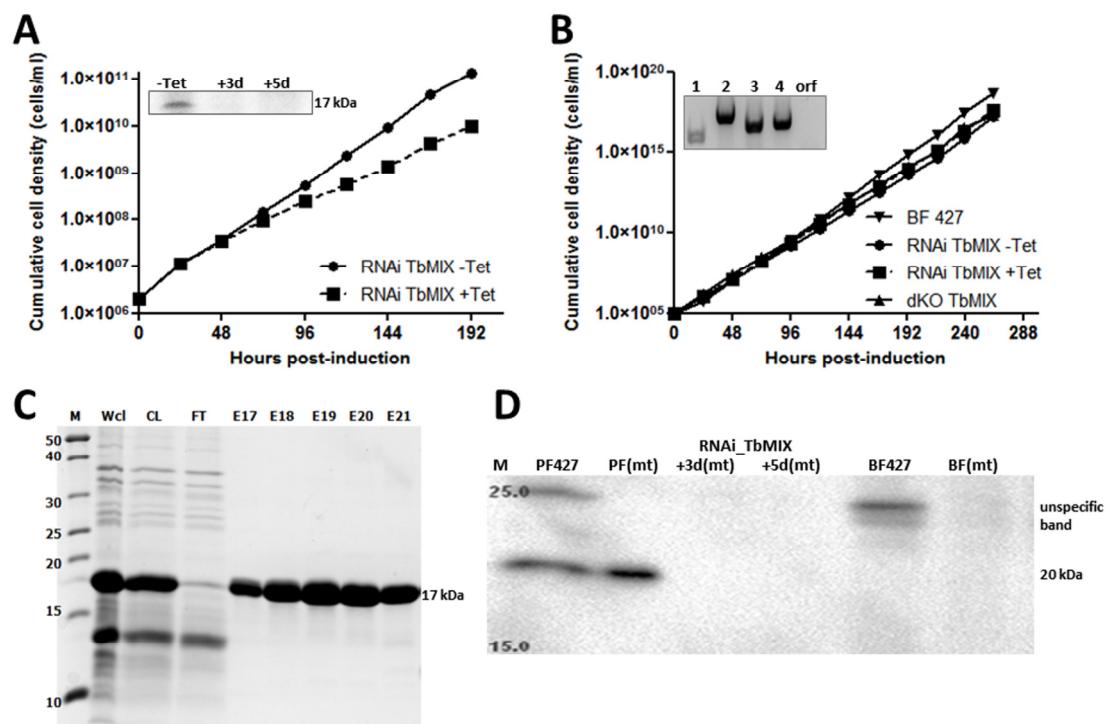


Figure 16: A – Growth curve of RNAi TbMIX in PF cells. Inlay shows western blot analysis of TbMIX expression upon induction of RNAi. **B – Growth curve of RNAi and genetically silenced dKO TbMIX in BF cells.** Inlay shows PCR analysis of BF dKO TbMIX cell line. **C – Purification profile of the TbMIX antigen.** Recombinant truncated TbMIX Δ 45 was purified from *E. coli* with sarkosyl. The expected protein size was 17 kDa. **D – Anti-TbMIX antibody verification by immunoblotting.** Antibody raised against TbMIX Δ 45 antigen was tested with the PF427 whole cell (1×10^7 cell/well), isolated mitochondria from parental cell line PF(mt) and RNAi TbMIX in PF (+3d and +5d), BF427 whole cells (1×10^7 cell/well), and isolated mitochondria BF(mt). M – marker, WCL – whole cell lysate, CL – cleared lysate, P – pellet, FT1 – flow through, W – wash, TeV – protease cleavage fraction, E – elution fraction.

3. SUMMARY

The presented doctoral thesis is a compilation of disparate projects, all aiming to explore mitochondrial processes in Kinetoplastid parasites *T. brucei* and *L. major*.

In Part I, I investigated the consequences of genetic knockout of mt release factor TbMrf1 on viability, energy metabolism, and virulence of BF trypanosome. Contrary to universally expected essential nature of Mrf1¹¹², I found that cultured cells can not only tolerate its loss but also adapt to the situation by employing a TbPth4 factor, a homolog of yeast codon-independent release factor-like protein. However, these adaptations are not enough to allow the parasite to establish a stable infection in a mouse model. The possible outcomes are discussed in research paper included in the results section of Part I.

In the second results section, I present research on two additional factors of translation termination phase in trypanosome, the mt N⁵-glutamine methyltransferase TbMTQ1 and the cytosolic release factor 1, TbeRF1. As a subject of my diploma project, I verified the localization of TbMTQ1 and performed tandem affinity purification to uncover its binding partners. During my doctoral studies, I continued in further characterization of TbMTQ1. The original *in vitro* approach was abandoned for lack of recombinant protein for downstream analyses in favor of *in vivo* studies using mutant *T. brucei* cell lines. From my results, I concluded that TbMTQ1 is not essential for trypanosome viability and maintenance of mt membrane potential levels, either *in vitro* or *in vivo* in an animal model.

Furthermore, I generated RNAi of a putative cytosolic release factor TbeRF1 and a cell line with endogenously tagged allele. I was persuaded by

rapid and distinctive growth phenotype and by its cytosolic localization that this protein is indeed the cytosolic class 1 release factor. Later, the genome-wide analyses assigned TbeRF1 as a protein with a putative role in mRNA-binding and TbeRF1 was annotated as ERF1 in TriTrypDB.

In Part II, I share my results from optimization of a rapid and reproducible fluorescent method to measure mt membrane potential (mmp) in permeabilized BF cells. The assay is based on the linear dependency of safranin O fluorescence quenching on the level of mt membrane potential. I was able to measure subtle differences in mmp occurring in BF cell and thus observe the decrease of mmp in RNAi ATPaseTb1 cell line, which was difficult to detect with other methods. Obtained data are a part of the manuscript in preparation (Šubrtová et al.).

In Part III, I attempted to develop the destabilization domain technique (dd) for use with mt localized essential targets. The idea behind the dd-technique project originated from the need to circumvent technical difficulties in working with mt targets in *Leishmania major*, which does not contain functional RNAi pathway. As a test subject, I used the LmMIX protein, a virulence factor targeted to the mitochondrion. However, neither one of designed approaches yielded a functional system for mt proteins expression regulation. The project was abandoned when more advantageous CRISPR/Cas9 system was optimized in eukaryotes. Nevertheless, the MIX protein remained in my focus and in part IV, I prepared recombinant antigen used for anti-TbMIX polyclonal antibody generation. In the process, I had to optimize solubilization protocol in order to purify hydrophobic and insoluble proteins. In the end, the resulting antibody detected TbMIX exclusively in PF lysates, not in BF. Although MIX is a promising attenuation factor in *Leishmania*, the project was suspended for lack of available tools. However, eventual investigation of this protein could employ mentioned CRISPR/Cas9 methodology with published results from both model organisms

4. REFERENCES

1. Claes, F., Büscher, P., Touratier, L. & Goddeeris, B. M. Trypanosoma equiperdum: Master of disguise or historical mistake? *Trends in Parasitology* **21**, 316–321 (2005).
2. Borst, P., Fase-Fowler, F. & Gibson, W. C. Kinetoplast DNA of Trypanosoma evansi. *Molecular and Biochemical Parasitology* **23**, 31–38 (1987).
3. Trindade, S., Rijo-Ferreira, F., Carvalho, T., Pinto-Neves, D., Guegan, F., Aresta-Branco, F., Bento, F., Young, S. A., Pinto, A., Van Den Abbeele, J., Ribeiro, R. M., Dias, S., Smith, T. K. & Figueiredo, L. M. Trypanosoma brucei Parasites Occupy and Functionally Adapt to the Adipose Tissue in Mice. *Cell Host & Microbe* **19**, 837–848 (2016).
4. Borst, P. & Cross, G. A. M. Molecular basis for trypanosome antigenic variation. *Cell* **29**, 291–303 (1982).
5. Reuner, B., Vassella, E., Yutzy, B. & Boshart, M. Cell density triggers slender to stumpy differentiation of Trypanosoma brucei bloodstream forms in culture. *Molecular and Biochemical Parasitology* **90**, 269–280 (1997).
6. Fenn, K. & Matthews, K. R. The cell biology of Trypanosoma brucei differentiation. *Current Opinion in Microbiology* **10**, 539–546 (2007).
7. Seed, J. R. & Wenck, M. A. Role of the long slender to short stumpy transition in the life cycle of the African trypanosomes. *Kinetoplastid Biology and Disease* **2**, 3 (2003).
8. Rico, E., Rojas, F., Mony, B. M., Szoor, B., MacGregor, P. & Matthews, K. R. Bloodstream form pre-adaptation to the tsetse fly in Trypanosoma brucei. *Frontiers in Cellular and Infection Microbiology* **3**, 78 (2013).
9. Stuart, K., Brun, R., Croft, S., Fairlamb, A., Gürtler, R. E., McKerrow, J., Reed, S. & Tarleton, R. Kinetoplastids: Related protozoan pathogens, different diseases. *Journal of Clinical Investigation* **118**, 1301–1310 (2008).
10. Croft, S. L. Kinetoplastida: new therapeutic strategies. *Parasite* **15**, 522–527 (2008).
11. Kolasinska-zwierz, P., Down, T., Latorre, I., Liu, T., Liu, X. S. & Ahringer, J. High-throughput decoding of anti-trypanosomal drug efficacy and resistance. *Cancer* **41**, 376–381 (2009).
12. Blum, J., Nkunku, S. & Burri, C. Clinical description of encephalopathic syndromes and risk factors for their occurrence and outcome during melarsoprol treatment of human African trypanosomiasis. *Tropical Medicine and International Health* **6**, 390–400 (2001).
13. Nok, A. J. Arsenicals (melarsoprol), pentamidine and suramin in the treatment of human African trypanosomiasis. *Parasitology Research* **90**, 71–9 (2003).

14. Alirol, E., Schrumph, D., Amici Heradi, J., Riedel, A., De Patoul, C., Quere, M. & Chappuis, F. Nifurtimox-eflornithine combination therapy for second-stage gambiense human African trypanosomiasis: Médecins Sans Frontières experience in the Democratic Republic of the Congo. *Clinical Infectious Diseases* **56**, 195–203 (2013).
15. Mesu, V. K. B. K., Kalonji, W. M., Bardonneau, C., Mordt, O. V., Blesson, S., Simon, F., Delhomme, S., Bernhard, S., Kuziena, W., Lubaki, J. P. F., Vuvu, S. L., Ngima, P. N., Mbembo, H. M., Ilunga, M., Bonama, A. K., Heradi, J. A., Solomo, J. L. L., Mandula, G., Badibabi, L. K., *et al.* Oral fexinidazole for late-stage African *Trypanosoma brucei* gambiense trypanosomiasis: A pivotal multicentre, randomised, non-inferiority trial. *Lancet* **391**, 144–154 (2017).
16. Barreto-de-Albuquerque, J., Silva-dos-Santos, D., Pérez, A. R., Berbert, L. R., Santana-van-Vliet, E. de, Farias-de-Oliveira, D. A., Moreira, O. C., Roggero, E., Carvalho-Pinto, C. E. de, Jurberg, J., Cotta-de-Almeida, V., Bottasso, O., Savino, W. & Meis, J. de. *Trypanosoma cruzi* Infection through the Oral Route Promotes a Severe Infection in Mice: New Disease Form from an Old Infection? *PLoS Neglected Tropical Diseases* **9**, e0003849 (2015).
17. Hemmige, V., Tanowitz, H. & Sethi, A. *Trypanosoma cruzi* infection: a review with emphasis on cutaneous manifestations. *International Journal of Dermatology* **51**, 501–508 (2012).
18. Teixeira, M. M., Gazzinelli, R. T. & Silva, J. S. Chemokines, inflammation and *Trypanosoma cruzi* infection. *Trends in Parasitology* **18**, 262–5 (2002).
19. World Health Organization. Chagas disease (American trypanosomiasis). (2017). Available at: <http://www.who.int/mediacentre/factsheets/fs340/en/>.
20. Leishmaniasis. (2016). Available at: <http://www.who.int/mediacentre/factsheets/fs375/en/>.
21. Hartley, M.-A., Ronet, C., Zangger, H., Beverley, S. M. & Fasel, N. Leishmania RNA virus: when the host pays the toll. *Frontiers in Cellular and Infection Microbiology* **2**, 99 (2012).
22. Ives, A., Ronet, C., Prevel, F., Ruzzante, G., Fuertes-Marraco, S., Schutz, F., Zangger, H., Revaz-Breton, M., Lye, L.-F., Hickerson, S. M., Beverley, S. M., Acha-Orbea, H., Launois, P., Fasel, N. & Masina, S. Leishmania RNA Virus Controls the Severity of Mucocutaneous Leishmaniasis. *Science* **331**, 775–778 (2011).
23. Robinson, J. I. & Beverley, S. M. Concentration of 2′C-methyladenosine triphosphate by *Leishmania guyanensis* enables specific inhibition of *Leishmania* RNA virus 1 by its RNA polymerase. *Journal of Biological Chemistry* jbc.RA117.001515 (2018).
24. Brettman, E. A. The Role of RNA Interference in the Control of *Leishmania* RNA virus 1 Infection. Ph.D. Thesis (Washington University in St. Louis, 2017).
25. Ghalib, H. & Modabber, F. Consultation meeting on the development of therapeutic vaccines for post kala azar dermal leishmaniasis. *Kinetoplastid Biology and Disease* **6**, 7 (2007).

References

26. Zijlstra, E., Musa, A., Khalil, E., El Hassan, I. & El-Hassan, A. Post-kala-azar dermal leishmaniasis. *Lancet Infectious Diseases* **3**, 87–98 (2003).
27. David Sibley, L. Invasion and intracellular survival by protozoan parasites. *Immunological Reviews* **240**, 72–91 (2011).
28. Rosenzweig, D., Smith, D., Opperdoes, F., Stern, S., Olafson, R. W. & Zilberstein, D. Retooling *Leishmania* metabolism: from sand fly gut to human macrophage. *FASEB Journal* **22**, 590–602 (2008).
29. Olliaro, P. L., Guerin, P. J., Gerstl, S., Haaskjold, A. A., Rottingen, J. A. & Sundar, S. Treatment options for visceral leishmaniasis: A systematic review of clinical studies done in India, 1980-2004. *Lancet Infectious Diseases* **5**, 763–774 (2005).
30. Kedzierski, L., Zhu, Y. & Handman, E. *Leishmania* vaccines: Progress and problems. *Parasitology* **133**, S87-112 (2006).
31. Titus, R. G., Gueiros-Filho, F. J., de Freitas, L. A. & Beverley, S. M. Development of a safe live *Leishmania* vaccine line by gene replacement. *Proceedings of the National Academy of Sciences of USA* **92**, 10267–10271 (1995).
32. Selvapandiyar, A., Duncan, R., Debrabant, A., Lee, N., Sreenivas, G., Salotra, P. & Nakhasi, H. L. Genetically modified live attenuated parasites as vaccines for leishmaniasis. *Indian Journal of Medical Research* **123**, 455–466 (2006).
33. Lueong, S., Merce, C., Fischer, B., Hoheisel, J. D. & Erben, E. D. Gene expression regulatory networks in *Trypanosoma brucei*: insights into the role of the mRNA-binding proteome. *Molecular Microbiology* **100**, 457–71 (2016).
34. Kolev, N. G., Ramey-Butler, K., Cross, G. A. M., Ullu, E. & Tschudi, C. Developmental Progression to Infectivity in *Trypanosoma brucei* Triggered by an RNA-Binding Protein. *Science* **338**, 1352–1353 (2012).
35. Hedges, S. B. The origin and evolution of model organisms. *Nature Reviews Genetics* **3**, 838–849 (2002).
36. Vanhamme, L. & Pays, E. Control of Gene Expression in Trypanosomes. *Microbiological Reviews* **59**, 223–240 (1995).
37. Teixeira, S. M., Paiva, R. M. C. de, Kangussu-Marcolino, M. M. & DaRocha, W. D. Trypanosomatid comparative genomics: contributions to the study of parasite biology and different parasitic diseases. *Genetics and Molecular Biology* **35**, 1–17 (2012).
38. Nelson, R. G., Parsons, M., Barr, P. J., Stuart, K., Selkirk, M. & Agabian, N. Sequences homologous to the variant antigen mRNA spliced leader are located in tandem repeats and variable orphans in *Trypanosoma brucei*. *Cell* **34**, 901–909 (1983).
39. Parsons, M., Nelson, R. G., Watkins, K. P. & Agabian, N. Trypanosome mRNAs share a common 5' spliced leader sequence. *Cell* **38**, 309–316 (1984).
40. Michaeli, S. Trans-splicing in trypanosomes: machinery and its impact on the parasite transcriptome. *Future Microbiology* **6**, 459–474 (2011).

41. Günzl, A. The pre-mRNA splicing machinery of trypanosomes: Complex or simplified? *Eukaryotic Cell* **9**, 1159–1170 (2010).
42. Gilinger, G. & Bellofatto, V. Trypanosome spliced leader RNA genes contain the first identified RNA polymerase II gene promoter in these organisms. *Nucleic Acids Research* **29**, 1556–1564 (2001).
43. Zamudio, J. R., Mitra, B., Zeiner, G. M., Feder, M., Bujnicki, J. M., Sturm, N. R. & Campbell, D. A. Complete cap 4 formation is not required for viability in *Trypanosoma brucei*. *Eukaryotic Cell* **5**, 905–915 (2006).
44. Bangs, J. D., Crain, P. F., Hashizume, T., McCloskey, J. A. & Boothroyd, J. C. Mass spectrometry of mRNA cap 4 from trypanosomatids reveals two novel nucleosides. *Journal of Biological Chemistry* **267**, 9805–9815 (1992).
45. Siegel, T. N., Hekstra, D. R., Wang, X., Dewell, S. & Cross, G. A. M. Genome-wide analysis of mRNA abundance in two life-cycle stages of *Trypanosoma brucei* and identification of splicing and polyadenylation sites. *Nucleic Acids Research* **38**, 4946–4957 (2010).
46. Clayton, C. E. Networks of gene expression regulation in *Trypanosoma brucei*. *Molecular and Biochemical Parasitology* **195**, 96–106 (2014).
47. Glover, L., Hutchinson, S., Alsford, S., McCulloch, R., Field, M. C. & Horn, D. Antigenic variation in African trypanosomes: The importance of chromosomal and nuclear context in VSG expression control. *Cellular Microbiology* **15**, 1984–1993 (2013).
48. Wickstead, B., Ersfeld, K. & Gull, K. The small chromosomes of *Trypanosoma brucei* involved in antigenic variation are constructed around repetitive palindromes. *Genome Research* **14**, 1014–1024 (2004).
49. Navarro, M. & Gull, K. A pool transcriptional body associated with VSG mono-allelic expression in *Trypanosoma brucei*. *Nature* **414**, 759–763 (2001).
50. Allen, C. L., Goulding, D. & Field, M. C. Clathrin-mediated endocytosis is essential in *Trypanosoma brucei*. *EMBO Journal* **22**, 4991–5002 (2003).
51. Field, M. C. & Carrington, M. The trypanosome flagellar pocket. *Nature Reviews Microbiology* **7**, 775–786 (2009).
52. Bakker, B. M., Mensonides, F. I. C., Teusink, B., van Hoek, P., Michels, P. A. M. & Westerhoff, H. V. Compartmentation protects trypanosomes from the dangerous design of glycolysis. *Proceedings of the National Academy of Sciences of USA* **97**, 2087–2092 (2000).
53. Michels, P. A. M., Bringaud, F., Herman, M. & Hannaert, V. Metabolic functions of glycosomes in trypanosomatids. *Biochimica et Biophysica Acta - Molecular Cell Research* **1763**, 1463–1477 (2006).
54. Colasante, C., Ellis, M., Ruppert, T. & Voncken, F. Comparative proteomics of glycosomes from bloodstream form and procyclic culture form *Trypanosoma brucei brucei*. *Proteomics* **6**, 3275–3293 (2006).

References

55. Škodová, I., Verner, Z., Bringaud, F., Fabian, P., Lukeš, J. & Horváth, A. Characterization of Two Mitochondrial Flavin Adenine Dinucleotide-Dependent Glycerol-3-Phosphate Dehydrogenases in *Trypanosoma brucei*. *Eukaryotic Cell* **12**, 1664–1673 (2013).
56. Bakker, B. M., Westerhoff, H. V. & Michels, P. A. M. Regulation and control of compartmentalized glycolysis in bloodstream form *Trypanosoma brucei*. *Journal of Bioenergetics and Biomembranes* **27**, 513–525 (1995).
57. Bakker, B. M., Michels, P. A. M., Opperdoes, F. R. & Westerhoff, H. V. Glycolysis in Bloodstream Form *Trypanosoma brucei* Can Be Understood in Terms of the Kinetics of the Glycolytic Enzymes. *Journal of Biological Chemistry* **272**, 3207–3215 (1997).
58. Bakker, B. M., Michels, P. A. M., Opperdoes, F. R. & Westerhoff, H. V. What Controls Glycolysis in Bloodstream Form *Trypanosoma brucei*? *Journal of Biological Chemistry* **274**, 14551–14559 (1999).
59. Butter, F., Bucerius, F., Michel, M., Cicova, Z., Mann, M. & Janzen, C. J. Comparative Proteomics of Two Life Cycle Stages of Stable Isotope-labeled *Trypanosoma brucei* Reveals Novel Components of the Parasite's Host Adaptation Machinery. *Molecular & Cellular Proteomics* **12**, 172–179 (2013).
60. Bochud-Allemann, N. & Schneider, A. Mitochondrial substrate level phosphorylation is essential for growth of procyclic *Trypanosoma brucei*. *Journal of Biological Chemistry* **277**, 32849–32854 (2002).
61. Acestor, N., Zíková, A., Dalley, R. A., Anupama, A., Panigrahi, A. K. & Stuart, K. D. *Trypanosoma brucei* Mitochondrial Respiratome: Composition and Organization in Procyclic Form. *Molecular & Cellular Proteomics* **10**, M110.006908 (2011).
62. Clarkson, A. B., Bienen, E. J., Pollakis, G. & Grady, R. W. Respiration of bloodstream forms of the parasite *Trypanosoma brucei brucei* is dependent on a plant-like alternative oxidase. *Journal of Biological Chemistry* **264**, 17770–17776 (1989).
63. Verner, Z., Škodová, I., Poláková, S., Ďurišová-Benkovičová, V., Horváth, A., Lukeš, J. Alternative NADH dehydrogenase (NDH2): intermembrane-space-facing counterpart of mitochondrial complex I in the procyclic *Trypanosoma brucei*. *Parasitology* **140**, 328–337 (2013).
64. Schnauffer, A., Clark-Walker, G. D., Steinberg, A. G. & Stuart, K. The F1-ATP synthase complex in bloodstream stage trypanosomes has an unusual and essential function. *EMBO Journal* **24**, 4029–4040 (2005).
65. Surve, S., Heestand, M., Panicucci, B., Schnauffer, A. & Parsons, M. Enigmatic Presence of Mitochondrial Complex I in *Trypanosoma brucei* Bloodstream Forms. *Eukaryotic Cell* **11**, 183–193 (2012).
66. Bringaud, F., Rivière, L. & Coustou, V. Energy metabolism of trypanosomatids: Adaptation to available carbon sources. *Molecular and Biochemical Parasitology* **149**, 1–9 (2006).

67. Vercesi, A. E., Docampo, R. & Moreno, S. N. J. Energization-dependent Ca²⁺ accumulation in *Trypanosoma brucei* bloodstream and procyclic trypomastigotes mitochondria. *Molecular and Biochemical Parasitology* **56**, 251–257 (1992).
68. Mazet, M., Morand, P., Biran, M., Bouyssou, G., Courtois, P., Daulouède, S., Millerioux, Y., Franconi, J. M., Vincendeau, P., Moreau, P. & Bringaud, F. Revisiting the Central Metabolism of the Bloodstream Forms of *Trypanosoma brucei*: Production of Acetate in the Mitochondrion Is Essential for Parasite Viability. *PLoS Neglected Tropical Diseases* **7**, e2587 (2013).
69. Schnauffer, A. An RNA Ligase Essential for RNA Editing and Survival of the Bloodstream Form of *Trypanosoma brucei*. *Science* **291**, 2159–2162 (2001).
70. Brown, S. V, Hosking, P., Li, J. & Williams, N. ATP synthase is responsible for maintaining mitochondrial membrane potential in bloodstream form *Trypanosoma brucei*. *Eukaryotic Cell* **5**, 45–53 (2006).
71. Bennett, M. C., Mlady, G. W., Kwon, Y.-H. & Rose, G. M. Chronic In Vivo Sodium Azide Infusion Induces Selective and Stable Inhibition of Cytochrome c Oxidase. *Journal of Neurochemistry* **66**, 2606–2611 (2002).
72. Miyadera, H., Shiomi, K., Ui, H., Yamaguchi, Y., Masuma, R., Tomoda, H., Miyoshi, H., Osanai, A., Kita, K. & Omura, S. Atpenins, potent and specific inhibitors of mitochondrial complex II (succinate-ubiquinone oxidoreductase). *Proceedings of the National Academy of Sciences of USA* **100**, 473–477 (2003).
73. Nakayama, K., Okamoto, F. & Harada, Y. Antimycin A: isolation from a new *Streptomyces* and activity against rice plant blast fungi. *Journal of Antibiotics* **9**, 63–6 (1956).
74. Bruni, A., R., C. A. & Scalell, P. The binding of atractyloside and oligomycin to liver mitochondria. *Biochimica et Biophysica Acta* **100**, 1–12 (1965).
75. Ochs, D. E., Otsu, K., Teixeira, S. M. R., Moser, D. R. & Kirchhoff, L. V. Maxicircle genomic organization and editing of an ATPase subunit 6 RNA in *Trypanosoma cruzi*. *Molecular and Biochemical Parasitology* **76**, 267–278 (1996).
76. Benne, R., Van Den Burg, J., Brakenhoff, J. P. J., Sloof, P., Van Boom, J. H. & Tromp, M. C. Major transcript of the frameshifted *coxII* gene from trypanosome mitochondria contains four nucleotides that are not encoded in the DNA. *Cell* **46**, 819–826 (1986).
77. Aphasizhev, R. & Aphasizheva, I. Mitochondrial RNA editing in trypanosomes: Small RNAs in control. *Biochimie* **100**, 125–131 (2014).
78. Aphasizheva, I. & Aphasizhev, R. RET1-Catalyzed Uridylylation Shapes the Mitochondrial Transcriptome in *Trypanosoma brucei*. *Molecular and Cellular Biology* **30**, 1555–1567 (2010).
79. Aphasizheva, I., Maslov, D., Wang, X., Huang, L. & Aphasizhev, R. Pentatricopeptide Repeat Proteins Stimulate mRNA Adenylation/Uridylation to Activate Mitochondrial Translation in Trypanosomes. *Molecular Cell* **42**, 106–117 (2011).

References

80. Bhat, G. J., Koslowsky, D. J., Feagin, J. E., Smiley, B. L. & Stuart, K. An extensively edited mitochondrial transcript in kinetoplastids encodes a protein homologous to ATPase subunit 6. *Cell* **61**, 885–894 (1990).
81. Etheridge, R. D., Aphasizheva, I., Gershon, P. D. & Aphasizhev, R. 3' adenylation determines mRNA abundance and monitors completion of RNA editing in *T. brucei* mitochondria. *EMBO Journal* **27**, 1596–1608 (2008).
82. Carnes, J., Soares, C. Z., Wickham, C. & Stuart, K. Endonuclease Associations with Three Distinct Editosomes in *Trypanosoma brucei*. *Journal of Biological Chemistry* **286**, 19320–19330 (2011).
83. Panigrahi, A. K., Ogata, Y., Zíková, A., Anupama, A., Dalley, R. A., Acestor, N., Myler, P. J. & Stuart, K. D. A comprehensive analysis of *Trypanosoma brucei* mitochondrial proteome. *Proteomics* **9**, 434–450 (2009).
84. Kang, X., Gao, G., Rogers, K., Falick, A. M., Zhou, S. & Simpson, L. Reconstitution of full-round uridine-deletion RNA editing with three recombinant proteins. *Proceedings of the National Academy of Sciences of USA* **103**, 13944–13949 (2006).
85. Cristodero, M., Seebeck, T. & Schneider, A. Mitochondrial translation is essential in bloodstream forms of *Trypanosoma brucei*. *Molecular Microbiology* **78**, 757–69 (2010).
86. Aphasizheva, I., Maslov, D. A. & Aphasizhev, R. Kinetoplast DNA-encoded ribosomal protein S12. *RNA Biology* **10**, 1679–1688 (2013).
87. Verner, Z., Basu, S., Benz, C., Dixit, S., Dobáková, E., Faktorová, D., Hashimi, H., Horáková, E., Huang, Z., Paris, Z., Peña-Díaz, P., Ridlon, L., Týč, J., Wildridge, D., Zíková, A. & Lukeš, J. Malleable Mitochondrion of *Trypanosoma brucei*. *International Review of Cell and Molecular Biology* **315**, 73–151 (2015).
88. Amunts, A., Brown, A., Toots, J., Scheres, S. H. W. & Ramakrishnan, V. The structure of the human mitochondrial ribosome. *Science* **348**, 95–98 (2015).
89. Ott, M., Amunts, A. & Brown, A. Organization and Regulation of Mitochondrial Protein Synthesis. *Annual Review of Biochemistry* **85**, 77–101 (2016).
90. Eperon, I. C., Janssen, J. W. G., Hoeijmakers, J. H. J. & Borst, P. The major transcripts of the kinetoplast DNA of *Trypanosoma brucei* are very small ribosomal RNAs. *Nucleic Acids Research* **11**, 105–125 (1983).
91. Schneider, A. Unique aspects of mitochondrial biogenesis in trypanosomatids. *International Journal for Parasitology* **31**, 1403–1415 (2001).
92. Agrawal, R. K. & Sharma, M. R. Structural aspects of mitochondrial translational apparatus. *Current Opinion in Structural Biology* **22**, 797–803 (2012).
93. Zíková, A., Panigrahi, A. K., Dalley, R. A., Acestor, N., Anupama, A., Ogata, Y., Myler, P. J. & Stuart, K. *Trypanosoma brucei* Mitochondrial Ribosomes. *Molecular & Cellular Proteomics* **7**, 1286–1296 (2008).

94. Maslov, D. A., Spremulli, L. L., Sharma, M. R., Bhargava, K., Grasso, D., Falick, A. M., Agrawal, R. K., Parker, C. E. & Simpson, L. Proteomics and electron microscopic characterization of the unusual mitochondrial ribosome-related 45S complex in *Leishmania tarentolae*. *Molecular and Biochemical Parasitology* **152**, 203–212 (2007).
95. Ridlon, L., Škodová, I., Pan, S., Lukeš, J. & Maslov, D. A. The importance of the 45 S ribosomal small subunit-related complex for mitochondrial translation in *trypanosoma brucei*. *Journal of Biological Chemistry* **288**, 32963–32978 (2013).
96. Vila-Sanjurjo, A., Lu, Y., Aragonez, J. L., Starkweather, R. E., Sasikumar, M. & O'Connor, M. Modulation of 16S rRNA function by ribosomal protein S12. *Biochimica et Biophysica Acta - Gene Structure and Expression* **1769**, 462–471 (2007).
97. Agarwal, D., Gregory, S. T. & O'Connor, M. Error-Prone and Error-Restrictive Mutations Affecting Ribosomal Protein S12. *Journal of Molecular Biology* **410**, 1–9 (2011).
98. Schneider, A., Martin, J. & Agabian, N. A nuclear encoded tRNA of *Trypanosoma brucei* is imported into mitochondria. *Molecular and Cellular Biology* **14**, 2317–22 (1994).
99. Tan, T. H. P., Pach, R., Crausaz, A., Ivens, A. & Schneider, A. tRNAs in *Trypanosoma brucei*: genomic organization, expression, and mitochondrial import. *Molecular and Cellular Biology* **22**, 3707–3717 (2002).
100. Tan, T. H. P., Bochud-Allemann, N., Horn, E. K. & Schneider, A. Eukaryotic-type elongator tRNA^{Met} of *Trypanosoma brucei* becomes formylated after import into mitochondria. *Proceedings of the National Academy of Sciences of USA* **99**, 1152–1157 (2002).
101. Alfonzo, J. D., Blanc, V., Estévez, A. M., Rubio, M. A. & Simpson, L. C to U editing of the anticodon of imported mitochondrial tRNA(Trp) allows decoding of the UGA stop codon in *Leishmania tarentolae*. *EMBO Journal* **18**, 7056–62 (1999).
102. Charriere, F., Helgadottir, S., Horn, E. K., Soll, D. & Schneider, A. Dual targeting of a single tRNA^{Trp} requires two different tryptophanyl-tRNA synthetases in *Trypanosoma brucei*. *Proceedings of the National Academy of Sciences of USA* **103**, 6847–6852 (2006).
103. Wohlgamuth-Benedum, J. M., Rubio, M. A. T., Paris, Z., Long, S., Poliak, P., Lukeš, J. & Alfonzo, J. D. Thiolation Controls Cytoplasmic tRNA Stability and Acts as a Negative Determinant for tRNA Editing in Mitochondria. *Journal of Biological Chemistry* **284**, 23947–23953 (2009).
104. Martin, N. C. Location alters tRNA identity: *Trypanosoma brucei*'s cytosolic elongator tRNA^{Met} is both the initiator and elongator in mitochondria. *Proceedings of the National Academy of Sciences of USA* **99**, 1110–1112 (2002).
105. Kuzmenko, A., Atkinson, G. C., Levitskii, S., Zenkin, N., Tenson, T., Hauryliuk, V. & Kamenski, P. Mitochondrial translation initiation machinery: Conservation and diversification. *Biochimie* **100**, 132–140 (2014).

References

106. Gaur, R., Grasso, D., Datta, P. P., Krishna, P. D. V., Das, G., Spencer, A., Agrawal, R. K., Spremulli, L. & Varshney, U. A Single Mammalian Mitochondrial Translation Initiation Factor Functionally Replaces Two Bacterial Factors. *Molecular Cell* **29**, 180–190 (2008).
107. Christian, B. E. & Spremulli, L. L. Preferential Selection of the 5'-Terminal Start Codon on Leaderless mRNAs by Mammalian Mitochondrial Ribosomes. *Journal of Biological Chemistry* **285**, 28379–28386 (2010).
108. Jones, C. N., Wilkinson, K. A., Hung, K. T., Weeks, K. M. & Spremulli, L. L. Lack of secondary structure characterizes the 5' ends of mammalian mitochondrial mRNAs. *RNA* **14**, 862–871 (2008).
109. Bonnefoy, N. & Fox, T. D. In vivo analysis of mutated initiation codons in the mitochondrial COX2 gene of *Saccharomyces cerevisiae* fused to the reporter gene ARG8 m reveals lack of downstream reinitiation. *Molecular and General Genetics* **262**, 1036–1046 (2000).
110. Williams, E. H., Butler, C. A., Bonnefoy, N. & Fox, T. D. Translation Initiation in *Saccharomyces cerevisiae* Mitochondria: Functional Interactions Among Mitochondrial Ribosomal Protein Rsm28p, Initiation Factor 2, Methionyl-tRNA-Formyltransferase and Novel Protein Rmd9p. *Genetics* **175**, 1117–1126 (2006).
111. Charrière, F., Tan, T. H. P. & Schneider, A. Mitochondrial initiation factor 2 of *Trypanosoma brucei* binds imported formylated elongator-type tRNAMet. *Journal of Biological Chemistry* **280**, 15659–15665 (2005).
112. Cristodero, M., Mani, J., Oeljeklaus, S., Aeberhard, L., Hashimi, H., Ramrath, D. J. F., Lukeš, J., Warscheid, B. & Schneider, A. Mitochondrial translation factors of *Trypanosoma brucei*: elongation factor-Tu has a unique subdomain that is essential for its function. *Molecular Microbiology* **90**, 744–755 (2013).
113. Agrawal, R. K., Spahn, C. M. T., Penczek, P., Grassucci, R. A., Nierhaus, K. H. & Frank, J. Visualization of Trna Movements on the Escherichia coli 70s Ribosome during the Elongation Cycle. *Journal of Cell Biology* **150**, 447–460 (2000).
114. Spremulli, L. L., Coursey, A., Navratil, T. & Hunter, S. E. Initiation and Elongation Factors in Mammalian Mitochondrial Protein Biosynthesis. Chapter in *Progress in Nucleic Acid Research and Molecular Biology* **77**, 211–261 (2004).
115. Tsuboi, M., Morita, H., Nozaki, Y., Akama, K., Ueda, T., Ito, K., Nierhaus, K. H. & Takeuchi, N. EF-G2mt Is an Exclusive Recycling Factor in Mammalian Mitochondrial Protein Synthesis. *Molecular Cell* **35**, 502–510 (2009).
116. Chiron, S. Mitochondrial Translation: Elongation Factor Tu Is Essential in Fission Yeast and Depends on an Exchange Factor Conserved in Humans but Not in Budding Yeast. *Genetics* **169**, 1891–1901 (2005).
117. Ito, K., Uno, M. & Nakamura, Y. Single amino acid substitution in prokaryote polypeptide release factor 2 permits it to terminate translation at all three stop codons. *Proceedings of the National Academy of Sciences of USA* **95**, 8165–8169 (1998).
118. Nakamura, Y., Ito, K. & Isaksson, L. A. Emerging Understanding of Translation Termination. *Cell* **87**, 147–150 (1996).

119. Duarte, I., Nabuurs, S. B., Magno, R. & Huynen, M. Evolution and diversification of the organellar release factor family. *Molecular Biology and Evolution* **29**, 3497–3512 (2012).
120. Barrell, B. G., Bankier, A. T. & Drouin, J. A different genetic code in human mitochondria. *Nature* **282**, 189–194 (1979).
121. Rorbach, J., Soleimanpour-Lichaei, R., Lightowlers, R. N. & Chrzanowska-Lightowlers, Z. M. A. How do mammalian mitochondria synthesize proteins? *Biochemical Society Transactions* **35**, 1290–1291 (2007).
122. Christian, B. E. & Spremulli, L. L. Evidence for an Active Role of IF3 mt in the Initiation of Translation in Mammalian Mitochondria. *Biochemistry* **48**, 3269–3278 (2009).
123. Plevoda, B., Span, L. & Sherman, F. The yeast translation release factors Mrf1p and Sup45p (eRF1) are methylated, respectively, by the methyltransferases Mtq1p and Mtq2p. *Journal of Biological Chemistry* **281**, 2562–71 (2006).
124. Kisselev, L., Ehrenberg, M. & Frolova, L. Termination of translation: Interplay of mRNA, rRNAs and release factors? *EMBO Journal* **22**, 175–182 (2003).
125. Noble, C. G. & Song, H. Structural studies of elongation and release factors. *Cellular and Molecular Life Sciences* **65**, 1335–1346 (2008).
126. Shin, D. H., Brandsen, J., Jancarik, J., Yokota, H., Kim, R. & Kim, S. H. Structural analyses of peptide release factor 1 from *Thermotoga maritima* reveal domain flexibility required for its interaction with the ribosome. *Journal of Molecular Biology* **341**, 227–239 (2004).
127. Inge-Vechtomov, S., Zhouravleva, G. & Philippe, M. Eukaryotic release factors (eRFs) history. *Biology of the Cell* **95**, 195–209 (2003).
128. Janzen, D. M. & Geballe, A. P. The effect of eukaryotic release factor depletion on translation termination in human cell lines. *Nucleic Acids Research* **32**, 4491–4502 (2004).
129. Le Goff, X., Philippe, M. & Jean-Jean, O. Overexpression of human release factor 1 alone has an antisuppressor effect in human cells. *Molecular and Cellular Biology* **17**, 3164–72 (1997).
130. Ito, K., Ebihara, K. & Nakamura, Y. The stretch of C-terminal acidic amino acids of translational release factor eRF1 is a primary binding site for eRF3 of fission yeast. *RNA* **4**, 958–972 (1998).
131. Eurwilaichitr, L., Graves, F. M., Stansfield, I. & Tuite, M. F. The C-terminus of eRF1 defines a functionally important domain for translation termination in *Saccharomyces cerevisiae*. *Molecular Microbiology* **32**, 485–496 (1999).
132. Heurgué-Hamard, V., Champ, S., Mora, L., Merkoulova-Rainon, T., Kisselev, L. L. & Buckingham, R. H. The glutamine residue of the conserved GGQ motif in *Saccharomyces cerevisiae* release factor eRF1 is methylated by the product of the YDR140w gene. *Journal of Biological Chemistry* **280**, 2439–2445 (2005).

References

133. Mora, L., Heurgué-Hamard, V., de Zamaroczy, M., Kervestin, S. & Buckingham, R. H. Methylation of bacterial release factors RF1 and RF2 is required for normal translation termination in vivo. *Journal of Biological Chemistry* **282**, 35638–45 (2007).
134. Pannekoek, Y., Langerak, A. A. J., Speijer, D., Buckingham, R. H., Ende, A. Van Der, Heurgué-Hamard, V., Langerak, A. A. J., Speijer, D., Buckingham, R. H. & Ende, A. Van Der. The N⁵-Glutamine S-Adenosyl- L -Methionine-Dependent Methyltransferase PrmC / HemK in *Chlamydia trachomatis* Methylates Class 1 Release Factors. *Journal of Bacteriology* **187**, 507–511 (2005).
135. Polevoda, B. & Sherman, F. Methylation of proteins involved in translation. *Molecular Microbiology* **65**, 590–606 (2007).
136. Colson, C., Lhoest, J. & Urlings, C. Genetics of ribosomal protein methylation in *Escherichia coli*. III. Map position of two genes, prmA and prmB, governing methylation of proteins L11 and L3. *Molecular & General Genetics* **169**, 245–50 (1979).
137. Amaro, A. M. & Jerez, C. A. Methylation of ribosomal proteins in bacteria: evidence of conserved modification of the eubacterial 50S subunit. *Journal of Bacteriology* **158**, 84–93 (1984).
138. Trobro, S. & Åqvist, J. A Model for How Ribosomal Release Factors Induce Peptidyl-tRNA Cleavage in Termination of Protein Synthesis. *Molecular Cell* **27**, 758–766 (2007).
139. Nakahigashi, K., Kubo, N., Narita, S. S. -i., Shimaoka, T., Goto, S., Oshima, T., Mori, H., Maeda, M., Wada, C. & Inokuchi, H. HemK, a class of protein methyl transferase with similarity to DNA methyl transferases, methylates polypeptide chain release factors, and hemK knockout induces defects in translational termination. *Proceedings of the National Academy of Sciences of USA* **99**, 1473–1478 (2002).
140. Schubert, H. L., Phillips, J. D. & Hill, C. P. Structures along the Catalytic Pathway of PrmC / HemK , an N⁵-Glutamine. *Biochemistry* **42**, 5592–5599 (2003).
141. Liu, P., Nie, S., Li, B., Yang, Z.-Q., Xu, Z.-M., Fei, J., Lin, C., Zeng, R. & Xu, G.-L. Deficiency in a Glutamine-Specific Methyltransferase for Release Factor Causes Mouse Embryonic Lethality. *Molecular and Cellular Biology* **30**, 4245–4253 (2010).
142. Soleimanpour-Lichaei, H. R., Kühl, I., Gaisne, M., Passos, J. F., Wydro, M., Rorbach, J., Temperley, R., Bonnefoy, N., Tate, W., Lightowlers, R. & Chrzanowska-Lightowlers, Z. mtRF1a Is a Human Mitochondrial Translation Release Factor Decoding the Major Termination Codons UAA and UAG. *Molecular Cell* **27**, 745–757 (2007).
143. Towpik, J., Chacińska, A., Cieśla, M., Ginalski, K. & Boguta, M. Mutations in the Yeast MRF1 Gene Encoding Mitochondrial Release Factor Inhibit Translation on Mitochondrial Ribosomes. *Journal of Biological Chemistry* **279**, 14096–14103 (2004).

144. Ishizawa, T., Nozaki, Y., Ueda, T. & Takeuchi, N. The human mitochondrial translation release factor HMRF1L is methylated in the GGQ motif by the methyltransferase HMPmC. *Biochemical and Biophysical Research Communications* **373**, 99–103 (2008).
145. Nozaki, Y., Matsunaga, N., Ishizawa, T., Ueda, T. & Takeuchi, N. HMRF1L is a human mitochondrial translation release factor involved in the decoding of the termination codons UAA and UAG. *Genes to Cells* **13**, 429–438 (2008).
146. Wesolowska, M. T., Richter-Dennerlein, R., Lightowers, R. N. & Chrzanowska-Lightowers, Z. M. A. Overcoming stalled translation in human mitochondria. *Frontiers in Microbiology* **5**, 374 (2014).
147. Chrzanowska-Lightowers, Z. M. & Lightowers, R. N. Response to ‘Ribosome Rescue and Translation Termination at Non-standard Stop Codons by ICT1 in Mammalian Mitochondria’. *PLoS Genetics* **11**, e1005227 (2015).
148. Gagnon, M. G., Seetharaman, S. V., Bulkley, D. & Steitz, T. A. Structural Basis for the Rescue of Stalled Ribosomes: Structure of YaeJ Bound to the Ribosome. *Science* **335**, 1370–1372 (2012).
149. Dujeancourt, L., Richter, R., Chrzanowska-Lightowers, Z. M., Bonnefoy, N. & Herbert, C. J. Interactions between peptidyl tRNA hydrolase homologs and the ribosomal release factor Mrf1 in *S. pombe* mitochondria. *Mitochondrion* **13**, 871–880 (2013).
150. Kiktev, D., Moskalenko, S., Murina, O., Baudin-Baillieu, A., Rousset, J. P. & Zhouravleva, G. The paradox of viable sup45 STOP mutations: A necessary equilibrium between translational readthrough, activity and stability of the protein. *Molecular Genetics and Genomics* **282**, 83–96 (2009).
151. Paushkin, S. V, Kushnirov, V. V, Smirnov, V. N. & Ter-Avanesyan, M. D. Interaction between yeast Sup45p (eRF1) and Sup35p (eRF3) polypeptide chain release factors: implications for prion-dependent regulation. *Molecular and Cellular Biology* **17**, 2798–2805 (1997).
152. Moskalenko, S. E., Chabelskaya, S. V., Inge-Vechtomov, S. G., Philippe, M. & Zhouravleva, G. A. Viable nonsense mutants for the essential gene SUP45 of *Saccharomyces cerevisiae*. *BMC Molecular Biology* **4**, 1–14 (2003).
153. Barbosa, E. & Moss, B. mRNA(nucleotide-2'-)methyltransferase from Vaccinia Virus. *Journal of Biological Chemistry* **21**, 7698–7702 (1978).
154. Schnierle, B. S., Gershon, P. D. & Moss, B. Cap-specific mRNA (nucleoside-O2'-)-methyltransferase and poly(A) polymerase stimulatory activities of vaccinia virus are mediated by a single protein. *Proceedings of the National Academy of Sciences of USA* **89**, 2897–2901 (1992).
155. Arhin, G. K. A protein related to the vaccinia virus cap-specific methyltransferase VP39 is involved in cap 4 modification in *Trypanosoma brucei*. *RNA* **12**, 53–62 (2006).
156. Armstrong, C. M. & Goldberg, D. E. An FKBP destabilization domain modulates protein levels in *Plasmodium falciparum*. *Nature Methods* **4**, 1007–1009 (2007).

References

157. Schimanski, B., Nguyen, T. N., Günzl, A. & Gu, A. Highly Efficient Tandem Affinity Purification of Trypanosome Protein Complexes Based on a Novel Epitope Combination. *Eukaryotic Cell* **4**, 1942–1950 (2005).
158. Alibu, V. P., Storm, L., Haile, S., Clayton, C. & Horn, D. A doubly inducible system for RNA interference and rapid RNAi plasmid construction in *Trypanosoma brucei*. *Molecular and Biochemical Parasitology* **139**, 75–82 (2005).
159. Wirtz, E., Leal, S., Ochatt, C. & Cross, G. A. M. A tightly regulated inducible expression system for conditional gene knock-outs and dominant-negative genetics in *Trypanosoma brucei*. *Molecular and Biochemical Parasitology* **99**, 89–101 (1999).
160. Chomczynski, P. & Sacchi, N. The single-step method of RNA isolation by acid guanidinium thiocyanate-phenol-chloroform extraction: twenty-something years on. *Nature Protocols* **1**, 581–5 (2006).
161. Yang, Z., Shipman, L., Zhang, M., Anton, B. P., Roberts, R. J. & Cheng, X. Structural Characterization and Comparative Phylogenetic Analysis of *Escherichia coli* HemK, a Protein (N5)-glutamine Methyltransferase. *Journal of Molecular Biology* **340**, 695–706 (2004).
162. Champ, S., Heurgue-Hamard, V., Champ, S., Engström, Å., Ehrenberg, M. & Buckingham, R. H. The hemK gene in *Escherichia coli* encodes the N5-glutamine methyltransferase that modifies peptide release factors. *EMBO* **21**, 769–778 (2002).
163. Gasteiger, E., Hoogland, C., Gattiker, A., Duvaud, S., Wilkins, M. R., Appel, R. D. & Bairoch, A. *Proteomics Protocols Handbook* (Humana Press, 2005).
164. Dean, S., Gould, M. K., Dewar, C. E. & Schnauffer, A. C. Single point mutations in ATP synthase compensate for mitochondrial genome loss in trypanosomes. *Proceedings of the National Academy of Sciences of USA* **110**, 14741–14746 (2013).
165. Dinçbas-Renqvist, V., Engström, Å., Mora, L., Heurgué-Hamard, V., Buckingham, R. & Ehrenberg, M. A post-translational modification in the GGQ motif of RF2 from *Escherichia coli* stimulates termination of translation. *EMBO Journal* **19**, 6900–6907 (2000).
166. Pierson, W. E., Hoffer, E. D., Keedy, H. E., Simms, C. L., Dunham, C. M. & Zaher, H. S. Uniformity of Peptide Release Is Maintained by Methylation of Release Factors. *Cell Reports* **17**, 11–18 (2016).
167. Lamour, N., Riviere, L., Coustou, V., Coombs, G. H., Barrett, M. P. & Bringaud, F. Proline Metabolism in Procyclic *Trypanosoma brucei* Is Down-regulated in the Presence of Glucose. *Journal of Biological Chemistry* **280**, 11902–11910 (2005).
168. Nicholls, D. G. & Ward, M. W. Mitochondrial membrane potential and cell death: mortality and millivolts. *Trends in Neuroscience* **23**, 166–174 (2000).
169. Mitchell, P. & Moyle, J. Estimation of Membrane Potential and pH Difference across the Cristae Membrane of Rat Liver Mitochondria. *European Journal of Biochemistry* **7**, 471–484 (2005).

170. Nicholls, D. G. The Influence of Respiration and ATP Hydrolysis on the Proton-Electrochemical Gradient across the Inner Membrane of Rat-Liver Mitochondria as Determined by Ion Distribution. *European Journal of Biochemistry* **50**, 305–315 (1974).
171. Scaduto, R. C. & Grotyohann, L. W. Measurement of Mitochondrial Membrane Potential Using Fluorescent Rhodamine Derivatives. *Biophysical Journal* **76**, 469–477 (1999).
172. Åkerman, K. E. O. & Wikström, M. K. F. Safranin as a probe of the mitochondrial membrane potential. *FEBS Letters* **68**, 191–197 (1976).
173. Perevoshchikova, I. V, Sorochkina, A. I., Zorov, D. B. & Antonenko, Y. N. Safranin O as a fluorescent probe for mitochondrial membrane potential studied on the single particle level and in suspension. *Biochemistry* **74**, 663–71 (2009).
174. Scanlon, J. A. B., Al-Shawi, M. K. & Nakamoto, R. K. A Rotor-Stator Cross-link in the F₁-ATPase Blocks the Rate-limiting Step of Rotational Catalysis. *Journal of Biological Chemistry* **283**, 26228–26240 (2008).
175. Walker, J. E. & Dickson, V. K. The peripheral stalk of the mitochondrial ATP synthase. *Biochimica et Biophysica Acta - Bioenergetics* **1757**, 286–296 (2006).
176. Rastogi, V. K. & Girvin, M. E. Structural changes linked to proton translocation by subunit c of the ATP synthase. *Nature* **402**, 263–8 (1999).
177. Allegretti, M., Klusch, N., Mills, D. J., Vonck, J., Kühlbrandt, W. & Davies, K. M. Horizontal membrane-intrinsic α -helices in the stator a-subunit of an F-type ATP synthase. *Nature* **521**, 237–240 (2015).
178. Zíková, A., Schnauffer, A., Dalley, R. A., Panigrahi, A. K. & Stuart, K. D. The F₀F₁-ATP synthase complex contains novel subunits and is essential for procyclic *Trypanosoma brucei*. *PLoS Pathogens* **5**, e1000436 (2009).
179. Gahura, O., Šubrtová, K., Váchová, H., Panicucci, B., Fearnley, I. M., Harbour, M. E., Walker, J. E. & Zíková, A. The F₁-ATPase from *Trypanosoma brucei* is elaborated by three copies of an additional p18-subunit. *FEBS Journal* **285**, 614–628 (2018).
180. Montgomery, M. G., Gahura, O., Leslie, A. G. W., Zíková, A. & Walker, J. E. ATP synthase from *Trypanosoma brucei* has an elaborated canonical F₁-domain and conventional catalytic sites. *Proceedings of the National Academy of Sciences of USA* **115**, 2102–2107 (2018).
181. Šubrtová, K., Panicucci, B. & Zíková, A. ATPaseTb2, a Unique Membrane-bound FoF₁-ATPase Component, Is Essential in Bloodstream and Dyskinetoplastic *Trypanosomes*. *PLoS Pathogens* **11**, e1004660 (2015).
182. Šubrtová, K. FoF₁-ATP synthase/ATPase in the parasitic protist, *Trypanosoma brucei*. Ph.D. Thesis (University of South Bohemia in České Budějovice, 2015).
183. Škodová-Sveráková, I., Horváth, A. & Maslov, D. A. Identification of the mitochondrially encoded subunit 6 of F₁F₀ ATPase in *Trypanosoma brucei*. *Molecular and Biochemical Parasitology* **201**, 135–138 (2015).

References

184. Nolan, D. P. & Voorheis, H. P. The mitochondrion in bloodstream forms of *Trypanosoma brucei* is energized by the electrogenic pumping of protons catalysed by the F1F0-ATPase. *European Journal of Biochemistry* **209**, 207–216 (1992).
185. Huang, G., Vercesi, A. E. & Docampo, R. Essential regulation of cell bioenergetics in *Trypanosoma brucei* by the mitochondrial calcium uniporter. *Nature Communications* **4**, (2013).
186. Robinson, K. A. & Beverley, S. M. Improvements in transfection efficiency and tests of RNA interference (RNAi) approaches in the protozoan parasite *Leishmania*. *Molecular and Biochemical Parasitology* **128**, 217–228 (2003).
187. Lye, L. F., Owens, K., Shi, H., Murta, S. M. F., Vieira, A. C., Turco, S. J., Tschudi, C., Ullu, E. & Beverley, S. M. Retention and Loss of RNA interference pathways in trypanosomatid protozoans. *PLoS Pathogens* **6**, e1001161 (2010).
188. Kolev, N. G., Tschudi, C. & Ullu, E. RNA interference in protozoan parasites: achievements and challenges. *Eukaryotic Cell* **10**, 1156–1163 (2011).
189. Chu, B. W., Banaszynski, L. A., Chen, L. & Wandless, T. J. Recent progress with FKBP-derived destabilizing domains. *Bioorganic & Medicinal Chemistry Letters* **18**, 5941–5944 (2008).
190. Bonger, K. M., Chen, L., Liu, C. W. & Wandless, T. J. Small-molecule displacement of a cryptic degron causes conditional protein degradation. *Nature Chemical Biology* **7**, 531–537 (2011).
191. Barbarino, J. M., Staats, C. E., Venkataramanan, R., Klein, T. E. & Altman, R. B. PharmGKB summary: Cyclosporine and tacrolimus pathways. *Pharmacogenetics and Genomics* **23**, 563–585 (2013).
192. Brasseur, A., Rotureau, B., Vermeersch, M., Blisnick, T., Salmon, D., Bastin, P., Pays, E., Vanhamme, L. & Pérez-Morgaa, D. *Trypanosoma brucei* FKBP12 differentially controls motility and cytokinesis in procyclic and bloodstream forms. *Eukaryotic Cell* **12**, 168–181 (2013).
193. Madeira da Silva, L., Owens, K. L., Murta, S. M. F. & Beverley, S. M. Regulated expression of the *Leishmania major* surface virulence factor lipophosphoglycan using conditionally destabilized fusion proteins. *Proceedings of the National Academy of Sciences of USA* **106**, 7583–7588 (2009).
194. Herm-Götz, A., Agop-Nersesian, C., Münter, S., Grimley, J. S., Wandless, T. J., Frischknecht, F. & Meissner, M. Rapid control of protein level in the apicomplexan *Toxoplasma gondii*. *Nature Methods* **4**, 1003–1005 (2007).
195. Banaszynski, L. A., Chen, L., chun, Maynard-Smith, L. A., Ooi, A. G. L. & Wandless, T. J. A Rapid, Reversible, and Tunable Method to Regulate Protein Function in Living Cells Using Synthetic Small Molecules. *Cell* **126**, 995–1004 (2006).
196. Azzu, V. & Brand, M. D. Degradation of an intramitochondrial protein by the cytosolic proteasome. *Journal of Cell Science* **123**, 3616–3616 (2010).

197. Leidhold, C. & Voos, W. Chaperones and proteases - Guardians of protein integrity in eukaryotic organelles. in *Annals of the New York Academy of Sciences* **1113**, 72–86 (2007).
198. Bulteau, A.-L., Szweda, L. I. & Friguet, B. Mitochondrial protein oxidation and degradation in response to oxidative stress and aging. *Experimental Gerontology* **41**, 653–657 (2006).
199. Koppen, M. & Langer, T. Protein degradation within mitochondria: Versatile activities of AAA proteases and other peptidases. *Critical Reviews in Biochemistry and Molecular Biology* **42**, 221–242 (2007).
200. Uboldi, A. D., Lueder, F. B., Walsh, P., Spurck, T., McFadden, G. I., Curtis, J., Likic, V. A., Perugini, M. A., Barson, M., Lithgow, T. & Handman, E. A mitochondrial protein affects cell morphology, mitochondrial segregation and virulence in *Leishmania*. *International Journal for Parasitology* **36**, 1499–1514 (2006).
201. Gorman, M. A., Uboldi, A. D., Walsh, P. J., Tan, K. S., Hansen, G., Huyton, T., Ji, H., Curtis, J., Kedzierski, L., Papenfuss, A. T., Dogovski, C., Perugini, M. A., Simpson, R. J., Handman, E. & Parker, M. W. Crystal structure of the *Leishmania* major MIX protein: A scaffold protein that mediates protein-protein interactions. *Protein Science* **20**, 1060–1068 (2011).
202. Yan, S., Martinez-Calvillo, S., Schnauffer, A., Sunkin, S., Myler, P. J. & Stuart, K. A low-background inducible promoter system in *Leishmania donovani*. *Molecular and Biochemical Parasitology* **119**, 217–223 (2002).
203. Schmidt, O., Pfanner, N. & Meisinger, C. Mitochondrial protein import: from proteomics to functional mechanisms. *Nature Reviews Molecular Cell Biology* **11**, 655–667 (2010).
204. Fegan, A., White, B., Carlson, J. C. T. & Wagner, C. R. Chemically controlled protein assembly: Techniques and applications. *Chemical Reviews* **110**, 3315–3336 (2010).
205. Rogers, M. B., Hilley, J. D., Dickens, N. J., Wilkes, J., Bates, P. A., Depledge, D. P., Harris, D., Her, Y., Herzyk, P., Imamura, H., Otto, T. D., Sanders, M., Seeger, K., Dujardin, J.-C., Berriman, M., Smith, D. F., Hertz-Fowler, C. & Mottram, J. C. Chromosome and gene copy number variation allow major structural change between species and strains of *Leishmania*. *Genome Research* **21**, 2129–2142 (2011).
206. Tripp, C. A., Myler, P. J. & Stuart, K. A DNA sequence (LD1) which occurs in several genomic organizations in *Leishmania*. *Molecular and Biochemical Parasitology* **47**, 151–160 (1991).
207. Hightower, R. C., Ruiz-Perez, L. M., Wong, M. L. & Santi, D. V. Extrachromosomal elements in the lower eukaryote *Leishmania*. *Journal of Biological Chemistry* **263**, 16970–6 (1988).
208. Arrebola, R., Olmo, A., Reche, P., Garvey, E. P., Santi, D. V., Ruiz-Perez, L. M. & Gonzalez-Pacanowska, D. Isolation and characterization of a mutant dihydrofolate reductase-thymidylate synthase from methotrexate-resistant *Leishmania* cells. *Journal of Biological Chemistry* **269**, 10590–6 (1994).

References

209. Ghorbal, M., Gorman, M., Macpherson, C. R., Martins, R. M., Scherf, A. & Lopez-Rubio, J.-J. Genome editing in the human malaria parasite *Plasmodium falciparum* using the CRISPR-Cas9 system. *Nature Biotechnology* **32**, 819–821 (2014).
210. Wagner, J. C., Platt, R. J., Goldfless, S. J., Zhang, F. & Niles, J. C. Efficient CRISPR-Cas9-mediated genome editing in *Plasmodium falciparum*. *Nature Methods* **11**, 915–918 (2014).
211. Shen, B., Brown, K. M., Lee, T. D. & Sibley, L. D. Efficient gene disruption in diverse strains of *Toxoplasma gondii* using CRISPR/CAS9. *mBio* **5**, e01114-14 (2014).
212. Peng, D., Kurup, S. P., Yao, P. Y., Minning, T. A. & Tarleton, R. L. CRISPR-Cas9-Mediated Single-Gene and Gene Family Disruption in *Trypanosoma cruzi*. *mBio* **6**, e02097-14-e02097-14 (2014).
213. Zhang, W.-W. & Matlashewski, G. CRISPR-Cas9-Mediated Genome Editing in *Leishmania donovani*. *mBio* **6**, e00861-15 (2015).
214. Duncan, S. M., Myburgh, E., Philipon, C., Brown, E., Meissner, M., Brewer, J. & Mottram, J. C. Conditional gene deletion with DiCre demonstrates an essential role for CRK3 in *Leishmania mexicana* cell cycle regulation. *Molecular Microbiology* **100**, 931–944 (2016).
215. Sollelis, L., Ghorbal, M., MacPherson, C. R., Martins, R. M., Kuk, N., Crobu, L., Bastien, P., Scherf, A., Lopez-Rubio, J.-J. & Sterkers, Y. First efficient CRISPR-Cas9-mediated genome editing in *Leishmania* parasites. *Cellular Microbiology* **17**, 1405–1412 (2015).
216. Urbaniak, M. D., Martin, D. M. A. & Ferguson, M. A. J. Global Quantitative SILAC Phosphoproteomics Reveals Differential Phosphorylation Is Widespread between the Procyclic and Bloodstream Form Lifecycle Stages of *Trypanosoma brucei*. *Journal of Proteome Research* **12**, 2233–2244 (2013).
217. Gunasekera, K., Wüthrich, D., Braga-Lagache, S., Heller, M. & Ochsenreiter, T. Proteome remodelling during development from blood to insect-form *Trypanosoma brucei* quantified by SILAC and mass spectrometry. *BMC Genomics* **13**, 556 (2012).
218. Wickstead, B., Ersfeld, K. & Gull, K. Targeting of a tetracycline-inducible expression system to the transcriptionally silent minichromosomes of *Trypanosoma brucei*. *Molecular and Biochemical Parasitology* **125**, 211–216 (2002).
219. Kolaskar, A. S. & Tongaonkar, P. C. A semi-empirical method for prediction of antigenic determinants on protein antigens. *FEBS Letters* **276**, 172–174 (1990).

5. SUPPLEMENTARY MATERIAL

Supplementary table 1: Sequences of oligonucleotides used in unpublished projects. Table is divided in two parts.

Primer	5' -> 3' sequence
TbeRF1-PTP_fw	GGGCCCTACAAGAGAAGAACTAC
TbeRF1-PTP_rv	ATAGCGGCCGCATAAAGTCGTCGTCG
TbeRF1-KD_fw	TATCTCGAGATCGTGGGGCTCGTGCTTGC
TbeRF1-KD_rv	TATGGATCCAGGCGCAACCAAACCTTGCGG
TbeRF1-qPCR_fw	AGCGTTCAAAGTGCCATCAC
TbeRF1-qPCR_rv	TCCTTGTTTTCTGCCGTGAG
TbMTQ1-5'UTR_fw	CACGCGGCCGCAATTGACGATTTGTGTG
TbMTQ1-5'UTR_rv	CACACGCGTCTCGAGATGTCACACAGCTCCAGG
TbMTQ1-3'UTR_fw	CACTCTAGAATTTAAATTATCCACGCGCTAAAC
TbMTQ1-3'UTR_rv	CACAGGCCTGCGGCCGCCACTTTCTTTC
TbMTQ1-5'UTR_ext_fw	CGATGAAGGTTGTTCAAGCC
TbMTQ1-3'UTR_ext_rv	CCTTGAAGGCTGCAATATGG
TbMTQ1-sKO_fw	CTTGCCGAATATCATGGTGG
TbMTQ1-sKO_rv	GTAATCCGGATCAGATCAGC
TbMTQ1-dKO_fw	TACTCGCCGATAGTGGAACC
TbMTQ1-dKO_rv	CGCGATGACTTAGTAAAGCAC
TbMTQ1_fw	CACGGATCCATGCGTCGATG
TbMTQ1_rv	CACAAGCTTTTAGTGGGAGG
9S rRNA	GGTACATATAGAACAACACTGT
12S rRNA	CCGCAACGGCTGGCATCC
A6 pre-edited_fw	GAGAAGCAAGGAGGAGAA
A6 pre-edited_rv	GCAAAGGCAATTCCCAAT
A6 edited_fw	TTGCCGCCATATTACAGT
A6 edited_rv	TCTATAACTCCAATAACAAACCAAAT
RPS12 pre-edited_fw	CGACGGAGAGCTTCTTTTGAATA
RPS12 pre-edited_rv	CCCCCACCCAAATCTTT
RPS12 edited_fw	CGTATGTGATTTTTGTATGGTTGTTG
RPS12edited_rv	ACACGTCGGTTACCGGAACT
Murf 5_fw	TGTTCCATTATTCATTTTGTGCATTAC
Murf 5_rv	TGTGTATAATGTTAAGTCAAATTAATAATGC
Lm_5'SSU_fw	TCTAGACAGATGGGAGAGATG
Lm_5'SSU_rv	CTCGAGCCAAGAGGCTTCAG
Lm_3'SSU_fw	GGTACCCACGCTTAGATGCAAAC
Lm_3'SSU_rv	AAGCTTCTGCCTGGCGGCTCC

Supplementary material

Primer	5' -> 3' sequence
LmMIX_ML	ATGCTCCGCCACACCGCGCGTTCGCATG
LmMIX_MHT_fw	ATAGGATCCATGCTCCGCCACAC
LmMIX_MHT_rv	ATAAAGCTTCGTGTGGGTCCG
eGFP_fw	TATGGATCCATGGGTGGCGGTGGATC
eGFP_rv	CCGACTAGTGGATCTAGACTTGTACAGCTCG
ML-eGFP_fw	TATGGATCCATGCTCCGCCACACCGCGCGTTCGCATGATGGGTGGCGGTGG
DST-IR_fw	ATGGCCAAGTTGACCAGT
DST-IR_rv	CCGGGGACAGGGGGAG
DD_fw	GGATCCATGGGAGTGCAGG
DD_rv (no STOP)	CGCACTAGTGAGCTCTCCGGTTTTAGAAGC
ML-DD_fw	TATGGATCCATGCTCCGCCACACCGCGCGTTCGCATGATGGGAGTGCAGGTGG
LmMIX_fw	ACTAGTATGCTCCGCCACAC
LmMIX_rv	GGATCCCGTGTGGGTCCG
DD_rv	GGTACCTCATTCCGGTTTTAG
TbMIX_KD_fw	GCGAGATCTGCTGTTATCAACGTAGCC
TbMIX_KD_rv	CTAAAGCTTGGCGTGTGTTGTTCCC
TbMIX_PAbII_fw	ATACATATGGCTGGGCCACTGGAGCTTC
TbMIX_PAbII_rv	TATAAGCTTTTCGTTGAGTCTACCCCCATTTGG
TbMIX_qPCR_fw	ACCAGTTGCGTAAGGAGGTAC
TbMIX_qPCR_rv	TCACATCTCGGTTGAGTCTACC
TbMIX_3'UTR_fw	GGGTCTAGAATTTAAATGCCGGACGTCTTGTGGTTCGAG
TbMIX_3'UTR_rv	TTTAGGCCTGCGGCCGCCCTGCCTCTTTGGTCACCGGC
TbMIX_5'UTR_fw	AAAGCGCCGCGGAAATGGTTTGACAGAAAAGG
TbMIX_5'UTR_rv	ACCACGCGTCTCGAGTCAATCCACGTTTGATCAAACG

Supplementary Information

Cultured bloodstream *Trypanosoma brucei* adapt to life without mitochondrial translation release factor 1

Michaela Procházková,^{a,b*} Brian Panicucci,^a Alena Zíková^{a,b,#}

Institute of Parasitology, Biology Centre ASCR, Ceske Budejovice, Czech Republic^a; Faculty of Science, University of South Bohemia, Ceske Budejovice, Czech Republic^b

Running title: Bloodstream *T. brucei* mitochondrial translation

#Address correspondence to Alena Zíková, azikova@paru.cas.cz

Phone: (420)-38-777-5482; Fax: (420)-38-531-0388

*Present address: Central European Institute of Technology, Masaryk University, Brno, Czech Republic

Key words: Trypanosoma, mitochondrion, RNAi, mitochondrial translation, mitoribosome, FoF1-ATPase

Supplementary Figure S1. Lack of TbMrf1 did not result in cells without kinetoplast DNA.

(a) Left panels: fluorescence microscopy of DAPI-stained BF 427, dKO TbMrf1 1wk and 7wk cells. Right panels: the DNA content and single tubular mitochondrion was visualized with DAPI and with a fluorescein isothiocyanate (FITC)-conjugated secondary antibody that recognizes a polyclonal primary antibody detecting F₁-ATPase subunit β , respectively. DIC - differential interference contrast; n – nuclei; k – kinetoplast.

(b) Quantification of the microscopy images based on the number of nuclei and kinetoplasts in more than 200 cells per cell line. Only normal cell types either in G1/S (1N1K) and G2/M (1N2K) phases or undergoing cytokinesis (2N2K) were detected.

Supplementary Figure S2. Ectopic overexpression of TbMrf1 in the background of TbMrf1 dKO decreases the sensitivity to oligomycin and carboxyatractyloside inhibitors

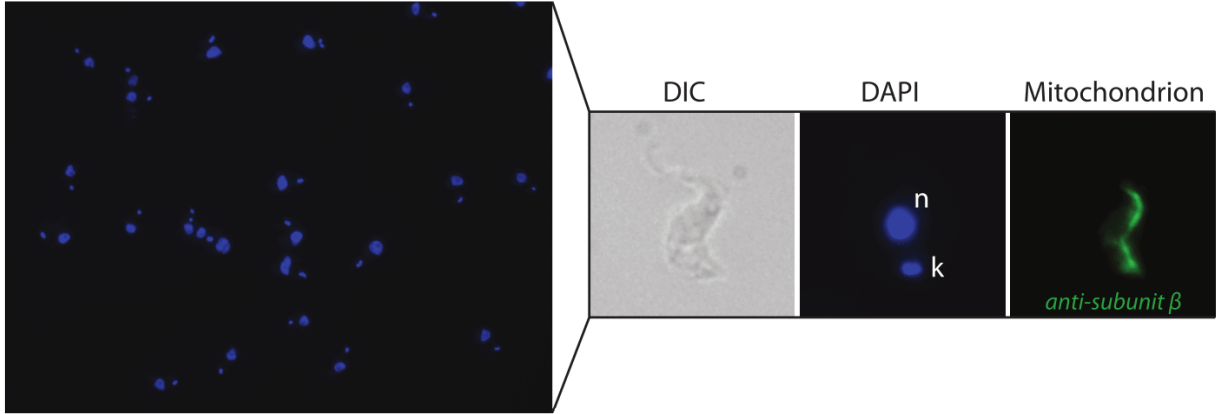
(a) Whole cell lysates from BF 427 cultures and cKO TbMrf1 7wk cells either noninduced (-tet) or induced (+tet) with tetracycline for 48 hours were probed with a specific anti-V5 antibody. An anti-APRT antibody was used as a loading control.

(b) The oligomycin and carboxyatractyloside sensitivity of cKO TbMrf1 7wk +tet cells was determined by an Alamar Blue assay. The dose-response curves were calculated using GraphPad Prism. Error bars represent the standard deviation calculated from three independent experimental replicates.

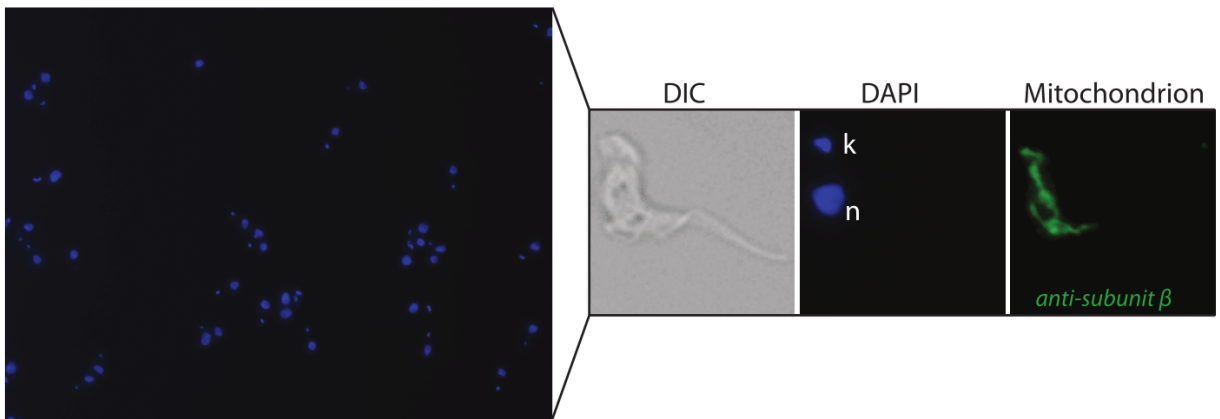
Supplementary Figure S1:

a

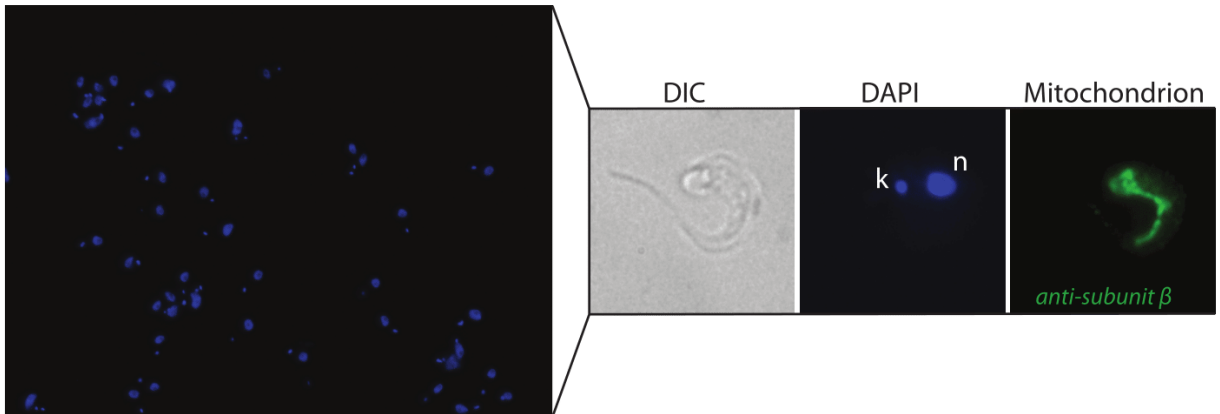
BF427



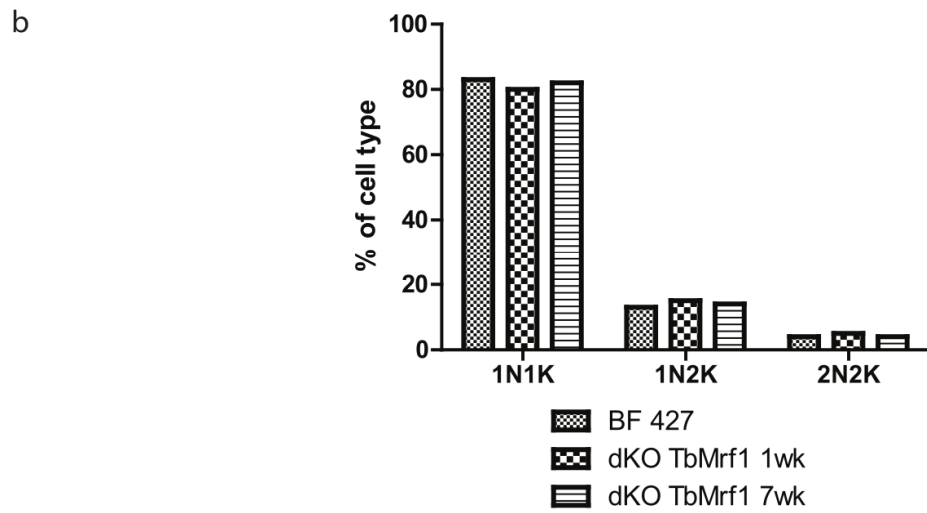
dKO TbMrf1 1wk



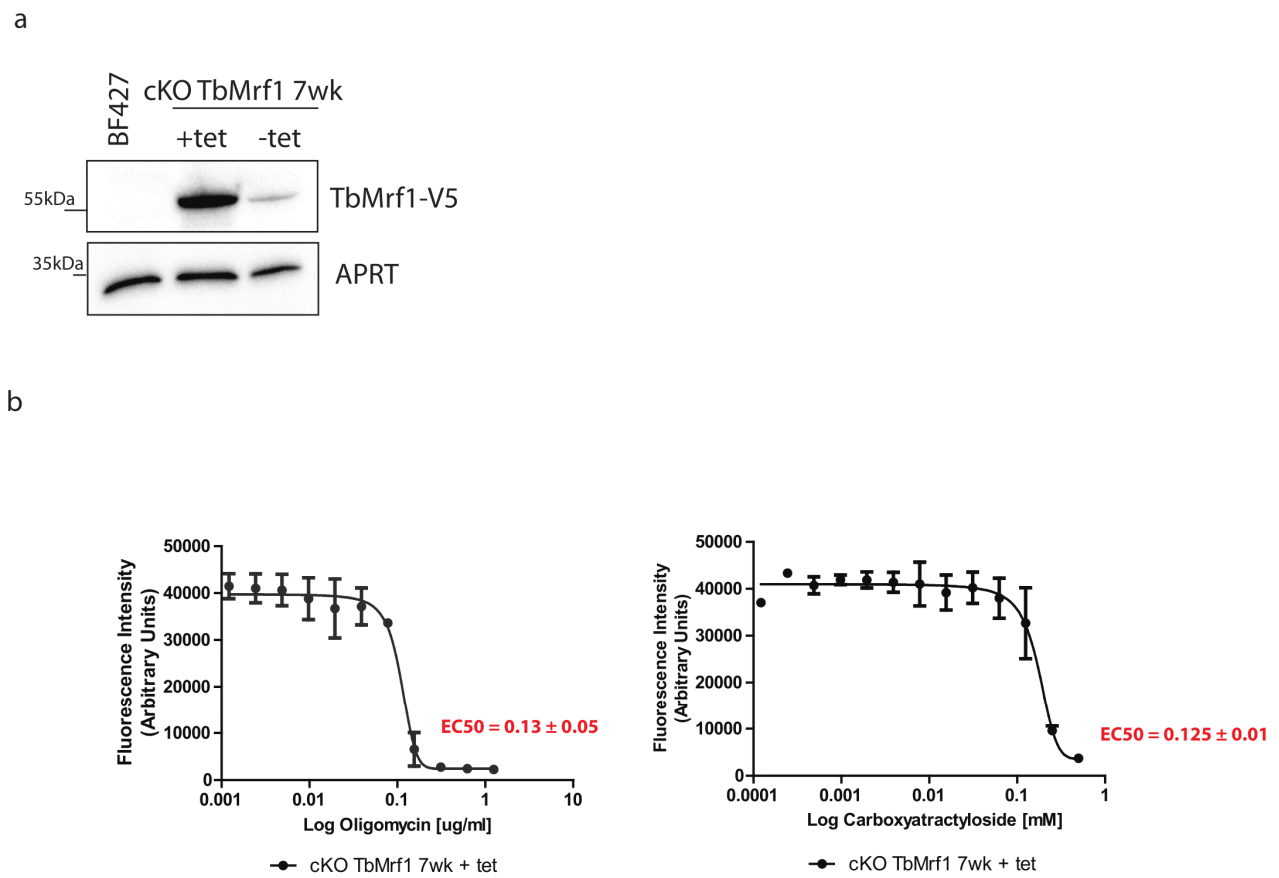
dKO TbMrf1 7wk



Supplementary Figure S1:



Supplementary Figure S2:



Supplementary Table S1: Oligonucleotides used in published research.

Primer name	Primer sequence
5'UTR_fw	TATGCGGCCGCTGTTCTATAACCGAGGACG
5'UTR_rv	AGGACGCGTCTCGAGATTCTTGGAATTGCTTGTACG
3'UTR_fw	GGGTCTAGAATTTAAATGAGAAGACGTGGGTGCCTAG
3'UTR_rv	TATAGGCCTGCGGCCGCTTGCCACTTTGGATCTGGG
5'UTR_ext_fw	AGTATTGGGCTATCGTCAGG
3'UTR_ext_rv	GAGGCAAATATGGTGAGAGC
sKO_fw	CTTGCCGAATATCATGGTGG
sKO_rv	GTAAATCCGGATCAGATCAGC
dKO_fw	TACTCGCCGATAGTGGAAACC
dKO_rv	CGCGATGACTTAGTAAAGCAC
TbMrf1_fw	ATAGGATCCATGAGGAATGCCCCATTGCTC
TbMrf1_rv	GCGAAGCTTTTACGTAACACAGTTGAAGTCG
TbMrf1 cKO_fw	CACAAGCTTATGAGGAATGCCC
TbMrf1 cKO_rv	CACGGATCCCGTAACACAGTTGAAG
β -tubulinqPCR_fw	TTCCGCACCCTGAAACTGA
β -tubulinqPCR_rv	TGACGCCGGACACAACAG
18S rRNA_fw	CGGAATGGCACCACAAGAC
18S rRNA_rv	TGGTAAAGTTCCCCGTGTTGA
12S rRNA_fw	GGGCAAGTCCTACTCTCCTTTACAAAG
12S rRNA_rv	TGAACAATCAATCATGGTAATAAGTAGACGATG
9S rRNA_fw	ATTAGATTGTTTTGTTAATGCTATTAGATG
9S rRNA_rv	ACGGCTGGCATCCATTTC
TbPth4qPCR_rv	TCTTTCAGAAACGATATGTG
TbPth4qPCR_fw	CTTCAGCAGATGATTCAC
TbPth4V5_fw	GGGAAGCTTATGAGTTGGTTAACTCCTTCAGG
TbPth4V5_rv	AAAGGATCCCCACAGCCCTTTGCGAG
TbPth4iSL_fw	ATTCTCGAGCCCGGGCAGAGACGAGGTAATTTCC
TbPth4iSL_rv	ACCAAGCTTGGATCCTGATCAGCTGTGTCTCATCC
TbMrf1qPCR_fw	ATGCAAAGCAGTTCCAACGC
TbMrf1qPCR_rv	ACACGACGTACCAACAGTTG

© for unpublished parts – Michaela Procházková

Contact: veselm08@gmail.com

All rights reserved

For non-commercial use only

Printed 2018 in Brno, Czech Republic

Mgr. Michaela Procházková

Curriculum Vitae



Husova čtvrt 1086, Rosice, 665 01
+420 728 913 633
michaela.veselikova@ceitec.muni.cz
<https://www.ceitec.cz/mgr-michaela-prochazkova/u89963>

DOCTORAL RESEARCH

“Mitochondrial gene expression in trypanosomatids”

In my research, I examined the ability of protozoan parasite *Trypanosoma brucei* to withstand loss of an essential translation factor - mitochondrial release factor 1 (TbMrfi). I found that the bloodstream form of trypanosome is not only able to survive complete knockout of TbMrfi but also adapt to its loss by previously unknown mechanism.

WORK EXPERIENCE

CURRENT, FROM FEB 2016 (FT)

CEITEC-MU Postdoc

As a member of Structural Virology research group led by Dr. Plevka, I am responsible for several projects. I work on structural analysis of honeybee sacbrood virus (SBV) and *Leishmania* RNA virus 1 (LRV 1) using combined means of crystallography and cryoEM. Furthermore, I became familiar with Focused ion beam milling of vitrified biological samples and employ this method to study a bacteriophage infection process in *Staphylococcus aureus*.

JUL 2015 – OCT 2015 (VISIT)

Laboratory of Dr. Ruslan Aphasizhev, Boston University Visiting scholar

I spent three months working with Dr. Aphasizhev on analysis of mitochondrial transcripts in my mutant cell lines. The research visit was also one of the university requirements for granting the Ph.D.

OCT 2010 – JAN 2016 (PT)

Institute of Parasitology, Biological Centre of CAS Laboratory technician

This position was granted to me during my Ph.D. studies.

REFERENCES

Dr. Pavel Plevka

POSITION Team leader
EMPLOYER CEITEC-MU
EMAIL pavel.plevka@ceitec.muni.cz

PUBLICATIONS

Procházková, M., Panicucci, B., Zíková, A. (2018). Cultured bloodstream *Trypanosoma brucei* adapt to life without mitochondrial translation release factor 1. *The Scientific Reports*, (8), 1-15.

Doleželová E., Terán D., Gahura O., Kotrbová Z., Procházková M., Keough D., et al. (2018). Evaluation of the *Trypanosoma brucei* 6-oxopurine salvage pathway as a potential target for drug discovery. *PLOS Neglected Tropical Diseases*, 12(2): e0006301.

EDUCATION

- 2010 – CURRENT **Doctor of Philosophy**
Molecular and Cell Biology and Genetics
University of South Bohemia
- 2008 – 2010 **Master of Science**
GRADUATED WITH HONOURS
Experimental Biology
University of South Bohemia
- 2005 – 2008 **Bachelor of Biology**
Biology
University of South Bohemia

AWARDS

- 2012 – 2013 **Student grant funding**
Grant Agency of University of South Bohemia

COMPUTER SKILLS

- BEGINNER EMAN2, Relion, SerialEM, CCP4, ITEX
INTERMEDIATE PyMOL, Coot, UCSF Chimera, IMOD

COMMUNICATION SKILLS

- CONFERENCES Oral Presentation, XV. Discussions in Structural Molecular Biology – 2018
POSTERS Poster at the 2nd iNEXT Annual User Meeting – 2017

SKILLS

Laboratory methods

I am skilled in molecular biology methods including molecular cloning, protein expression and purification, and immunoblotting methods. Furthermore, I am familiar with tissue culture maintenance, biochemical assays, and fluorescent dyes applications.

Instrumentation

I am an independent operator of Vitrobot and TEM microscope – Tecnai F20 in both room temperature and cryo mode. I became proficient in operating Versa3D dual beam system for FIB milling of vitrified biological samples for subsequent cryo electron tomography using Titan Krios TEM instrument.

IN ČESKÉ BUDĚJOVICE

SIGNATURE